Applications of Lumping Kinetics Methodology to Complex Reactive Mixtures

by

Mustafa Adam Amhammed

A thesis submitted for the degree of Doctor of Philosophy in

Heriot-Watt University

Chemical Engineering

Institute of Mechanical, Process and Energy Engineering
School of Engineering and Physical Sciences

September 2013

ABSTRACT

The thesis concerns a comprehensive study to develop and assess the predictive capabilities of a lumping model for the kinetics of complex reaction mixtures containing a large number of reacting components. Two types of lumping models were developed to reduce the number of reaction kinetics, namely a discrete and a continuum lumping model. These models were applied on three different problems.

In the first case study, a continuum model was developed for a mixture of n-paraffins (waxes) produced from the Fischer-Tropsch process; the paraffins range from C_5 to C_{70} and undergoing catalytic hydrocracking. The model was run with two types of the reactant-type distribution functions to describe the yield of products from the isomerisation and cracking reactions. The model was used to study the effect of the operating conditions on the model parameters and the yield composition. Experimental data were used to optimise the model parameters. The optimal parameters were used to predict the product distribution of n-paraffins hydrocracking and their conversion. The new in this case study was used the carbon number as label in the continuum lumping model and to study how the effect of D(k) on the yield distribution. Good agreements have been obtained when running the model with D(k) employed a gamma function but it needs more time to solve the model than when employing a power law relation for D(k).

In the second case study, both primary and secondary reaction kinetics of the pyrolysis of lignin were investigated by using the discrete lumping methodology. Two mathematical models were developed which consider the product as three lumps whilst the lignin was assumed to be an additional lump. The model's results were validated against experimental data. In addition, a continuum lumping model was developed for the cracking of the tar to obtain lighter components. The novelty in this case study is to develop a kinetic model including primary and secondary reaction kinetics for the pyrolysis of lignin in a fluid bed pyrolyser and to study how the continuum lumping model for tar can be linked to the discrete lumping model.

In the third case study, a model based on the continuum lumping approach was proposed to predict the molecular weight distribution of polymers during batch polymerisation. The result obtained from a continuum model was assessed, at this stage, only qualitatively; nevertheless, by analysing the weight distribution and the average of such distribution, conclusions were reached to assess the predictive capability of the lumping methodology. It is the first time that the continuum model with a yield distribution function is used to predict the molecular weight distribution of the polymerisation at various times.

DEDICATION

This thesis is dedicated to my Parents, my wife, my brothers and sisters, who have supported me through this period of study.

DECLARATION STATEMENT

ACADEMIC REGISTRY

Research Thesis Submission

Name*:*	Mustafa Adam		
School/PGI:	School of Engineering and Physical Sciences		
Version: *(i.e. First, Resubmission, Final)*	First	Degree Sought (Award **and** Subject area)	**PhD** in Chemical Engineering

Declaration

In accordance with the appropriate regulations I hereby submit my thesis and I declare that:

1) The thesis embodies the results of my own work and has been composed by myself
2) Where appropriate, I have made acknowledgement of the work of others and have made reference to work carried out in collaboration with other persons
3) The thesis is the correct version of the thesis for submission and is the same version as any electronic versions submitted*.
4) my thesis for the award referred to, deposited in the Heriot-Watt University Library, should be made available for loan or photocopying and be available via the Institutional Repository, subject to such conditions as the Librarian may require
5) I understand that as a student of the University I am required to abide by the Regulations of the University and to conform to its discipline.

* *Please note that it is the responsibility of the candidate to ensure that the correct version of the thesis is submitted.*

Signature of Candidate*:*		Date:	

Submission

Submitted By *(name in capitals):*	MUSTAFA ADAM
Signature of Individual Submitting:	
Date Submitted:	

For Completion in the Student Service Centre (SSC)

Received in the SSC by *(name in capitals):*			
Method of Submission *(Handed in to SSC; posted through internal/external mail):*			
E-thesis Submitted **(mandatory for final theses)**			
Signature:		Date:	

ACKNOWLEDGMENTS

I would like to thank my supervisor Prof. Raffaella Ocone for providing me the work on such a scientifically interesting project and I would like to express my sincere gratitude for her help, guidance and support in this research. The scientific discussions with her have always been very insightful and I will always be indebted to her for all knowledge she shared with me. She always assisted me with all technical and non-technical issues during this research. Her encouragement and interest led this work to be completed successfully in a timely manner. Special thanks to my second supervisor Dr Arrighi Valeria for all help and support.

Last but not at the least, I would to express my warmest regards to my wife and my family members for their unconditional love and support without which I could have never completed this dissertation.

TABLE OF CONTENT

Contents

LISTS OF FIGURES

LISTS OF TABLES

NOMENCLATURE

Symbols

A	Constant
B	Constant
C	Constant
D	Constant
E	Activation energy
C_i	Carbon number of the species i
C(t)	Concentration of the lump
D(k)	Species-type distribution function generic spices in mixture
L	Length chain
L_l	Longest chain
Ls	Shortest chain
N	Total number of species
P	Pressure, bar
P_0	Reference pressure, bar
R	Gas constant
T	Temperature, K
T_0	Reference temperature, K
W	Molecular weight
a_0,a_1	Model parameters
c_0	Total initial concentration or Initial Concentration
c(k,t)	Continuous concentration-reactivity function at time t

$c(w,t)$	concentration of reactant with molecular weight w, at time t in the continuous mixture
h	Plank's constant, J S/molecule
h(x)	Distribution function
k	reaction rate constant, h^{-1}
k_0	Pre-exponential factor, h^{-1}
k_G, k_T, k_C	Rate constant for Gas, Tar and Char from lignin, s^{-1}
k_{GT}	Rate constant for Gas from Tar, s^{-1}
kB	Boltozmann constant, J/K
k_{max}	rate constant of species with longest chain or highest molecular weight, h^{-1} or s^{-1}
M_N & M_w	Number average and weight average molecular weight
p(k,K)	Yield distribution function
p(W,w)	Yield distribution function
q	Model parameter
t	Resistance time, t=1/WHSV
t_v	Gases vapour resistance time
S_0	Constant
x_i	Weight fraction of reactant of type i
w_l, w_G, w_T, w_C	Weight fraction of Lignin, Gas, Tar and Char

Greek letters

Θ	Normalised length chain or molecular weight
α	Model parameter
η,ζ	Model parameter
Γ	Gamma function

Abbreviations

CCD	Central Composite Design
CN	Carbon Number
CSTR	Continuous Stirred Tank Reactor
FB	Fluidised Bed
FCC	Fluid catalytic cracking
FID	Flame Ionization Detector
FT	Fischer-Tropsch
GC/MS	Gas Chromatograph/Mass Spectrometry
HDM	Hydrodemetalization
HDN	Hydrodenitrogenation
HDS	Hydrodesulfurization
HS	Hydride shift
ICFAR	Institute for Chemical and Fuel from Alternative Resources
ID	Internal Demeter
LIK	Langmuir Isotherm dominated Kinetics
LPG	Liquid Petroleum Gas
MCR	Micro-Carbon Residue
MD	Middle Distillate
MFD	Mechanical Fluidised Bed
MS	Methyl Shift
MW	Molecular Weight
PCP	Protonated CycloPropane
PRF	Plug Flow Reactor
PRK	Primary Reaction Kinetic
PSRK	Primary and Secondary Reaction Kinetic
TBP	True Boiling Point

VGO	Vacuum Gas Oil
VLE	Vapour Liquid Equilibrium
WHSV	Weight Hour Space Velocity

LIST OF PUBLICATIONS DURING THIS STUDY

Journal Papers:

- Adam, M., Calemma, V., Galimberti, F., Gambaro, C., Heiszwolf, J., Ocone, R. (2012).”Continuum lumping kinetics of complex reactive systems”. Chemical Engineering Science, **76(**9): 154-164.
- Adam, M., Arrighi, V., Ocone, R. (2012). “Continuum lumping modelling for step growth polymerisation mechanism”. Chemical Engineering Research and Design. **90**(12): 2287-2292.
- Adam, M., Ocone, R., Mohammad, J., Berruti, F., Briens, C. (2013). “Kinetic Investigations of Kraft Lignin Pyrolysis”. Industrial & Engineering Chemistry Research. **52**(26): 8645-8654

Conference Presentations:

- M. Adam, V. Arrighi, R. Ocone, “Continuum Lumping Modelling for Polymerisation Kinetics”, AIChE Annual Meeting, Minneapolis, October 2011.
- M. Adam, J. Mohammad, F. Berruti, C. Briens, R. Ocone, “Pyrolysis of lignin: Discrete and Continuum Lumping Kinetics Applied to Experiments in a Mechanically Fluidised Reactor”. 21st Conference on Fluidised Bed Combustors, June 2012, Napoli, Italy.
- R. Ocone, M. Adam, F. Berruti, C. Briens, “Pyrolysis of Lignin”, AIChE Annual Meeting, Pittsburgh, November 2012.
- M. Adam, R. Ocone, C. Briens, F. Berruti, “A strategy for kinetic parameter estimation in the pyrolysis of lignin”, BioEnergy IV, Otranto, Italy, June 2013.

Other achievements:

- Win the poster competition for first year PhD.

CHAPTER 1.

Preface

1.1 Introduction

Models are an integral part of any type of industrial activity. The most scientific and technically useful models are expressed in mathematical terms. Models can rely on relatively few equations or present greater complexity. One of the most important features of a model is to achieve agreement between the model predictions and the modelled experimental data. A model may be used as a predictive tool for design and control and/or used for process optimisation. In the chemical reaction arena a mathematical model can attempt to describe the thermodynamics, the kinetics or the combined kinetic and thermodynamic aspects of the system under scrutiny. Mathematical models can give a deeper understanding of complex chemical reaction kinetics, particularly in mixtures with large number of compounds.

Ideally a kinetic model, describing a given reactive system, should include all the reactions that each single component in the feed undergoes. Kinetic models mainly rely on the rate of reaction and its dependence on the other variables such as temperature, concentration and pressure. Models for the chemical kinetics can provide an essential tool to understand the mechanisms of chemical processes. When dealing with mixtures of many components, the kinetic model should take into account all the reactions which the components in the reactive mixture undergo, while in reality this is a difficult task due to the complex chemistry and to the lack of kinetic data. To solve these problems, researchers have proposed two mains approaches to model the kinetics of multi-component mixtures: lumped and detailed molecular models. And a model simplification and order reduction are becoming central problems in the study of complex reaction systems by the researcher. The reduced system should be simpler mathematically and contain fewer unknown parameters than the full model. System reduction can involve both the reactive mechanisms and the dimensions (i.e. number of components) of the system. In reducing a system to one of lower dimensionality, it may follow rules based on experience, trial and error or based on mathematical constraints.

Mathematical rules guarantee the condition under which the reduction is carried out and they can furnish insights into the range of validity of the results obtained. Okino and Mavrovouniotis (1998) have reported three different methods that can be used to carry out system reduction: i) lumping, ii) sensitivity analysis, and iii) time-scale analysis. In the lumping reduction, the original variables are transformed to a lower dimensional vector. The transformation based on physical properties or on the reactivity of the compounds. Sensitivity analysis reduction system seeks to determine and eliminate species and reactions based on their impact on designated important species. Time-scale analysis reduction system focuses on generating non-stiff reduced models.

A lumped kinetic model is one of the ways to treat a large and complex reaction mixture containing a large number of reacting components. In general, most lumped kinetic models have been developed usually along two lines: the first is called partition-based lumping and the second is called total lumping. In the partition–based lumping models, a reaction mixture is partitioned into a finite number of kinetic lumps and the reactions among them are tracked; in the total lumping models all reactions are lumped into a single pseudo-species. By lumping the reactive species into a lower number of imaginary groups the dimensionality of the problem is reduced. In simple terms, lumping is based on the reduction of the number of components of the complex mixture into a lower number of representative components still able to describe the behaviour of the original mixture. The problem with the lumping methodology is that it is not able to describe in detail the kinetic behaviour of each individual component of a complex mixture. However, in general, one is often interested only in some lumped quantities which are easily amenable to measurements, for example the total concentration of a whole class of components, or the total selectivity of a reaction network. Consequently, lumping models can be a powerful tool to describe the simplified problem.

1.2 Aim of the work

The thesis is aimed at assessing the descriptive capabilities of the lumping methodology with particular emphasis to the continuum lumping theory. The appropriateness of the lumping methodology is investigated by studying the kinetic behaviour of three selected problems, namely hydrocracking of paraffins, pyrolysis of biomass and batch polymerisation.

1.3 Motivation of this research

This session presents a brief introduction of the three case studies selected and identifies how the lumping methodology is applied to the problems at hand.

It should be pointed out that these three case studies, i.e., understanding and modelling the kinetics reaction of the components in the complex mixture for designing a new reactor and to control the reaction inside the reactor can be done by lumping methodology.

CASE STUDY (I) - Hydrocracking of Paraffins

The Fischer-Tropsch (FT) process leads to the formation of a range of n-paraffins (>90%) with small percentages of alcohols and olefins. The FT products are characterised by a wide distribution of molecular weights which can be described through the Anderson-Schulz-Flory model (Dry, 2002). A large fraction of FT products is characterised by a boiling point higher than 370 °C (waxes), and those products are a suitable source for the production of high quality transportation fuels such as diesel. Another fraction consists of middle distillates (MD) (150-370 °C) having very poor cold flow properties (i.e. high melting point) that hampers their use as a transportation fuel. The hydrocracking process leads to an increase of MD yields and to the formation of iso-paraffins. Iso-paraffins have a strong influence on cold flow properties of the product as well as on the cetane number (Calemma et al., 2005; Collins et al., 2006).

The hydrocracking reaction of n-paraffins over bifunctional catalysts has been studied intensively by Martens et al. (1986) and Schulz and Weitkamp (1972). Weitkamp (1982) investigated the product distribution and the isomer composition of long chain on a Pt/Cay zeolite catalyst. Later, Froment and co-worker (1987) developed “lumped kinetic models” for the hydrocracking studying the reaction of different pure n-paraffins. In these models, the reaction products were divided into main classes, or lumps, which correspond to n-paraffins, iso-paraffins and cracked products (Baltanas, et al., 1983).

An alternative approach, which is presented in this study, is the continuum lumping methodology. In this study the continuum lumping methodology is applied to a mixture of n-paraffins (waxes) ranging from C_5 to C_{70} undergoing catalytic hydrocracking. A large number of reactions take place in the catalytic reactions of n-parafins, such as dehydrogenation reactions, isomerisation reactions, cracking reactions, and hydrogenation reactions. A continuum lumping kinetics model is shown to be appropriate to describe the yield of components produced from the isomerisation and cracking reactions. The model relies on assuming that the isomers form a single lump (for example, n-C_{14} and iso-C_{14} are considered as a one lump) and the dehydrogenation and hydrogenation reactions are ignored. In reality, the n-paraffins react along two consecutive reaction pathways, where the normal paraffins are first isomerised into mono-branched isomers which undergo subsequent isomerisation steps and cracking reaction according to the scheme below:

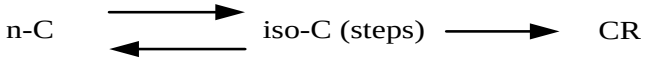

Figure 1.1. n- paraffin hydrocracking reaction mechanism.

In this work, the intermediate step (Fig. 1.1) is ignored; this is a consequence of the fact that in this study the carbon number was chosen as the label that univocally identify the components within the mixture; such label cannot distinguish between isomers (more on the labelling of the components will be said in Chapter three). The continuum lumping kinetics model has been already applied to the hydrocracking of heavy oil fraction based on true boiling point as a label and it has been shown that it well describes the observed experimental data (Elizalde, et al., 2009).

CASE STUDY (II) – Pyrolysis of Lignin

Lignin is an organic polymer and it is the second most abundant renewable carbon source on earth, after cellulose. Lignin is not a single compound but many complex polymers; the commonality between all of them is their phenylpropane structure, that is, a benzene ring with a tail of three carbons. In their natural unprocessed

form, the lignin molecular weight may reach 15000 or more. The utilisation of lignin (biomass) as a renewable energy source is considered as a solution to environmental problem and the security of energy supply (Xu, et al, 2011).

From the description of some of the available kinetic studies, it appears evident that the detailed mechanisms for the pyrolysis of lignin are difficult to detect and assumptions are made to simplify the rather complex reaction network. Nevertheless, in many practical applications, one is interested in the formation of the product yield and knowledge of the apparent reaction kinetics can be sufficient for practical purposes. Based on the consideration that the lumping methodology has been successfully used in modelling the kinetics of complex reactive systems (e.g. Astarita and Ocone, 1988) and wood pyrolysis (Thurner and Mann, 1981), three models are proposed in this study for the pyrolysis of lignin. Two discrete lumping models are developed to describe the kinetics of primary and primary and secondary reactions of pyrolysis of Kraft lignin. Subsequently, a continuum model is developed to describe the upgrading (fractionation) of the produced tar. In this study, the following aspects were considered:

a) Experimental investigation of the pyrolytic characteristics of simulated Kraft lignin.

b) Acquisition of the kinetic parameters of the pyrolytic reaction of the lignin.

It should be noticed that this second case study is different from the previous one, since it introduces the discrete lumping procedure alongside the continuum lumping one.

CASE STUDY (III) – Batch Polymerisation

This case study has been selected for its intrinsic difference from the previous case studies: whilst those deal with the breakage of long chain components, here the creation of longer chains is considered. This choice is dictated by the objective for investigating the flexibility of the lumping methodology, and therefore to see whether the continuum lumping model could be used to predict the molecular weight distribution for polymerisation.

Polymers are usually characterised by a high molecular weight. Depending on the kinetic mechanism, polymerisation reactions proceed by a step growth or chain growth process (Cowie and Arrighi, 2008). In this thesis, the kinetics of polymerisation is considered; the study does not consider other aspects of the problem such as reactor type or heat and mass transfer. The aim has to develop a model based on the continuum lumping approach to predict the molecular weight distribution during polymerisation and to assess the suitability of continuum lumping approach in polymerisation. The study focuses on the step growth polymerisation only, since we think that the underlying kinetic mechanism is amenable to be described through a continuum lumping procedure. The use of continuum modelling in polymerisation was applied by McCoy and Madras, (2001); however the use of a yield distribution function, as presented in this work, is novel. The method of employing a yield distribution function was first introduced to describe the hydrocracking of an oil cut (Laxminarasimhan et al, 1996) and was shown to give good predictions for the distribution of cracked products at various times. In polymerisation, the feed is very well characterised and therefore, the validity of the modelling procedure can be tested without any uncertainty related to the characterisation of the feed composition, as is the case in hydrocracking; consequently, polymerisation will furnish a more precise way to assess the predictive capabilities of yield function.

1.4 Objectives

The following objectives will have to be met for the three case studies selected:

I) *CASE STUDY (I)*:

a) Develop a model for the hydrocracking of a mixture of n-paraffins (waxes) with a wide range of molecular weight (from C_5 to C_{70}); most efforts to develop this model have depended on continuous lumping in which the feedstock is divided into several lumps based on carbon number.

b) Examine how the reactants influence the solution from the model. Specifically, this point is investigated by referring to a function, D(k) introduced by Chou and Ho (1988) which is responsible for the characteristic of the feedstock.

c) Validate the model against the experimental data.

d) Evaluate the effect of the operating conditions (such as temperature, pressure, weight hour space velocity, and feed hydrogen ratio) on the model parameters.

II) *CASE STUDY (II)*:

a) Develop a discrete model for lignin pyrolysis to determine the reaction rate parameters and to identify the composition of the pyrolysis products.
b) Validate the model against experimental data.
c) Apply the continuum lumped kinetics model to the upgrading of the tar produced from lignin pyrolysis. Evaluate the effect of weight hour space velocity and kinetic rate constant on the molecular weight distribution.

III) *CASE STUDY (III)*

a) Develop a continuum kinetics model which could predict the molecular weight distribution of the polymer at various times.
b) Study how the yield distribution function can be extended to polymerisation.
c) Evaluate the effect of the rate constant and weight hour space velocity on the yield product.

1.5 Structure of the thesis

The thesis consists of a total of six chapters. Chapter one gives a brief introduction to kinetics mathematical modelling and to the aims of the project.

Chapter Two gives a review of the literature on lumping methodology and system reduction, including the model formulation and a description of the system reduction.

Chapter Three introduces the kinetic model developed for the hydrocracking of paraffins (waxes) and explains the mathematical procedures for determining the model parameters. The experimental procedure utilised for obtaining the data used for the model validation is introduced as well. Validation of the model parameters are

presented for different experimental conditions such as temperature, pressure, weight hour space velocity and hydrogen to feed ratio.

Chapter Four presents the kinetic approaches developed for modelling the pyrolysis of Kraft lignin and explains the mathematical procedures for the determination of the kinetic parameters that describe the primary and secondary reactions. The experimental procedure and results are presented in this chapter too.

Chapter Five presents the continuum lumping modelling for step growth polymerisation mechanism and the results from the model. An investigation on how the reactivity of the components and the reaction time affect the components yield distribution is also presented.

Finally, Chapter Six summarises the thesis conclusions and addresses the future work.

CHAPTER 2.

Literature Review

In this chapter, a literature review on kinetic modelling of complex reaction system and model application is presented. Some system reduction methods discussed in this chapter are used for the formulation of the model for the kinetic reaction presented in the next chapters.

2.1 System reduction and lumping methodology formation

In a number of industrial processes the feedstock is constituted by a large number of chemical species in measurable quantities. Each of these species can undergo a large number of reactions. Precise kinetic studies should take into account all the reactions that each single component in the feedstock undergoes; in practice, this is a difficult task due to the complex chemistry and to the lack of kinetic data. Different methods have been used to describe the hydrocracking process and they have been recently reviewed by Ancheyta et al. (2005). The main four strategies that have been published for modelling order reduction are: a) lumping (discrete and continuous lumping approach), b) single-event kinetic method, c) sensitivity analysis, and d) Time-scale analysis (Okino et al., 1998).

Ho (2008) gave an overview of mathematical methods available for the system mathematical reduction. In general, an isothermal system can be described by a set of differential equations expressing the mass balance equation as following:

$$\frac{dC}{dt} = f(C)\ ,\ C(0) = C_f \tag{2.1}$$

where (C_f) is the vector of the feed concentration , f is the function that in general represents the sum of concentrations of the elementary reaction that the system undergoes and t is the space time for a plug-flow reactor or for a batch reactor. If the number of reactions is R, then:

$$f = \sum_i^R v_i r_i(C) \tag{2.2}$$

where v_i and r_i are the stoichiometric vector and the reaction rate of the ith elementary reaction respectively. The goal is to reduce the dimensionality of the system by introducing a new system of equations that can mimic the behaviour of the original system. If the system is first order, then $f = -Kc$, where K is the $n \times n$ matrix of rate constants k_{ij}. The equation 2.1 becomes:

$$\frac{d\hat{c}}{dt} = \hat{f}(\hat{c}; \hat{k}), \qquad \hat{c}(t_0) = \widehat{c_0} \tag{2.3}$$

Where $\hat{c}$ is the species vector in the reduced model (dimension of matrix in reduced model $\hat{n}$ < dimension of matrix in original model n), $\hat{k}$ is the vector of rate constants in the reduced system, and $\hat{f}$ is the kinetics vector.

2.1.1 Lumping

Lumping is one of the methodologies used to reduce a large reactive system to a much simpler and more tractable one. A reactant vector (such as species concentration vector and rate constant vector) is transformed into a lower dimensional vector of pseudo-species so that the kinetic equations become easier to solve and fewer parameters need to be determined experimentally. This methodology relies on identifying the individual components of the mixture through properties such as the true boiling point (TBP), the carbon number (C), and/or the molecular weight (MW). Lumping models have been developed along two lines: partition-based lumping and total lumping (Ho, 2008). In the partition-based lumping the reaction mixture is partitioned into a finite number of kinetic lumps and the reactions among them are

tracked. Each lump often contains reactants that have similar chemical or physical properties. However, in total lump, all reactants are lumped into a single pseudo-species, whether the reactants have similar physicochemical properties or not. If all reactions are assumed to be first order the concentration of the total lump at time t can be calculated by:

$$C(t) = \sum_i c_{if} \exp(-k_i t) \tag{2.4}$$

where C_{if} is the feed concentration of the ith reactant and k_i the rate constant. The aim is to predict an overall kinetics $\frac{dC}{dt} = -R(C)$. Complete information on feed properties and reactivity spectra is required to find C(t) and R(C). The main advantage of the lumping technique is that only a small amount of experimental data is required for parameter estimations and the method reduces the number of complex reaction in the system. An example for fluid catalytic cracking (FCC) of gas oil is shown in Fig. 2.1; here the model has ten lumps and 20 reactions based on physical and chemical properties (Jacob et al., 1976). The kinetic scheme in Fig. 2.1 shows that a paraffinic molecule in the P_h lump will form paraffinic molecules in the P_t lump, molecules in G (gasoline) lump and C (gas plus coke)lump. While the molecules in the P_t can only crack to form molecules in G lump and C lump. Likewise, a naphthenic molecule in N_h can crack to form naphthenic molecules in N_l, G and C lumps. The aromatic ring molecules in the A_h can crack to form A_l, C_{AL}, G and C lumps. The aromatic carbon atoms molecules C_{Ah} can crack to form C_{Al} and C lumps. The gasoline cannot form from C_{Ah} and C_{Al}. There is no interaction between the paraffinic, naphthenic, and aromatic groups in this model.

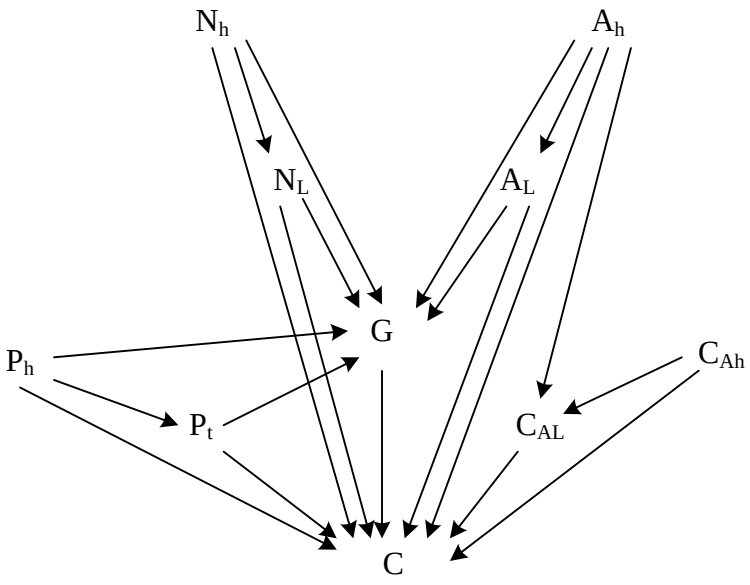

Figure 2.1. Ten-lump kinetic model for FCC. P_h=wt% paraffins, 340°C+; P_t=wt% paraffins, 220-340 °C; N_h=wt% naphthenes, 340 °C+; N_L= wt% naphthenes, 220-340°C; C_{Ah}=wt% aromatic carbon atoms, 340°C+; C_{AL}=wt% aromatic substituent groups, 220-340°C; A_h=wt% aromatic substituent groups, 340°C+; A_L=wt% aromatic substituent groups, 220-340°C; G=gasoline lump (C5-220°C); C= C_1 to C_4 + coke

Lumping implies system reduction by reducing the number of the components in the original mixture and substituting them with pseudo-components or lumps. However, the new system must be able to furnish insights into the dynamics of the components (reactants and yields). The new mixture can behave exactly or approximately as the original one. Under the hypothesis of a monomolecular liner system, the kinetic equation at all possible compositions is given by:

$$d\bar{m}/dt = -\bar{\bar{K}} \times \bar{m} \tag{2.5}$$

where $\bar{m}$ is the vector of the mass m of all components in the mixture and $\bar{\bar{K}}$ is a $n \times n$ matrix of pseudo-kinetic constants. The procedure is exactly the same if concentrations are considered instead.

2.1.1.1 Discrete lumping methodology

The main step in performing discrete lumping consists in developing rules to group each component of the original mixture that lead to a lower dimensionality

system. The "grouping" is performed based on common characteristics, such as true boiling point or molecular weight range of the hydrocarbons, where usually the reactivity of the components and pseudo-components are identified. In this approach, a small number of products and various series and parallel reactions are selected to predict the yields. Model parameters are chosen to fit the experimental data. The predictive performance of the discrete lumping models is quite sufficient for many applications although they are not giving a very accurate predictive power. Success of the discrete lumping models lies in the ease of application and integration into the reactor model, considering the limited number of reactions and participation rate parameters (Lababidi and AlHumaidan, 2011).

Stangeland (1974) developed a discrete lumping approach for the modelling of conversion kinetics in hydrocracing based on ordinary differential equations with a suitable yield distribution function. The yield distribution function is based on the boiling point of each of the pseudo-components that characterize the cut. The model involved three parameters A, B, and C. The parameter A contains the rate constants of the reactions while the yield distribution is controlled by parameters B and C. The assumption of first order kinetics reaction was the main advantage of this model to simplify the model. A three lump model with three reactions for the catalytic cracking of oil gas was proposed by Weekman and Nace (1970), consisting of residue (gas oil), gasoline boiling fraction (C_5- 410 °F), and gas plus coke as one lump. The gas plus coke lump contain in addition to coke, butane and hydrocarbon lighter than butane. In this model two parallel reactions to produce gasoline and gas plus coke and serial reaction to produce gas and coke from gasoline are considered in isothermal fixed, moving, and fluid bed reactors with negligible inter-particle diffusion. They have suggested that for oil gas cracking the rate is to be second order and for gasoline first order. This model was extended to ten lumps with 20 reactions by Jacob et al. (1976). Here the feedstock was divided into paraffins, aromatic rings, naphthenes and aromatic substituent groups in light (473-618 K) and heavy (+618 K) fractions. The gases, gasoline, and coke lumps are the same as in the three lumps model. Yen et al. (1987) and Lee et al. (1989) expanded the three lump model developed by Weekman and Nace (1970) into a four lump by separating the coke and gases lumps. The model involves parallel cracking of gas oil to gasoline, gas, and coke, with following cracking of the gasoline to gas and coke.

Krishna and Sexena (1989) introduced a different approach for hydrocarbon cracking based on the concept of axial dispersion with three parameters. This results in a simple model form with a minimum number of model parameters. The model employed seven lumps: sulphur compounds are considered to be a heavy lump and the other lumps are heavy and light aromatics, heavy and light naphthanes and heavy and light paraffins as presented in Fig 2.2. The pseudocomponents are considered light when they are formed from fractions with boiling points below the cut temperature (T_{cut}). The model was validated against the experimental data and that requires the estimation of kinetic parameters which are then compared with the experimental data. Mohanty et al. (1991) applied the kinetic model that was developed by Stangeland (1974) for a two-stage vacuum gas oil hydrocracker process. The feed and yields were lumped into 23 pseudocomponents and pseudo-homogeneous first order reactions were assumed. Each lump characterised by its boiling range. Ancheyta et al. (1997) presented a strategy for estimating the kinetic constants of a five lumps model in a fluid catalytic cracking (FCC) unit. They divided the gas lump in four lumps scheme into LPG lump and dry gas as in Fig. 2.3. They suggested evaluating the kinetic parameters included in the five lumps model by using three and four lumping model parameters which will be the same for all models.

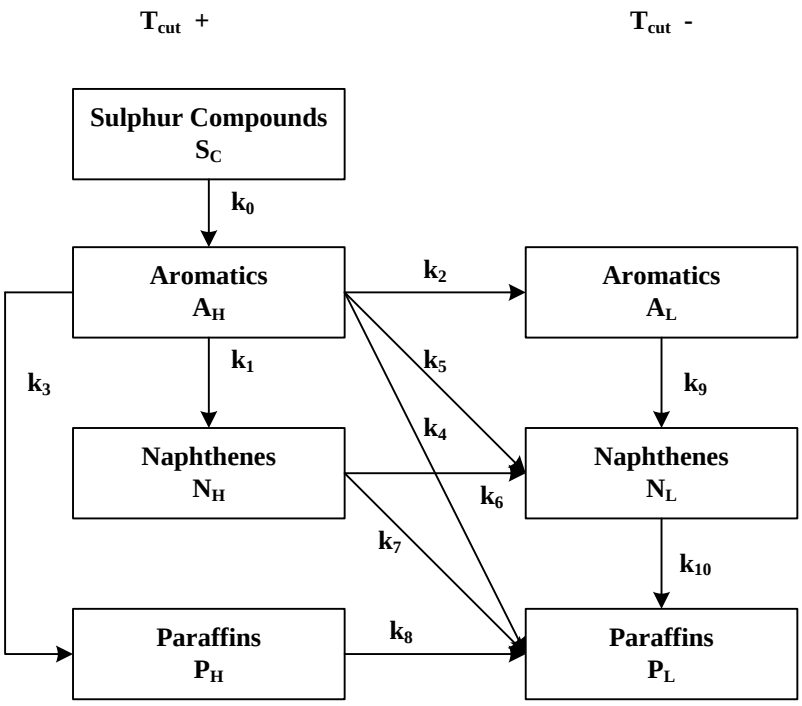

Figure 2.2. Reactive network for hydrocracking proposed by (Krishna and Saxena, 1989)

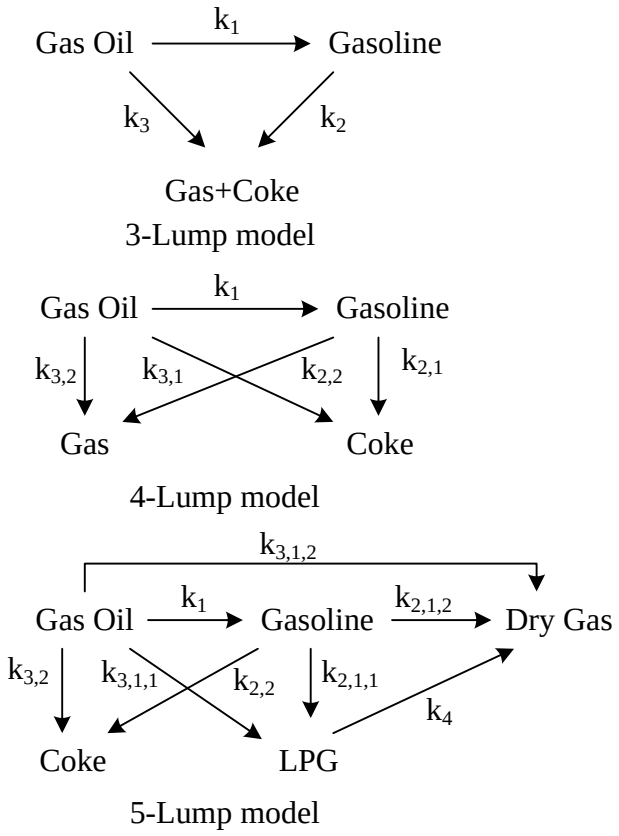

Figure 2.3. Reaction schemes for cracking kinetic lumping models (Ancheyta, 1997)

Later, Ancheyta and Sotelo (2002) applied a discrete lumping technique to the catalytic cracking of vacuum gas oil. The model consists of 6 lumps and 12 reactions (parallel and consecutive). The most important products considered in this model are gasoline (C_5-493 K), C_4's (butane, i-butane and butens), C_3's (propane and propylene), dry gas (H_2, C_1-C_2), coke, and unconverted VOG. The reactive network for the model is presented in Fig. 2.4. A second order reaction was assumed for VOG cracking and the gasoline, C_4's, and C_5's were assumed to crack according a first order reaction. de Almeida and Cuirardello (2005) presented a 5-lump kinetic model for hydroconversion of Marlim vacuum residue. 26 coefficients were estimated for the kinetic model. The reactions between micro-carbon residue (MCR) and easy residue (VReasy) were considered to be reversible, while the other reactions were irreversible. Both thermal and catalytic reactions were considered to occur in parallel in this model. Fig. 2.5 shows the reaction network for hydro-conversion in the model. Another five lumps kinetic model was developed by Bollas et al. (2007) for the prediction of the fluid catalytic cracking (FCC) product distribution. The reactant-products mixture was divided into five lumps according to their carbon number and boiling point range as: gas oil (with TBP in the range of 170 - 510 °C), gasoline (C_5-221 °C), liquefied product gas (C_3 –

C_4), dry gas ($C_1 - C_2$, H_2, and H_2S) and coke. The paths of catalyst deactivation were studied by this model to improve the product prediction. The model reaction network of catalytic cracking process that assumed by Bollas is presented in Fig 2.6.

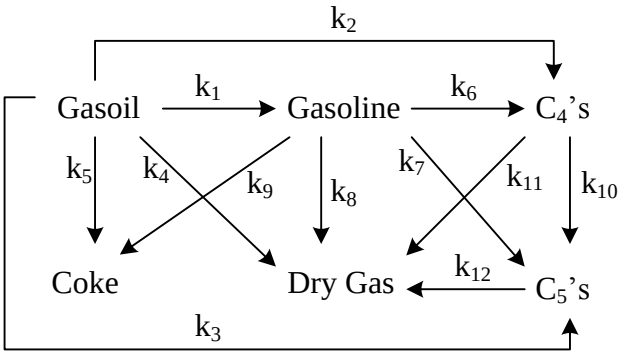

Figure 2.4. Kinetic model proposed by (Ancheyta, 2002)

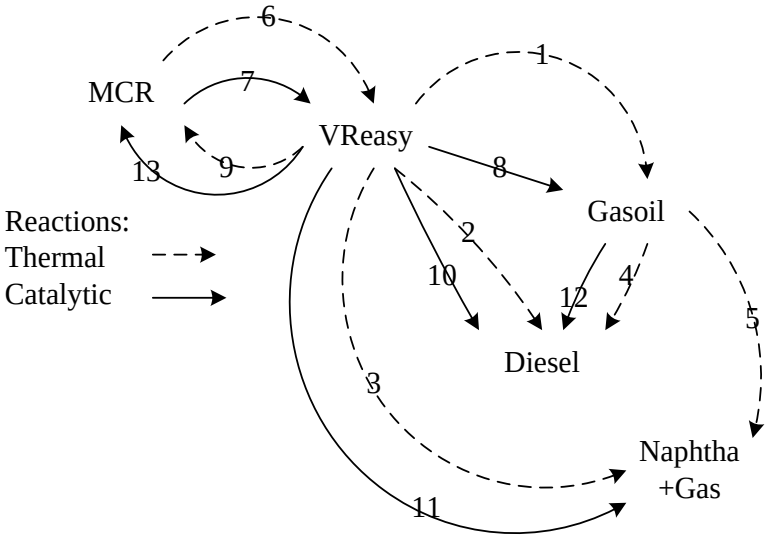

Figure 2.5. Reaction network for hydroconversion (Almeida and Gurirardello, 2005)

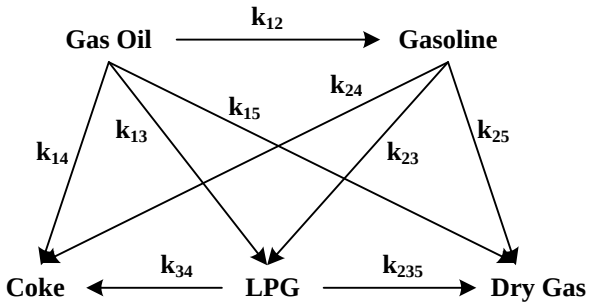

Figure 2.6. Schematic diagram of the five-lump model (Bollas et al., 2007)

Balasubramanian and Pushpavanam (2008) developed a discrete lump kinetic model from continuous kinetics for hydrocracking of vacuum gas oil using true boiling point and carbon number as the basis to identify the hydrocarbon cuts. Isomerisation and cracking are the two typical reactions that were considered by this model to model the hydrocracking process. Three different stoichiometric kernels (random scission, symmetric, and exponential) were used to identify the nature of the reactions and to determine the product yield distribution in the kinetic model. That is, random scission stoichiometric kernel was proposed for both true boiling point and carbon number basis models, exponential form kernel was proposed for the true boiling point basis lumped model, and symmetric kernel was proposed for carbon number basis lumped model. The model considered five lumps (gases, gasoline, kerosene, gas oil and residue) to model the hydrocracking reaction. Later, Krishna and Balasubramanian (2009) provided an analytical solution for the full stoichiometry based discrete lumped kinetic model. In this study, a general true boiling point basis discrete model for hydrocracking was presented to account for the cracking reaction occurring within the lumps. A general full stoichiometry of the hydrocracking reaction was represented as: $C_r \xrightarrow{k_{i,j,r}} C_i + C_j$, where r varies from 1 to N_L, i and j vary from 1 to r, N_L is the number of lumps considered, C_r is the molar concentration of the hydrocarbons present in the lump r, and $k_{i,j,r}$ represents the kinetic constant for cracking of reactant lump r into two products, lumps i and j. The authors assumed that the cracking is a binary process in which only two yields are formed in each cracking reaction. Also, a first order and irreversible cracking reaction were included in the assumptions.

Mazloom, et al. (2009) developed kinetic models for thermal and catalytic pyrolysis of scrap tyres by using a discrete lumping methodology. In this model, the reactant and yield mixture in terms of selected boiling cuts (lumps) were described by a boiling point distribution and the conversion of the heavier to lighter lumps was described in terms of series and parallel reactions. The thermal pyrolysis kinetic model consists of four lumps with four kinetic reaction constants while the catalytic pyrolysis kinetic model consists of five lumps with five kinetic reaction constants. Sadighi et al. (2010) presented a model that describes the hydrocracking of vacuum gas oil in a pilot scale reactor charged with a zelolite-base catalyst using lump first order kinetics. The proposed model divides vacuum gas oil into 4-lumps as: VGO, distillate, naphtha, and gas. The model includes twelve kinetic parameters which should be estimated from experimental data if all pathways of reaction are considered. However, in this study, three route passes and one activation energy coefficient were omitted; thus the number of coefficients was reduced to five. Fig. 2.7 illustrates the process pathways associated in this model. The difference between this model and the previous ones was its consideration of the hydrogen consumption which was implemented in the kinetic model by using a quadratic response surface model that modelled the unit mass of hydrogen consumed per unit mass of converted VGO.

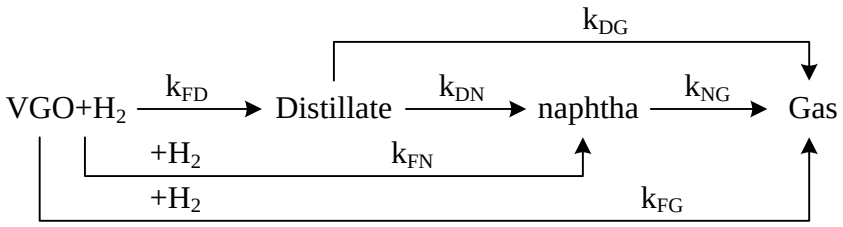

Figure 2.7. 4-lump kinetic model proposed by (Sadighi, 2010)

Discrete lumping methodology treats the components in a complex mixture individually or in groups, and transforms them on the basis of their reactivity (Okino and Mavrovouniotis 1998). The discrete method needs a complete description of the kinetic scheme. . Discrete lumping can be linear or nonlinear. Discrete linear lumping attempts the transformation into the lower order system through matrix operations. This information can be gained from the actual components and reactions, but it is also possible to use discrete lumping to further simplify the system of empirical. For a

system of monomolecular reactions, the linear kinetics of Eq. 2.5 can be written as in terms of concentration of the original system:

$$\frac{d\bar{c}}{dt} = \overline{\overline{K'}}.\bar{c} \tag{2.6}$$

where $\bar{c}$ is the vector on n dimensions of the concentrations and $\overline{\overline{K'}}$ is a square matrix of the rate constants. The diagonal elements of $\overline{\overline{K'}}$ are k_{ii} which represent the sum of the rate constants corresponding to the total consumption of component i, while the other elements are k_{ij} which represents the rate constants of the conversion of component j to component i. If discrete lumping is attempted, and the transformation is linear, lumps should be constructed such that:

$$\bar{c'} = \overline{\overline{M}}.\bar{c} \tag{2.7}$$

where $\bar{c'}$ a vector of dimensions $n' < n$ representing the concentration of the lumped compounds (or pseudo-components) and $\overline{\overline{M}}$ is the lumping matrix of dimension $n' \times n$. Eq. 2.7 represents a Linear Projective Transformation. The system is exactly lumpable if there exists a matrix $\overline{\overline{K''}}$ such that the kinetic behaviour of the lumped system can be described by:

$$\frac{d\bar{c'}}{dt} = \overline{\overline{K''}}.\bar{c'} \tag{2.8}$$

where $\overline{\overline{K''}}$, having dimensions $n' \times n'$.

The lumping is named approximate or exact depended on the solution of the lumping differential equation system does or does not have error compared to that given by the original system (Li et al., 1994).

2.1.1.1.1 Exact lumping

There are two methods of exact lumping to treat the components in a complex mixture: linear and nonlinear kinetics. Linear or nonlinear lumping is employed depending on lumping transformation type. Therefore, if the lumping transformation is linear, it would be called linear lumping otherwise it is called nonlinear lumping.

a) Linear kinetics

Wei and Kuo (1969) derived a necessary and sufficient condition for exact lumping of the linear monomolecular system, whose kinetic behaviour is given by eq. (2.8), to obtain the lumped solution, can be written as:

$$\bar{\bar{M}}.\overline{\overline{K'}} = \bar{\bar{M}}.\overline{\overline{K''}} \tag{2.9}$$

If λ_i are the eigenvalues and x_i are the eigenvectors of matrix $\overline{\overline{K'}}$, the system is lumpable if one of the following two conditions is satisfied:

$$\bar{\bar{M}}.x_i = 0 \tag{2.10}$$

Or

$$\overline{\overline{K''}}.\left(\bar{\bar{M}}.x_i\right) = \lambda_i.(\bar{\bar{M}}.x_i) \tag{2.11}$$

The matrix $\overline{\overline{K''}}$ has only n'' eigenvectors which derive from the eigenvector x_i and they are obtained from $\bar{x}_i'' = \bar{\bar{M}}.x_i$.

Wei and Kuo showed a direct construction of the matrix $\overline{\overline{k''}}$ from eigenvectors and eigenvalues of the matrix $\overline{\overline{k'}}$. By transposing Eq. (2.9), the following relation is obtained:

$$\overline{\overline{K'}}^T.\bar{\bar{M}}^T = \overline{\overline{K''}}^T.\bar{\bar{M}}^T \tag{2.12}$$

Eq. (2.12) says that the mapping of $\overline{\overline{k'}}^T$ on $\overline{\overline{M}}^T$ produces a matrix which remains in the same vector space and then $\overline{\overline{M}}^T$ is an invariant of $\overline{\overline{K'}}^T$. Considering a given eigenvalue, lets say λ_1, the simplest $\overline{\overline{K'}}^T$ invariant subspace can be obtained through the straight line containing x_1 : that $\overline{\overline{K''}}^T . x_1 = \lambda_1 . x_1$ means any vector $\alpha\, x_1$ upon mapping by $\overline{\overline{K'}}^T$ produces another vector $\alpha\lambda_1 x_1$ still belonging to the same straight line. Then, one can seek for $\overline{\overline{K'}}^T$ invariant subspace and $\overline{\overline{M}}$ can be obtained in this way.

b) Nonlinear kinetics

The first extension of the monomolecular (first order reactions) system, which published by Wei and Kuo (1969), to Bimolecular Reaction Systems was performed by Li (1984) who explored the necessary and sufficient conditions for exact lumping. Subsequently Li and Rabitz (1989) extended the methodology to nonlinear reaction systems using invariant subspace of the reaction system. The equations of the exactly lumped system would be:

$$\frac{d\bar{c'}}{dt} = -\overline{\overline{M}} . f(\overline{\overline{M'}} . \bar{c'}) \tag{2.13}$$

where $\overline{\overline{M'}}$ is one of the generalized inverses of $\overline{\overline{M}}$ satisfying

$$\overline{\overline{M}} . \overline{\overline{M'}} = \overline{\overline{I_{n'}}} \tag{2.14}$$

$\overline{\overline{M'}}$ does not affect the form of the lumping equation in the exact case.

In the case of non-linear kinetics, the necessary and sufficient condition for exact lumping of a nonlinear kinetic is that the transpose of the Jacobian matrix of $f(\bar{c})$, $\overline{\overline{J}}^T$, has non-trivial common invariant subspaces M. The lumping matrix $\overline{\overline{M}}$ is then constructed with the basis vectors of M. The conclusion which can be drawn at this point is that the system is exactly lumpable depends on $\overline{\overline{M}}$ and $\bar{f}$.

To find a lumping matrix, the nontrivial invariant subspace of $\bar{\bar{J}}^T(\bar{c})$ for the whole composition space should be determined in the first step. Different approaches to determine the nontrivial invariant subspace $\bar{\bar{J}}^T(\bar{c})$ were developed by Li and Rabitz (1989, 1990). One approach showed that the non-trivial invariant subspace of $\bar{\bar{J}}^T(\bar{C})$ can be obtained by decomposing $\bar{\bar{J}}^T(\bar{C})$ in the following way:

$$\bar{\bar{J}}^T(\bar{C}) = \sum_{k=1}^{m} a_k(\bar{c}).\overline{\overline{A_k}} \tag{2.15}$$

where $m < n^2$, a_k are parameters that are function of $\bar{c}$; $\overline{\overline{A_k}}$'s are constant matrices which form the basis of $\bar{\bar{J}}^T(\bar{c})$. One possible way is then to find the common invariant subspace of all $\overline{\overline{A_k}}$'s which are contained in the invariant of the matrix $\sum_{k=1}^{m} \overline{\overline{A_k}}$. At this point, it is worth noting that the transformation dictated by Eq. 2.6 and the transformation for the Jacobian as in Eq. 2.15 are both linear. Consequently, nonlinear kinetics is restricted to invariant subspaces dictated by linear transformations. The optimisation problem and to find $\bar{\bar{M}}$ one needs to solve the following:

$$\min Z(\bar{c}) = tr \sum \bar{\bar{M}}\, \bar{\bar{A}}_k^T \left(\bar{\bar{I}}_n - \bar{\bar{M}}^T\, \bar{\bar{M}}\right) \bar{\bar{A}}_k \bar{\bar{M}}^T \tag{2.16}$$

Subject to $\bar{\bar{M}}.\overline{\overline{M'}} = \overline{\overline{I_{n'}}}$

2.1.1.1.2 Approximate lumping

The aim of approximate lumping is to minimise some measures of inconsistencies between the dynamic of the original and lumped systems (Ho, 2008). The analysis reported in this paragraph is based on the works of Wei & Kuo (1969) and Liao & Lightfoot (1988). Initial conditions play an important role to give a first insight whether exact lumping is possible. Indeed, one can define the lumping error as:

$$\bar{e}(t) = \bar{\bar{M}}.\bar{c}(t) - \bar{c'}(t) \tag{2.17}$$

Differentiating Eq. (2.17) one obtains:

$$\frac{d\bar{e}}{dt} = \overline{\overline{K''}}.\bar{e} - \left(\overline{\overline{K''}}.\overline{\overline{M}} - \overline{\overline{K'}}.\overline{\overline{M}}\right)\bar{c} \tag{2.18}$$

If the lumping is exact, the condition expressed by Eq. (2.9) must be satisfied, implying:

$$\frac{d\bar{e}}{dt} = \overline{\overline{K''}}.\bar{e} \tag{2.19}$$

If the initial condition is $\bar{c'}(0) = \overline{\overline{M}}.\bar{c}(0)$, then $e(t) = 0$ for all t. If $\bar{c'}(0) \neq \overline{\overline{M}}.\bar{c}(0)$, $e(t)$ decays rapidly to zero.

In most practical applications, it is very likely that $\overline{\overline{M}}.\overline{\overline{K}}' \neq \overline{\overline{K}}''\ \overline{\overline{M}}$; however, lumping is still possible and one has to define the acceptable degree of approximation. In general, one needs to look at the error function and then aim to find error very close to zero for all t.

Li and Rabitz (1990) developed a general treatment of approximate lumping and proved that the error of the approximately lumped model depends on the choice of $\overline{\overline{M}}$ and $\overline{\overline{M'}}$, if Eq. (2.13) is still applied to describe the approximately lumping system. $\overline{\overline{M}}^T$ is proven to be a good choice for $\overline{\overline{M'}}$ when $\overline{\overline{M}}$ has orthonormal rows. To simplify the lumping model $\overline{\overline{M}}$ is required to have orthonormal row i.e,

$$\overline{\overline{M}}.\overline{\overline{M}}^T = \overline{\overline{I_{n'}}} \tag{2.20}$$

when $\overline{\overline{M}}^T$ is chosen for $\overline{\overline{M'}}$

Li et al. (1994) developed a method which is inherently a non-linear lumping procedure for a chemical kinetic system. Successively, incorporation of time-scale separation techniques were developed (Li et al, 1993). In general terms, the formulation

of the nonlinear lumping procedure starts by defining a new way to lump the concentration.

$$\hat{c} = H(c) \tag{2.21}$$

Then, with the definition given in Eq. (2.21) the reaction, Eq. (2.8), becomes:

$$\frac{d\hat{c}}{dt} = H_c[\bar{H}(\hat{c})\,]f[\bar{H}(\hat{c})] \tag{2.22}$$

where H_c is the Jacobian matrix of H and $\bar{H}$ is the generalised inverse of H, satisfy the relation:

$$H.\bar{H} = I_{n'} \tag{2.23}$$

This procedure defines a nonlinear projective transformation.

To avoid difficulty to find a reliable method to attempt the transformation of H and $\bar{H}$; Li et al. showed that when a system of reaction, Eq. (2.6) can be separated along time scales into:

$$d\bar{y}/d\tau = f^1(\bar{y}, \bar{z}; \bar{k}) + \varepsilon f^2(\bar{y}, \bar{z}; \bar{k}) \tag{2.24}$$

$$d\bar{z}/d\tau = g^1(\bar{y}, \bar{z}; \bar{k}) + \varepsilon g^2(\bar{y}, \bar{z}; \bar{k}) \tag{2.25}$$

where $\bar{y}$ and $\bar{z}$ are the vectors of concentrations reacting along the slow and fast time scales respectively. f and g are operators and ε is a small positive parameter which arises due to the separation between the magnitudes of reaction rates in a chemical system. ε is defined based on the fast time variable τ, as $\tau = t/\varepsilon$.

Approximate nonlinear lumping can be attempted by transforming the original system of reaction, Eq. (2.6) in terms of a series containing the small perturbation parameter:

$$\frac{dc_i}{dt} = f_i(\bar{c}) = Ac_i \qquad i = 1, \dots, n \tag{2.26}$$

where the operator A is defined as:

$$A = \sum_1^n f_i(\bar{c}) \frac{\partial}{\partial c_i} \tag{2.27}$$

Limitation of the method lies in the need to know the relative time scales of the reactions a priori, as it depends on the proper introduction of ε.

2.1.1.2 Continuous lumping methodology

In contrast to the discrete lumping, the continuum lumping assumes that the properties of each individual component (e.g., reactivity, concentration, volatility) are described through suitable component indexes, for example the boiling point or the molecular weight. Continuum lumping models carrying the best predictive capabilities for product yield from discrete lumping models and, therefore, are a step toward recognizing the chemical and physical properties of the diversity of heavy hydrocracking feedstock. The continuum approach is only one of the methodologies which have been attempted for describing a complex reactive mixture of various components, all undergoing similar types of reactions, e.g. cracking, pyrolysis, oligomerisation, etc. When the mixture has an infinite number of species, it becomes impossible to identify the species individually, but a distribution of species can be identified. The continuous lumping may be particularly convenient when a large number of species is involved and they are measured in a continuous fashion, e.g. in a chromatogram or a boiling point curve. In continuous lumping, it is convenient to introduce an index, *x*, and to identify the "species" $A(x)dx$ as the sub-mixture whose index (e.g. retention time, boiling point etc.) lies in the range $(x, x + dx)$. In other

words, some sort of "lumped" reactants to the real mixture and their collective behaviour is determined. As an example, in the hydrodesulfuration of oil cut, one is not interested in the individual sulphur species, but only in the reduction of the total sulfur content, and therefore the overall hydrodesulfuration kinetics is of interest. It is important to notice that the label is continuous variable, and therefore one is not constrained to take values that are integers.

The theory for treatment of a complex mixture as a continuous one was first developed by De Donder (1931). He analysed the general scheme for ethane hydrogenolysis and showed that the overall rate of reaction can be described in terms of lumped reactions relating the information of stable adsorbed C_2H_x species and transition states from gas-phase ethane and dihydrogen. Acrivos and Amundson (1955) applied the notion of the continuous mixture on distillation. This idea has been applied to polymerisation too by Zeeman and Amundson (1965). Aris and Gavalas (1966) presented mathematically the description of continuous mixture where the continuous description is introduced for polymerisation and cracking reactions

Aris (1968) extended the methodology considering specific kinetics of reactions in continuous mixtures. This methodology was applied to solve the problem where all the reactions are first order and irreversible. In his description the index (or label) x is taken as a positive number and a function $c(x)$ can be defined in the interval $[0, \infty)$ so that $C(a,b) = \int_a^b c(x)dx$ is the total concentration of the material with index in the interval (a,b). Because the reactions are irreversible, the derivative of the concentration with respect to retention time $c(x,t)$ is negative unless $c(x,t)$ is zero. And since the reactions are first order, the only relevant parameter of any species x is the kinetic constant $k(x)$ that can be written as $k'x$ where k' is the average value of $k(x)$ at t equal to zero. Therefore, the kinetic equation of rate of reaction $r(x,t)$ in a batch (or PFR) reactor has the form:

$$-c_t(x,t) = r(x,t) = xc(x,t) \tag{2.28}$$

This integrates to:

$$c(x,t) = c(x,0)e^{-xt} \tag{2.29}$$

The total concentration, C(t), can be obtained by integrating Eq. (2.29) over all components:

$$C(t) = \int_0^\infty c(x,0)e^{-xt}dx \tag{2.30}$$

That is, $C(t)$ is the Laplace transform of $c(x,0)$, with the dimensionless time t playing the role of the transform parameter. For the overall rate consumption, $-\frac{dC}{dt}$ is given by the first moment of $c(x,t)$:

$$-\frac{dC}{dt} = \int_0^\infty xc(x,0)e^{-xt}dx \tag{2.31}$$

Ho and Aris (1987) followed the same methodology to consider non-first order kinetic reactions. The above methodology does not extend directly to systems that are not first-order; this problem is often indicated as the single component identity (SCI). The SCI requirement is that, when all components in the mixture have the same values of the kinetic parameters, the lumping and unlumping descriptions have to coincide with each other. The mathematical form, which only satisfies for linear kinetics, of the SCI requirement given by Ho and Aris (1987) is:

$$\int_0^\infty F(\boldsymbol{P}(x), C(0)\delta(x-x^*), t)dx = F(\boldsymbol{P}(x^*), C(0), t) \tag{2.32}$$

where $\boldsymbol{P}$ is the vector of the kinetic parameters (e.g., $k's$). The analytical form of the function $F(\,)$ is determined by the form of the function $\frac{dc}{dt}$.

Astarita and Ocone (1988) gave the first possible method to solve the SCI problem by introducing and clearly taking into account the interactions between reactants for a reaction system. The key assumption is that the kinetics of each reaction

is dependent on the kinetics of each other reaction in the mixture and is called cooperative kinetics. Physically this assumption implies that in a mixture of reactants exhibiting similar chemical behaviour, the rate of disappearance of reactant x is likely to depend on the whole spectrum of concentration $c(y,t)$. The model is written similarly to Eq. (2.28) with the addition of an interaction function, K, as:

$$r(x,t) = xc(x,t)f[K(y)c(y,t)] \tag{2.33}$$

where $f[\,]$ is a function of a weighted concentration distribution function $c(y,t)$. In general the weighting factor $K(\,)$ depends on both x and y, namely $K(x,y)$, however the key assumption of uniformity implies that the kernel K does not depend explicitly on the component label x, then being $K(y)$. This assumption was applied by Astarita and Ocone (1988, 1992) to bimolecular reaction and to catalytic reaction governed by Langmuir isotherm adsorption.

Aris (1989) introduced an alternative approach to resolve the SCI paradox, the so-called bivariate description, labelling each reactant with two variables. The analysis of this approach is carried out in two steps: first order reactions are lumped in the first step to generate nonlinear kinetics which is lumped in the second step.

Chuo and Ho (1988) proposed an approach for continuous lumping of nonlinear reaction by introducing a reaction type distribution function that allows the continuous representation to transform to a discrete representation for kinetics of arbitrary linearity. This approach approximates the finite sum over reactants type i, as an integral over the reactive k. $D(k_i)$ can be used as the Jacobian of the i to k coordinate transformation to define the reaction concentration over an interval Δi to be:

$$C_i(t)\Delta i = c(k_i,t)D(k_i)\Delta k_i \tag{2.34}$$

The total reactant concentration lump can be expressed as:

$$C(t) = \int_0^\infty c(k,t)D(k)dk \tag{2.35}$$

where c(k,t) is the concentration of species k, $D(k)$ is the reactant type distribution function and the term $D(k)dk$ is the total reactant types with k between k and $k + dk$. The distribution function D(k) must be satisfied or normalized so that:

$$\frac{1}{N} \int_0^\infty D(k)dk \approx 1 \tag{2.36}$$

where N is a total number of reactant types

The focal point of the analysis is the appropriate choice of the $D(k)$ when dealing with a mixture of reaction, also the function $D(k)$ plays an important role in defining the condition of volatility of the continuous approach (Ho and White, 1995). The SCI can be easily established for any kinetics, as shown below:

$$C(t) = \int_0^\infty c(k,t)\delta(k - k^*)dk = c(k^*,t) \tag{2.37}$$

where δ is the delta function, which one obtains corresponding to the only reactant present.

Laxminaraasimhan et al (1996) introduced a yield distribution function $p(k,K)$ to address the problem of maximizing the liquid yield in hydrocracking of vacuum gas oil mixture. They assumed the hydrocracking rate constant (reactivity) k to be a monotonic function of boiling point. And $p(k,K)$ determines the amount of species that is formed with reactivity k from the cracking of the species with reactivity K. This function was developed by analysis of experimental data on the yield of hydrocracking reported in the literature. A skewed Gaussian –type distribution function is used to represent $p(k,K)$. In a plug flow-type reactor, the mass balance equation for the components with reactivity k can be expressed with an integro-differential equation in the k-space as follows:

$$\frac{dc(k,t)}{dt} = -k.c(k,t) + \int_{k}^{k_{max}} p(k,K).K.c(K,t).D(K).dK \quad (2.38)$$

The yield distribution function must satisfy the following properties:

a) The value of $P(k,K) = 0\,, \quad for\ k \geq K$, since the species of reactivity k cannot yield to itself upon cracking and since dimerisation and other similar reactions are not significant in hydrocracking.

b) $P(k,K) > 0$ and has a finite, small nonzero value when $k = 0$ because the smallest reactivity components are formed in traces and it should always be a positive value.

c) The function must satisfy the following equation: $\int_{0}^{K} P(k,K).D(k)\,dk = 1$

The mass balance equation is written in the k (reactivity) space. The species type distribution function $D(K)$ accounts for the cracking of all species with reactivity K.

2.1.1.3 Lumping applications

The lumping methodology has been applied to a number of diverse fields such as oil industry and petrochemicals. The goal of the refining process is converting heavy oil into suitable feedstocks for second conversion processes. Catalytic cracking is the most common sub-process in the refining. Both discrete and continuous lumping theory has been applied in oil refining and this is considered a good example for comparing and contrasting the two approaches.

Blanding (1953) studied the conversion of heavy oil to gasoline based on two lumps. The first lump contained all the components that have a boiling point above the gasoline rang (unconverted lump) and the second lump formed by everything else. He assumed the unconverted lump reacts with second order kinetics and each component within the lump reacts with first order kinetics. Weekman and Nace (1970) added gas lump (hydrocarbons have 4 or less carbon atoms) and coke lump to the original system

which studied by Blanding. It was assumed that the feedstock cracking following second order kinetic, whilst the gasoline products degrade with first order kinetics.

Balasubramanian and Pushpavanam (2008) presented a discrete lump kinetic model for hydrocracking from continuous kinetics using carbon number and true boiling point as the basis. Isomerisation and cracking are the typical global reactions which occur in hydrocracking of the VGO. The cracking reactions assumed to be first order, irreversible and isothermal.

Applied the continuous lumping approach in the petrochemical industry is dated back to Ho and Aris (1987), Aris (1989), Aris and Astarita (1989), Astarita (1989), Astarita and Nigam (1989), Astarita and Ocone (1988, 1989), Chou and Ho (1988, 1989), and Li and Ho (1991). Applications and examples are reported in their studies.

The continuous theory provides a unifying framework for gaining insights into a mixture's behaviour and explaining much seemingly peculiar behaviour in catalytic hydroprocessing. Some examples of information that one can gain from a lumping study are as follows (Ho, 2008):

a) The hydrodesulfuration of petroleum typically exhibit an overall order between 1.2 and 3.8, whereas individual sulphur species desulfurises at a first order.
b) High activity catalysts give rise to lower overall order than low activity catalysts.
c) The overall hydrodesulfuration order decreases with increasing the temperature.
d) The overall order for the PFR is higher than for CSTR.

Mazloon et al. (2009) applied two types of lumping approaches (discrete and continuous lumping) on a pyrolysis of scrap tyres. The boiling point distribution of the reactant mixture was used to describe the lumps. In the discrete lumping approach, the conversion of heavy components to lighter was described in terms of series and parallel first order. Elizalde et al (2010) presented a continuous kinetic lumping approach on heavy crude oil and studied how the pressure together with temperature and space

velocity affects the model parameters. Lababidi and AlHumaidan (2011) applied a continuous approach on hydrocracking of atmospheric residue feedstock associated with a hydrotreatment. The hydrotreatment process consists of three types of hydrotreating catalysts [hydrodesulfurisation (HDS), hydrodemetalisation (HDM), and hydrodenitrogenation (HDN)].

2.1.2 Single-event methodology

The single-event method is a structure-oriented approach, which utilises most of the information obtained with modern analytical techniques, and has been proposed for some catalytic processes. The single event model retains all the information of the reaction pathways of the individual feed components and reactions (Froment, 2005). In the single-event model the lumps are defined according to the structure of the reactants in the mixture (Ancheyta, 2005). This method was developed by Froment and co-workers (Baltanas et al., 1989 and Vynckier and Froment, 1991) for modelling complex reaction system.

Baltanas et al. (1989) used a computer algorithm which was devised by Clymans et al. (1984) to generate a network of elementary steps involving carbinium ions for hydrocracking of paraffins, taking into account all the reactions involving each molecule. Due to the molecular approach, the number of kinetic parameters that can describe the kinetic behaviour of the hydrocracking of feedstock is limited. The single-event model was extended by Vynckier and Froment (1991) to complex feedstocks and introduced the explanation of lumping coefficients to formulate rate expressions. Feng et al. (1993) applied the single-event kinetics approach to the catalytic cracking of parafins on RE-Y zeolite catalysts and single-event rate parameters are estimated for the cracking, accounting for the thermodynamic constraints. Svoboda et al. (1995) estimated single event rate coefficients for both isomerisation and cracking reactions of octane on a Pt/Us-Y zeolite catalyst over a wide range of experimental conditions. Schwetzer et al. (1999) validated a single-event kinetic model for cracking the Fischer-Tropsch products to produce very high quality of middle distillate. Martens et al. (2000) used a single event kinetic model for the hydrocracking of parafins (C_8-C_{12}) on Pt/US-Y zeolites catalyst.

Froment (2005) has reviewed the single event model, which takes account of all reaction pathways detail of individual feed components and intermediate reactions. This approach has been applied successfully for many complex reaction systems, amongst which are catalytic cracking of oil fraction, hydrocracking, isomerisation, catalytic reformer, alkylation, methanol-to-olefins, and olefin oligomerisation. Martinis and Froment (2006) applied the single-event kinetics to the alkylation of isobutene with butenes over proton-exchanged Y-zeolites. The number of model parameters reduced from 3130 to 14 when used the single-event kinetics approach.

The first step in the single event approach is to determine all the element steps involved in the various transformations that happen in the reactor. The basic idea of the single-event approach is to link rate constant to molecular structure to reduce the number of rate coefficients, which depend only on the type of reactor and the type of molecule (Surla et al., 2011). Single-event is used to model the frequency factors of the steps happening on the acidic site of the catalyst. In the single-event approach, the effect of molecular structure on the frequency factor is described with transition state theory and statistical thermodynamics. The rate coefficient in the single-event can be formalised as (Shahrouzi, et al., 2008; Kumar, 2006):

$$k = \frac{k_B T}{h} \exp\left(-\frac{\Delta G^{0\#}}{RT}\right) = \frac{k_B T}{h} \exp\left(\frac{\Delta S^{0\#}}{R}\right) \exp(-\frac{\Delta H^{0\#}}{RT}) \qquad (2.39)$$

Where is the k rate coefficient of an elementary step, k_B is the Boltozmann constant (J/K), h is Planck's constant (J. S/molecule), R is the Gas constant (J/mol.K), T is temperature (K), ΔG is the standard Gibbs free energy of reaction, ΔH is standard enthalpy of activation (J/mol), and ΔS is the standard entropy of activation (J/mol. K). According to statistical thermodynamics, the standard entropy of a species is determined by adding the contribution from various motions of the species such as translation, vibration, and rotation.

$$S^0 = S^0_{trans} + S^0_{vib} + S^0_{rot} \qquad (2.40)$$

The rotational contribution (S_{rot}^{0}) is composed of two terms, the intrinsic term ($\widehat{S^{0}}$) and a term due to symmetry number (σ) change, which depends on the geometry of the molecule.

$$S_{rot}^{0} = \widehat{S_{rot}^{0}} - Rln(\sigma) \tag{2.41}$$

Accounting for the effect of chirality, the S_{rot}^{0} is given by:

$$S_{rot}^{0} = \widehat{S_{rot}^{0}} - Rln(\frac{\sigma}{2^{n}}) \tag{2.42}$$

where n is a number of chiral centres in the molecule and the term ($\frac{\sigma}{2^{n}}$) is called the global symmetry number and is represented by (σ_{gl}).

The difference in standard entropy between reactant and activated complex due to symmetry changes is given by:

$$\Delta S^{0\#} = \Delta S_{int}^{0\#} + Rln(\frac{\sigma_{gl}^{r}}{\sigma_{gl}^{\#}}) \tag{2.43}$$

where the subscripts r and # refer to the reactant and activated complex, respectively and $\Delta S_{int}^{0\#}$ is the intrinsic standard entropy. When substituting equation (2.43) into equation (2.39), the effect of changes in symmetry in going from reactant to activated complex on the rate coefficient of a monomolecular elementary step, i.e., becomes:

$$k = \left(\frac{\sigma_{gl}^{r}}{\sigma_{gl}^{\#}}\right)\frac{k_B T}{h}\exp\left(\frac{\Delta S_{int}^{0\#}}{R}\right)\exp(-\frac{\Delta H^{0\#}}{RT}) \tag{2.44}$$

The rate coefficient of an elementary step (k) can be written as a multiple of the single-event rate coefficient ($\tilde{k}$) as:

$$k = n_e \tilde{k} \tag{2.45}$$

where the number of single-events (n_e) is equal to the ratio of the global symmetry numbers of the reactant and activated complex:

$$n_e = \left(\frac{\sigma_{gl}^{r}}{\sigma_{gl}^{\#}}\right) \tag{2.46}$$

Since the effect of structure between the reactant and activated complex has been factored out by introducing the number of single-events n_e, the rate coefficient of the elementary step k now in fact characterizes the reaction step at a fundamental level.

A single-event frequency factor $\tilde{A}$ does not depend on the structure of the reactant and the activated complex, it can be defined as:

$$\tilde{A} = \frac{k_B.T}{h} \exp\left(\frac{\Delta S^{\circ}}{R}\right) \tag{2.47}$$

where S° is the standard entropy. The Arrhenius from of the single-event rate coefficient is given by:

$$\tilde{k} = \tilde{A}.\exp\left(\frac{E_a}{RT}\right) \tag{2.48}$$

2.2 Summary

The main aim in this chapter is to give a briefly summarised about kinetic models reduction of complex reaction system, application in a number of diverse fields and the causes of selecting the lumping methodology in this study.

Model reduction is important to describe the complex chemical reaction network where the feedstocks contain many components. It is easier to solve the differential equation if the number of the independent components is reduced. The common approaches used to simplify the complex kinetic chemical reaction system follow four classes: time-scale analysis, sensitivity analysis, lumping, and single event. The selection of the model reduction methodology depends on the kinetic information available, composition, structure of component reaction, and the accuracy required.

The time scale method identifies the different scales over which species react, and the fast time scale reaction and species are assumed to be at steady state. The generalised application of this technique is difficult because the identification of fast and slow reactions does not clearly show which are the exact fast and slow species; therefore, the reduce model may not be a valid approximation of the reaction kinetics. This method has been successfully applied for enzyme catalysis and combustion. However, the sensitivity analysis approach seeks to determine and eliminate insignificant reactions and species on the basis of their impact on designated important species; it means that, only a subgroup of the original species remain in the reduced model. The disadvantage this approach is as the number of important species increases, sensitivity analysis is likely to provide substantial model order reduction. Reduction by sensitivity analysis has been applied to pyrolysis and combustion.

In the lumping approach, the reaction vector is transformed to one lower dimensional vector of pseudo-species, therefore the kinetics equations become easier to solve and a few parameters need to be experimentally determined. The resulting pseudo-species may be linear or non-linear combinations of the original species. The rate constant coefficients for the global conversion of lumps are estimated from the experimental values after simplifying a reaction network between these lumps.

Discrete and continuum lumping approaches have the same target to reduce the parameters for description of the complex reactions. Discrete lumping has been presented showing its systematic development in terms of pseudo-components. The selection of the lumps is not easy; it is often based on experience and in some cases it is a procedure based on trial and error. When a very rigorous procedure is followed, as in

those based on finding the invariant subspaces for determining the lumping scheme, the mathematics can be very cumbersome. Moreover, when the system is nonlinear, the results obtained can be difficult to interpret and lumped system can be difficult to compare with a real reduced system. To some extent, continuum lumping may appear to be easier to perform than discrete lumping, but it shows an inability to give detailed information. The number of kinetic parameters increases with increasing number of lumps. In some cases, the continuum lumping can be derived directly from the discrete lumping when the number of components becomes very large. When the exact composition and reaction are unknown the continuum lumping is very convenient, since the continuous procedure does not present the possibility of including information of kinetic detailed into the problem formulation. The major limitation of using discrete and continuum lumping kinetic approaches is that the kinetic parameters depend on the composition of the feedstock. Consequently, with every different feedstock the kinetic model needs to be refitted and new parameters have to be estimated. However, in the single-event method a complete reaction network is constructed, taking into account all the reactions involving each molecule. The kinetic parameters in this method are independent of the feedstock and hydrodynamic conditions. However, if this method applied without any simplifying assumption, originates a huge number of elementary steps even for relatively simple molecules, that makes its use difficult for complex mixture for example Fischer-Tropsch waxes. The single event approach has been applied only to a limited number of hydrocracking cases, mainly to feed-stock constituted of few components.

The lumping methodology is used in this study because it is used widely for reduction of a large system of reactive species to a more manageable one and it can give useful information that can be used in design, although it does not furnish information on the fundamental chemistry of the process. The following table summarises some study used lumping approach for system reduction such as hydrocracking, pyrolysis, etc.

Reference	Approach	Summary
Laxminarasimhan and Verma (1996)	Continuous	A hydrocracking study is vacuum gas oil. The hydrocracking rate constant k has been assumed to be a monotonic function of true boiling point. The model introduced a skewed Gaussian distribution function to determine product yield distribution of hydrocracking reaction $(p(k, K))$. A simple power law type was used to describe $D(k)$ (species-type distribution function).
Mazloom et al. (2009)	Discrete and Continuous	The kinetics of scrap tyre was described in terms of discrete and continuous lumping models. The lumps were described in terms of the boiling point distribution. The conversion of heavier lumps to lighter lumps in the discrete model was considered in terms of consecutive and parallel reactions. In continuous model the reacting mixture was considered as a continuous lump where boiling point used to describe the distribution of the species within the lump. Results indicated that the continuous model give more agreement with experimental data than discrete model.
Elizalde et al. (2009)	Continuous	A hydrocracking in a fixed bed reactor for Maya crude oil. The true boiling point distillation curve is a monotonic function of reactivity k. In this study the model parameters were accurately correlated with reaction temperature. The study showed four model parameters linear trend with temperature whereas only one parameter almost constant.
Elizade et al. (2010)	Continuous	The model was used to study the effect of pressure, temperature and space velocity on hydrocracking kinetics of heavy crude oil. The model parameters were correlated explicitly with

		temperature and pressure. The developed correlations were used to predict distillation curves at different conditions.
Lababidi and AlHumaidan (2011)	Continuous	A kinetic model used to describe the undergoing reaction of hydrocracking associated with the hydro-treatment of atmospheric residue. The main concept in this model was that the rate constant of hydrocracking was assumed as a monotonic function of the true boiling point. The effect of different catalyst types on the model parameters was investigated by this model.
Calemma et al (2000)	Discrete	A kinetic model developed to investigate the hydroisomerization and hydrocracking of n-hexadecane, n-octacosane and n-hexatriacntane in a stirred micro-autoclave. The kinetics of hydroisomerization and hydrocracking of n-alkanes was described adequately by a reaction network where the conversion of n-paraffins occurs by three competitive reactions and the iso-paraffins as a primary product by hydroisomerization further reacts to give cracking products.
Pellegriniet al.(2004,2008) and Gambaro et al. (2010)	Discrete	A lumping kinetic model was developed to describe the hydrocracking of Fischer-Tropsch waxes (C4-C70 mixture of n-paraffins). The lumped model based on the expression proposed by Froment (1987). A Langmuir-Hinshelwood-Hougen-Watson has been followed, accounting for physisorption by means of the Langmuir isotherm. The model introduces of the complete form of the rate expressions for isomerisation and cracking that is merely the consequence of the higher number of parameters used in the, but

		derives from a higher meaningfulness of the model.
The present work	Continuous and Discrete	This research proposed the development of a lumping methodology model, which deals with complex reactivity mixture. The continuous modelling will be developed for catalytic hydrocracking of Fischer-Tropsch wax (n-paraffins) based on molecular weight (chain length) as a monotonic function of reactivity k. To increase the model efficiency two types of species-type distribution function $D(k)$ will be studied. The second proposed in this research to show that the developed continuous lumping model can be linked to a discrete lumping model in lignin pyrolysis. The final proposed in this research is to assess the capability of developing model as applied to polymerisation

Table 2.1. Summary of some lumping study

CHAPTER 3.

Case (I) - Continuum Lumping Kinetics of n-Paraffins

The synthesis gases (CO_2 and H_2) are converted by using the Fischer-Tropsch (FT) process into n-paraffins (waxes) whose distribution covers a wide range of molecular weights. These paraffins (waxes) are essentially free from aromatic components, sulphur and nitrogen but contain a small amount of olefins and alcohol. A large fraction of FT products is characterised by a boiling point higher than 370 °C and the middle distillates (MD) (150-370) show very poor cold flow properties that hamper their use as a transportation fuel. Therefore the hydrocracking catalytic process is used to improve the FT product by increasing the MD yields to form iso-parafins which have a strong influence on the properties of the product such as cetane number. In this chapter, the suitability of the continuum lumping approach to describe the yield of the hydrocracking of paraffins (FT waxes) in a catalytic reactor is reported.

In this study it is assumed that n-paraffin and is-paraffin for each component can be taken as one lump because n-paraffin and iso-paraffin has the same carbon number and molecular weight for each component.

3.1 Introduction

Hydrocracking is considered, one of the most suitable processes for the production of high quality middle distillates (Gary and Handwerk, 1994). The hydrocracking process improves octane number for the gasoline fraction and raises the product ratios of iso-butane to n-butane in the butane fraction. The process involves complex chemistry and a variety of reactions, such as isomerisation, hydrogenation, dehydrogenation, C-C bond scission, hydrogen transfer, ring saturation, and dealkylation (Laxminarasimhan and Verma, 1996).

3.1.1 Chemistry of hydrocracking catalyst

The hydrocracking is a catalytic cracking process used to convert complex feedstock like vacuum gas oil into lower boiling products such as gasoline, kerosene and diesel. The hydrocracking of n-paraffins is carried out on dual-function catalysts consisting of a metal and an acid function. The acid function is responsible for the cracking and isomerisation reactions, whereas the hydrogenation/dehydrogenation reaction is provided by metals. The type of acid function can be amorphous oxides, crystalline zeolites or hybrid supports (mixture of zeolite and amorphous oxides), however the metal function can be noble metals (platinum) or non-noble metal (molybdenum). The following steps are the elementary steps and reactions that were used by Gamba et al. (2009) for hydrocracking of paraffin over the bifunctional catalysis:

- Dehydrogenation of n-paraffins
- Protonation of olefins
- Carbenium ion hydride shift
- Carbenium ion methyl shift
- Protonated cyclopropane
- Carbenium ion cracking through B-scission
- Deprotonation of carbenium ions
- Hydrogenation of olefins

Fig. 3.1 shows some steps that may occur in the paraffinic species and Fig. 3.2 illustrates the steps in the hydrocracking of mononaphthenes. Fig 3.3 shows an example of different possible reaction paths that can occur in the hydrocracking of a tetranaphthene during hydrocracking.

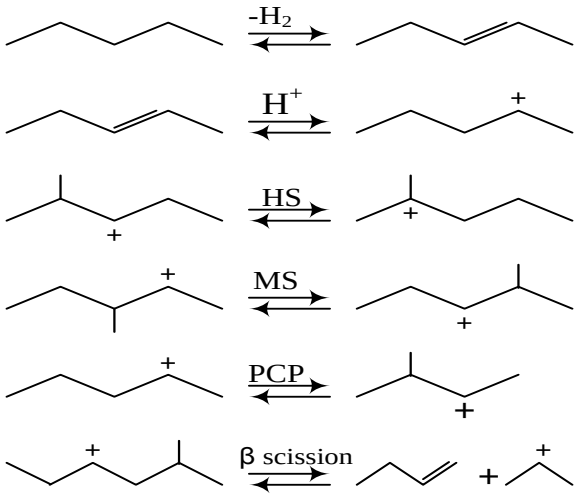

Figure 3.1. Steps of paraffins hydrocracking

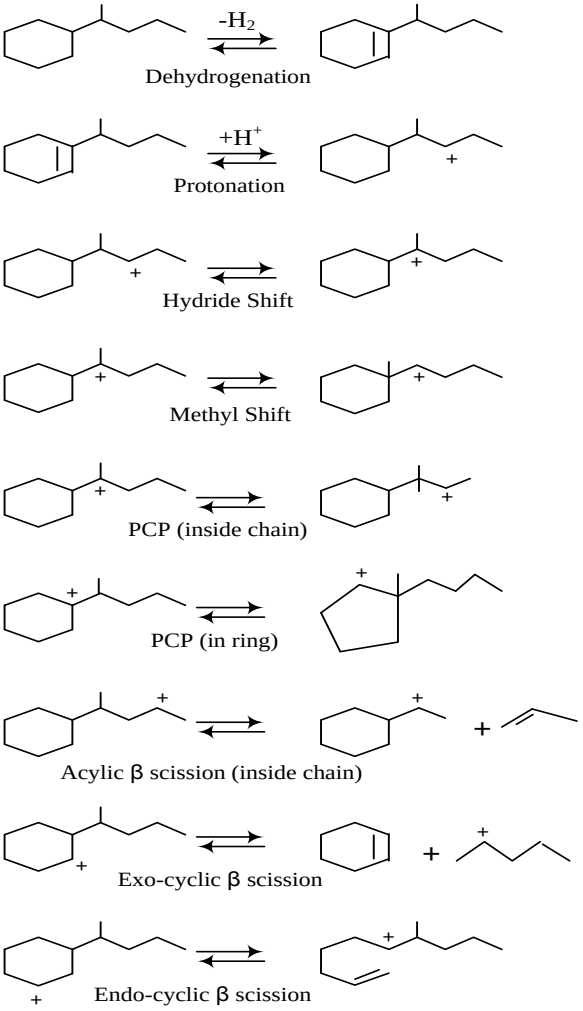

Figure 3.2. Steps of mono-ring naphthenes hydrocracking

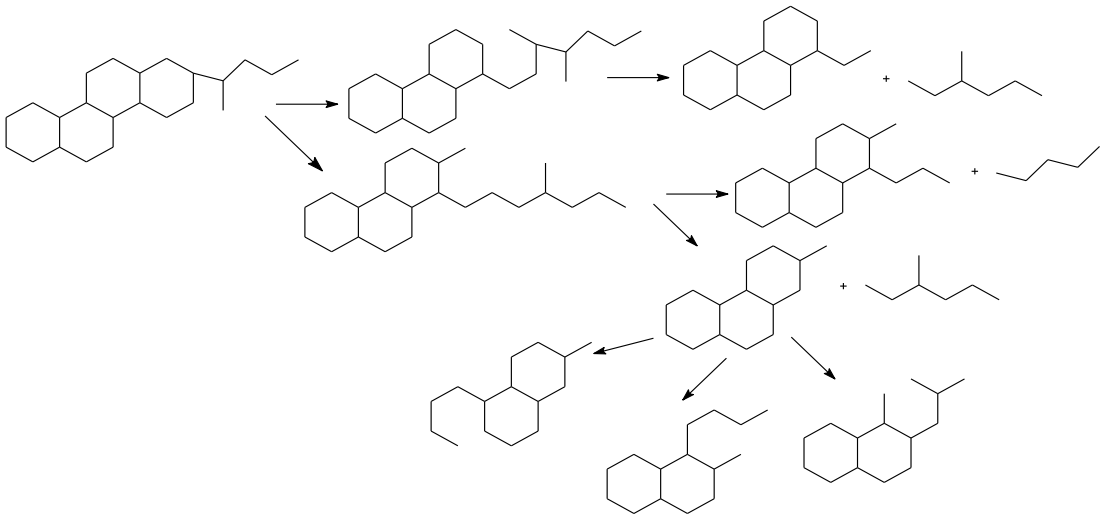

Figure 3.3. Reaction network of tetranaphthene

3.1.2 Hydrocracking of waxes

The hydrocracking reaction of n-paraffins over bifunctional catalysts has been studied intensively by Martens et al (1986) and Schulz and Weitkamp (1972). These works are outstanding in the definition of the hydrocracking reaction mechanism, mainly concerning the formation of branched products. Later, Froment (1987) introduced "lumped kinetic models" for the hydrocracking of different pure n-paraffins. In these models the reacting products were divided into main classes (or lumps) which correspond to n-paraffins, iso-paraffins and cracked products. Calemma et al. (2000) investigated the hydroisomerisation and hydrocracking of long chain n-alkanes on a Pt/amorphous SiO_2-Al_2O_3 catalyst at different temperatures and pressures. The reaction pathway and kinetic parameters for each n-alkanes were determined. Pellegrini et al. (2004) developed a lumped model based on an appropriate number of pseudocomponents (lumped model) proposed by Froment. In this model the feedstock components are divided into five lumps (C_1-C_4, C_5-C_9, C_{10}-C_{14}, C_{15}-C_{22}, and C_{22+}) and the products are constituted of n-paraffins and iso-paraffins without specifying the kind of isomers.

Calemma et al (2005) investigated the effect of the operating conditions on the hydroconversion of Fischer-Tropsch waxes and the quality of the middle distillate. The isomer content of C_{10-14} and C_{15-22} fractions of the hydrocracking products were determined by adequate linear quadratic models. Pellegrini et al (2007) adopted their previous work (2004) to model the material balance for each of the 138 components of

the feed mixture (70 n-paraffines, 67 iso-paraffins, and H_2). They assumed that the cracking of the reactants happens in the middle (i.e., C_{40} gives two C_{20} and C_{69} gives a C_{35} and a C_{34}). De Klerk (2007) proposed a thermal cracking model that is valid for n-paraffins (hard wax) up to C_{120}. It was based on the Voge et al. (1949) and Kossiakoff et al. (1943) description to describe thermal cracking of wax. Rate constant $k(n)$ of the carbon number is calculated by using: $k(n) = kB(n-1)(1.57n - 3.9)$, where B is the correlation constant to relate k to $k(n)$. The equation of material balance consists of two terms in the model: the first term is the first order thermal cracking rate to consume the species, while the second term gives the production rate of the species.

Pellegrini et al. (2008) presented a model for the hydrocracking of Fischer-Tropsch waxes that considers vapour-liquid equilibrium (VLE). The VLE in this model is described by the Soave-Redlich-Kwong (RSK) equation of state, which was extrapolated up to C_{70}. The hypothesis made in this model was that the cracking of the C-C bond occurred in the middle of the chain. Different multiplying factors to the vapour and liquid phase are used in the model to improve the model prediction. The model was successively simplified by Gamba et al. (2009) and applied to the catalytic hydrocracking of (FT) waxes over a bifunctional catalyst at different operating conditions. Here the improvement was achieved by introducing a probability function for cracking. They assumed that A represents the cracking probability of the $n_C - 7$ bonds (where n_C is the carbon number of the cracked paraffins) and $A/2$ is the cracking probability of the third bond and of the $(n_C - 3)$th bond as: $(n_C - 7) * A + 2A/2 = 1 \; and \; A = 1/(nc - 6)$. For example, when starting from n-C_8, paraffins will break giving rise to $2An^0$ moles (where n^0 is the initial value of the paraffin moles) of each product between C_4 and C_{nc-4} and to An^0 mols of C_3 and C_{nc-3}.

Moller et al. (2009) developed a two-phase reactor model, which combines elementary hydrocracking kinetics and vapour liquid equilibrium, for describing the hydrocracking of FT wax. The model is based on elementary β-scission kinetics applied to paraffin species lumped by carbon number. β-scission is the kinetic rate controlling step assumed in this model and all other steps are assumed to be either fast or at equilibrium. The β-scission reaction steps of n-paraffin lumps is divided into types A, B1, B2, and C kinetics to simplify the model. Recently, the kinetic model to describe

the hydrocracking of (FT) waxes based on Langmuir-Hinshelwood-Hougen-Watson approach was developed by Gambaro (2011). The kinetic and thermodynamic constants were defined as functions of the chain length to reduce the number of model parameters. All the hypotheses of the model by Gamba et al (2009) were adopted to further improve the quality of the fitting and possibly its prediction capability against experimental data.

The aim of this work is to investigate the robustness of the continuum lumping approach to describe the product composition of hydrocracking process of normal paraffins, and to study how the operating parameters affect the model parameters.

3.2 Labelling the reactants

Labelling the reactants is the first step for performing the continuum lumping methodology. The label (or index) can be any particular characteristic which unequivocally identifies the reactants. For example, one can choose the kinetic constant, the boiling point, the mass, etc. provided that a unique relationship between the components and the chosen label exists. The label, say x, is taken over the interval $[0, \infty)$ and, if the variable of interest is the concentration, the initial concentration of the species in the interval $(x, x + dx)$ is given by:

$$c(x, 0)dx = c_0.h(x)dx \tag{3.1}$$

where c_0 is the total initial concentration and $h(x)$ is a distribution function which must be normalised so that the mass conservation is assured:

$$\int_0^\infty c_0.h(x)dx = 1 \tag{3.2}$$

If such a correspondence between components and label can be established, and a distribution function is introduced, then the lumped (global) variables, at each time, can be obtained by the relevant integration over the label. As an example, let us

consider the chosen label being the kinetic rate constant k, then the global (lumped) concentration of the mixture, $C(t)$, can be defined and it can be calculated as follows:

$$C(t) = \int_0^\infty c(k,t).D(k)dk \tag{3.3}$$

where $c(k,t)$ is the concentration of the species with reactivity k at the considered time t and $D(k)$ is the reactant type distribution function. The reactant type distribution function describes the mixture with respect to the particular label chosen. In the case at hand, having chosen the reactivity as the label (expressed in terms of kinetic constant, k); $D(k)$ represents the distribution of reactivity of the various components. Consequently, $D(k)dk$ represents the reactant type with a rate constant between k and $k + dk$. The reactant type distribution function and its properties will be considered in detail in section 3.3.2.

Astarita and Ocone (1988) explain in detail the role that the kinetic constant plays in the continuous lumping. In particular one should remember that each component needs to be labelled univocally through an index. If one considers a collection of species, all characterised by linear kinetics, the kinetic behaviour of each component is completely identified by the value of the kinetic constant, k, and hence k can be used as a label. The situation is more complex in the case of nonlinear kinetics. However, some important results are reported here since they are relevant to the present analysis. Nonlinear kinetics, except for the case where the kinetic equation is of the power-law form (Astarita, 1985), requires always more than one label to identify univocally each species. This is only for some physical justification. The first label can be used to generate desirable first level aliases and the second label can then be used to distribute them over a spectrum of reaction rates (Aris and Astarita, 1989). For instance, if one considers the classical case of a Langmuir isotherm dominated kinetics (LIK), the kinetic equation for each reactant takes the following form:

$$-\frac{dc}{dt} = \frac{k.c}{1+K.c} \tag{3.4}$$

where k is a frequency factor and K is a normalizing factor for concentration. They identify each component in a mixture there is no reason to expect that the sorbability K has the same value for all components (Astarita and Ocone, 1988).

3.3 The kinetics model

The cracking process of the paraffins (waxes) could happen in the gas phase or mixed phase. Gas phase processes typically operate at a temperature around 620 °C, while mixed phase processes operate in the temperature range 450-540 °C (de Klerk, 2007). Therefore, there are four operating parameters affecting the catalytic cracking of the paraffins, namely temperature, pressure, H_2/feed ratio, and weight hourly space velocity (WHSV). WHSV is defined as the weight of feed flowing per unit weight of the catalyst per hour (inverse of the space velocity). In this work, experimental data has been used in conjunction with a model for catalytic cracking of n-paraffins (waxes) where each species is identified through its carbon number (CN). The kinetic scheme, reported in Fig. 3.4 below, is a proposed simplification for the catalytic cracking reactions occurring in the trickle bed reactor.

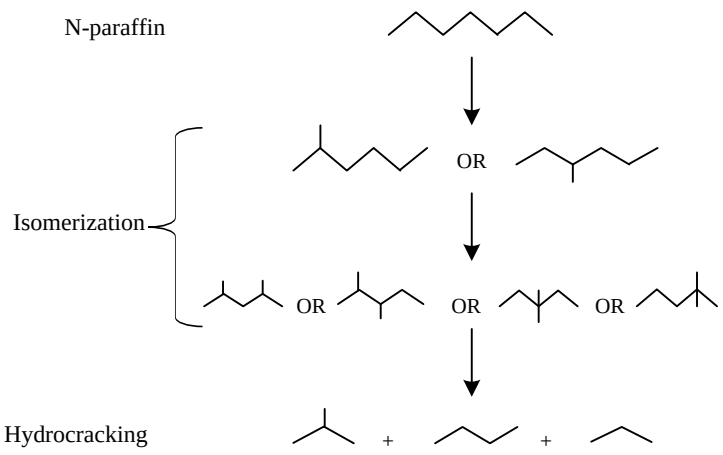

Figure 3.4. The simplified kinetic scheme of n-heptanes hydroconversion.

In this work the system considered a conversion of n-paraffins (waxes) occuring through a series of consecutive reactions, where the n-paraffins are first isomerised into mono-branched isomers which undergo subsequent isomerisation steps and cracking reaction as show in Fig. 3.4 to produce low molecular weight components (iso and normal paraffins have low molecular weight). The isomerisation reactions of the n-

parraffins could be predicted by the continuum lumping methodology. The starting point, as any continuum lumping problem would be to attempt to label the species to distinguish two isomers having the same carbon number, in principle. Suppose that such a property has been identified and measured: that can be, as an example, the boiling point; however, any other property, which can label univocally each isomer, could be equally used. Since for the development of this study, the carbon number, L_i, has been chosen as a label, different isomers are indistinguishable: L_i is not the relevant label to separate n-paraffins from iso-paraffins and the model proposed cannot distinguish between different isomers. If all the isomers are saturated, the molecular weight is also a property which will not distinguish between different isomers. Differences can be detected only if other properties, which are different for the different classes of isomers, are available. It is also worth noting that within the continuous lumping theory, the two classes of isomers could possibly be considered as only two lumps and therefore a possibility could be to model them through a discrete 2-lump model. The global reactions that, starting from n-C, furnish the cracked products CR, have therefore been considered in formulating the present model.

In this study, the feedstock is characterised through the chain length of its components; consequently, the various components are univocally identified by their carbon number, which is then adopted as the mixture label. The normalised chain length of the species is then defined as:

$$\theta = \frac{L_i - L_s}{L_l - L_s} \tag{3.5}$$

where L_i is the chain length (carbon number) of the generic component i and L_s and L_l represent the shortest and longest chain in the reaction mixture, respectively. The chain length is identified here with the carbon number. θ can take values between 0 and 1. Fig. 3.5 shows the distribution of θ for the system at hand where $L_s = 1$ and $L_l = 70$

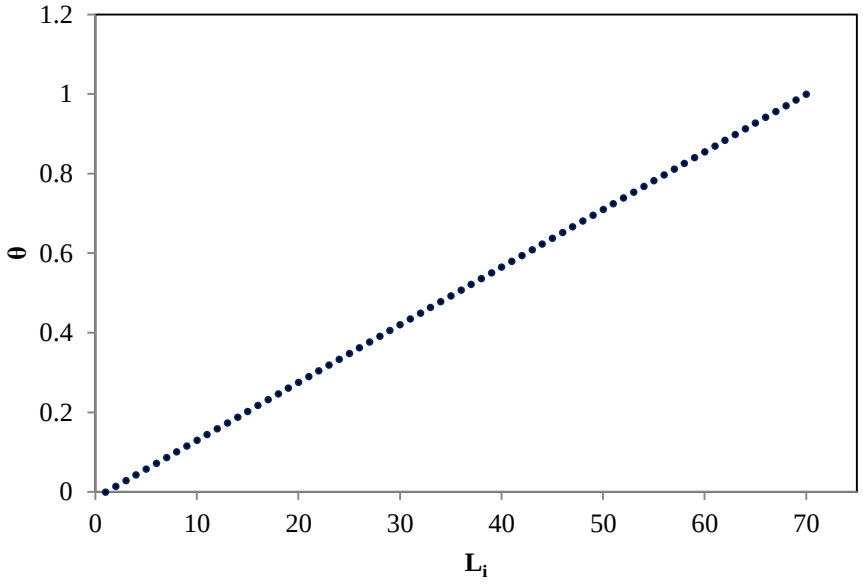

Figure 3.5. Normalised chain length (carbon number) versus carbon number

The continuous function $c(\theta, t)$ is then introduced and it represents the distribution of components at any given time t; $c(\theta, t)d\theta$ represents the fraction of the species with length chain between θ and $\theta + d\theta$ at time t.

The specific problem that aimed to solve it in this work corresponds to obtaining the solution of Eq. 3.3. Since the relationship is presented in terms of reactivity, one would need to establish the transformation from the θ-space to the k-space; this is achieved by establishing the (monotonic) relation between k and θ . Various relationships have been proposed in the literature and, for the space transformation; in this work selected one which derives directly from Eq. 3.6 below where a power law relation is used for transforming the space of carbon numbers into the space of reactivity.

The power law relation is one which has been widely used to transform the k-space into the θ –space (Laxminarasimhan et al, 1996 and Ancheyta et al., 2005):

$$\frac{k}{k_{max}} = \theta^{1/\alpha} \tag{3.6}$$

where k_{max} is the highest reactivity in the mixture. The assumption is made that k_{max} is associated with the component having the longest chain length and α is a model constant. α can take any positive value as in most of the literature. It is worth noting that when $\alpha = 1$, k increases linearly with the carbon number. Fig. 3.6 shows the behaviour of k for various values of α and $k_{max} = 4.24\ (h^{-1})$.

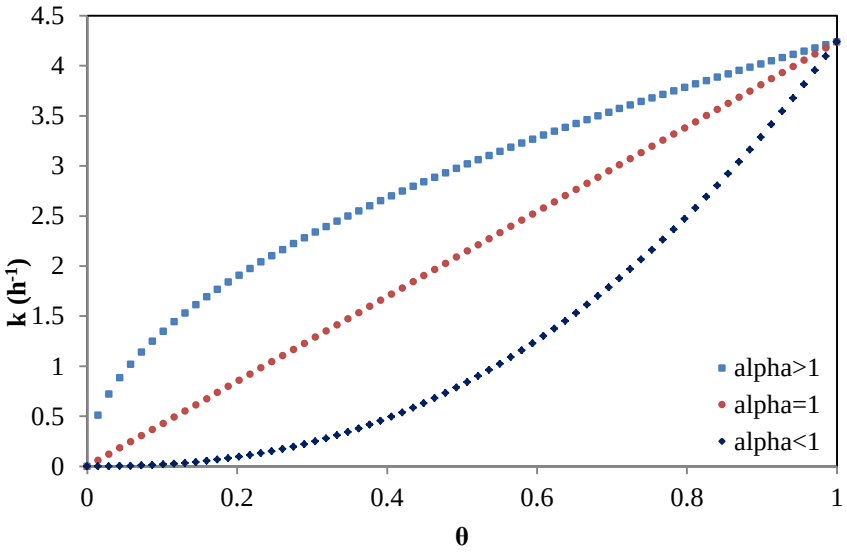

Figure 3.6. The exponential distribution function

3.3.1 Material balance equation

In a plug flow-type reactor, the material balance for the generic species of reactivity k, furnishes the following equation (Laxminarasimhan et al, 1996 and Ancheyta et al., 2005):

$$\frac{dc(k,t)}{dt} = -k.c(k,t) + \int_{k}^{k_{max}} p(k,K).K.c(K,t).D(K).dK \qquad (3.7)$$

where $p(k,K)$ represents the yield distribution function and determines the amount of formation of the species with reactivity k from the species with reactivity K greater than k, $c(k,t)$ is the concentration of species with a reactivity of k, and $D(K)$ is the species type distribution.

The term on the left-hand side represents the time variation of the concentration of the generic component of reactivity k, whilst the first term on the right-hand side represents the disappearance of the same component due to cracking. The function in the integral represents the formation of the component of reactivity k due to the cracking of all components of reactivity $K > k$.

The procedure chosen is the one utilised by Laxminarasimham et al. (1996). As one can deduce from the problem formulation, to proceed with a solution, one needs to assign an explicit form to $D(k)$.

3.3.2 The reaction-type distribution function

As already pointed out, Eq. 3.3 defines the so called direct lumping problem: given complete information about the feed, one is seeking to find $C(t)$. This implies that the label for each reactant is assigned. However, if one wants to find a value for $C(t)$ Eq. 3.3 would need to be solved. In practical terms, this implies that we need to know the specific form of $D(k)$. $D(k)$ was introduced by Chou and Ho (1988) to describe the transformation from the label space to the kinetic space and consequently it has a well-defined physical meaning. $D(k)$ depends on the type of reactants in the feed and, very importantly, it is independent of the feed concentration.

The focal point of the analysis is then the appropriate choice of $D(k)$; also, $D(k)$ plays an important role in defining the region of validity of the continuous approach (Ho and White, 1995). $D(k)$ can be determined by carrying out experiments on a model compound which mimics the behaviour of the mixture. The model compound is independent of the concentrations of each species. Conversely, the precise value of the concentration of the reactants, $c(k,t)$, does not pose any restriction to the implementation of the continuum approach, being only the number of component and $D(k)$ the discriminatory factors for implementing the continuum lumping methodology. $D(k)$ determines the solution of Eq. 3.3 by inputting information on how the kinetic constants are spaced in k-space and defining the relative reactivity of the reactive species. Consequently, depending on the specific form that $D(k)$ takes, the specific reactivity of different feeds can be represented.

In the specific problem considered in this study, $D(k)$ represents the transformation from the space L (chain length, or carbon number) to the space k. Despite defining it in correspondence of the discrete points L, as the number of components becomes very large, $D(k)$ can be treated as a continuous function. $D(k)dk$ represents the number of species type with rate constant between k and $k + dk$ and must satisfy the following relation:

$$N = \int_0^\infty D(k)dk \tag{3.8}$$

where N is the number of species in the reaction mixture.

The *D(k)* expresses the interdependence between the reactivity of the various components is clearly seen by considering the following expression:

$$D(k_i) = \frac{\Delta i}{\Delta k_i} = \frac{(i+1)-i}{k_{i+1}-k_i} = \frac{1}{\Delta k_i} \tag{3.9}$$

From Eq. 3.9 it follows that, depending on the value of Δk_i, $D(k)$ can be positive, negative or infinite. $\Delta k_i > 0$ implies that components with larger carbon number have a larger reactivity; conversely, if $\Delta k_i < 0$ components with larger carbon number have a smaller reactivity. However, $\Delta k_i = 0$ describes the case where all the components have the same reactivity.

The reaction type distribution function can be expressed as a function of the label; this is obtained by using the relation between the generic component i and θ.

$$D(k) = \frac{di}{dk} = \frac{di}{d\theta}.\frac{d\theta}{dk} = N.\frac{d\theta}{dk} \tag{3.10}$$

Two different situations are analysed in this work, and they correspond to different forms chosen for the function $D(k)$: *Case A* will be used to indicate the

situation where *D(k)* is a power-law relation, whilst *Case B* indicates the case where $D(k)$ is expressed through a gamma function. Experimental evidence of the hydrocracking process confirms that the reactivity increases as the carbon number increases; therefore *Case A* is the appropriate one for treating hydrocracking. However, to show the generality of the approach, *Case B* is considered as well and the issues arising when additional model parameters are introduced are then discussed. *Case B* is formulated trying to accommodate a more flexible way to describe the reactivity of a mixture; this makes it possible to accommodate the possibility that the reactivity is not a monotonic function of the label. The aim is to show how the numerical programme can be modified by including any other expression for $D(k)$ if necessary.

3.3.2.1 Case A: (The power law relation)

If the power law relation is used Eq. 3.6, then the corresponding expression for $D(k)$ is obtained by substituting the derivative of Eq. 3.6 into Eq. 3.10 as follows:

$$D(k) = \frac{N.\alpha}{k_{max}^{\alpha}} k^{\alpha-1} \tag{3.11}$$

Eq. 3.11 contains two parameters, namely α and k_{max}. Fig. 3.7 shows the behaviour of $D(k)$ as a function of the chain length, L_i, for various values of α where N is the number of species, equal to 70 in this study. The value of k_{max} used in Eq. 3.11 can be obtained through the value of $D(k)$ and its expression. Additionally, (k_{max}) can be estimated through relationships available in the literature through fitting of experimental data.

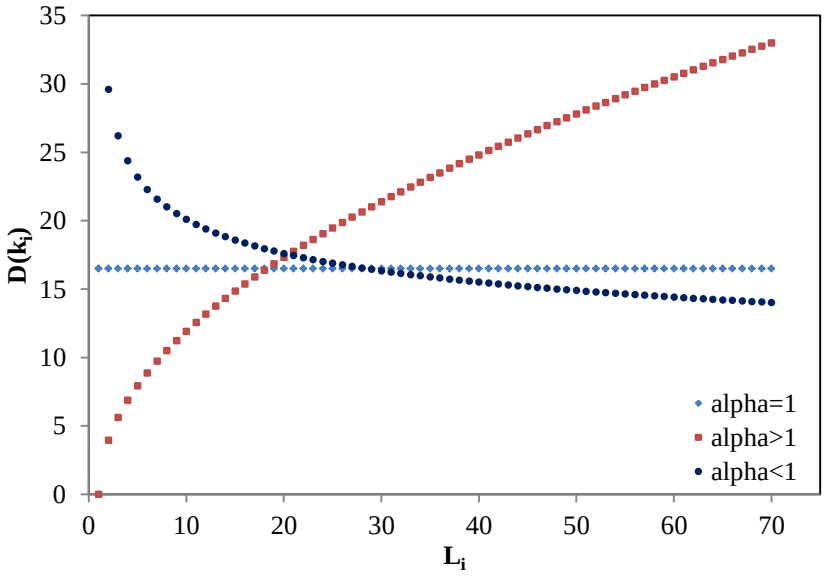

Figure 3.7. $\boldsymbol{D(k_i)}$ as a function of the chain length (carbon number) $\boldsymbol{L_i}$ (*Case A*).

Fig. 3.8 represents the typical behaviour of $D(k)$ as a function of k for *Case A*. In Fig. 3.8 the values of N and k_{max} used are the same as in Fig. 3. 7.

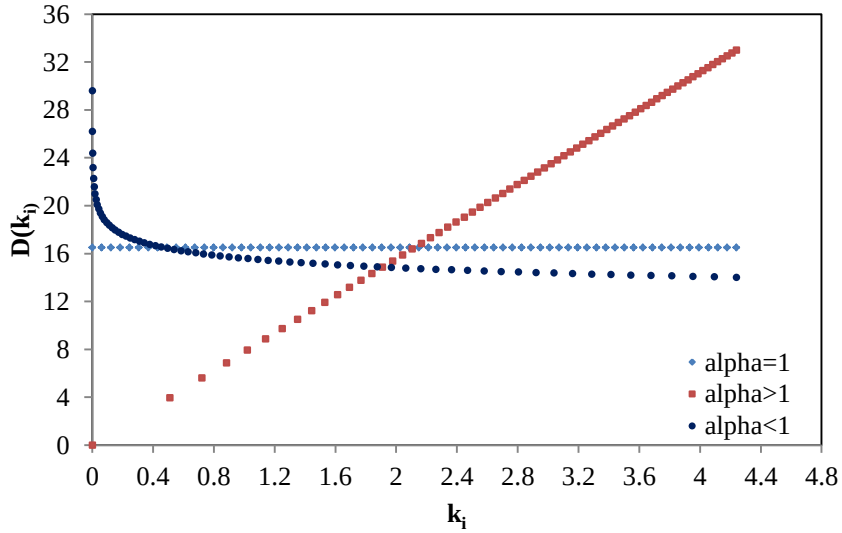

Figure 3.8. The reaction type distribution as a function of the reactivity (*Case A*).

3.3.2.2 Case B: (The gamma function)

An alternative way to express the reaction-type distribution would be to consider an expression more flexible than the power law. A powerful expression, able to accommodate a large number of kinetics is the "gamma" distribution; the distribution used in this work is an adaptation from Chou and Ho (1989):

$$D(k) = q.k^{\eta}e^{-\xi.k} \tag{3.12}$$

where q is a normalisation parameter (Chou and Ho, 1988); η and ξ are parameters that determine the shape of the distribution. Specifically, the distribution has a maximum for $k = \frac{\eta}{\xi}$. η and ξ determine the "sharpness" and asymmetry of the distribution and therefore are related to the relative reactivity of the species. The exponential distribution is recovered if $\eta = 0$ and $D(0) \neq 0$; physically this means that the mixture contains unconvertible species. In the limits of $\eta \to \infty$ and $\xi \to \infty$, with $\frac{\eta}{\xi} \to const$, the function becomes a delta function centred at $\frac{\eta}{\xi}$. Hence, it is clear that the values of the additional parameters introduced with $D(k)$ are related again to the relative reactivity of the components and should not show a strong dependence on the operating conditions.

For this specific function, Eq. 3.12, conservation of mass implies that the following condition is satisfied:

$$N = \int_0^{\infty} D(k)dk = \frac{q.\Gamma.(\eta+1)}{\xi^{\eta+1}} \tag{3.13}$$

where $-1 < \eta < \infty$ and $\xi > 0$, N is the number of spices, and Γ is the gamma function. Fig. 3.9 shows the typical behaviour of $D(k)$ as a function of k_i, where Eq. 3.5 is still used to express the variation of k with θ. Various values of α are reported.

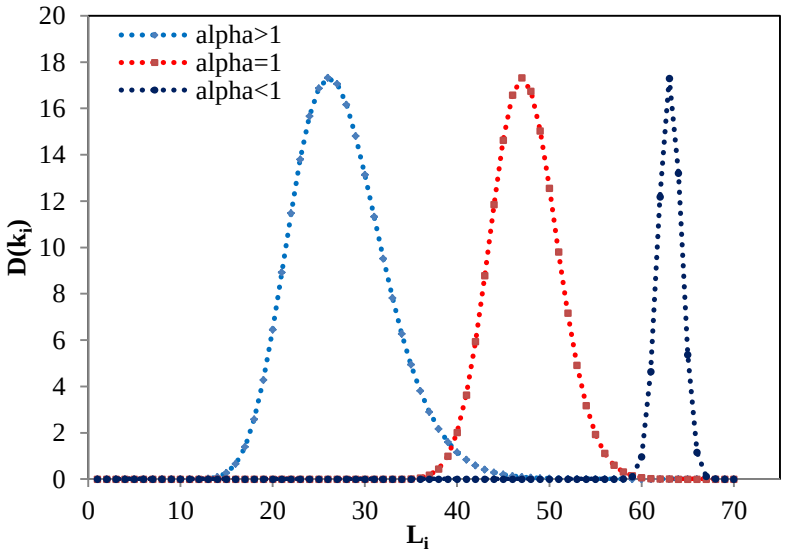

Figure 3.9. $\boldsymbol{D(k_i)}$ as a function of the carbon number $\boldsymbol{L_i}$ (*Case B*).

Fig. 3.10 shows the behaviour of $D(k_i)$ as a function of k_i. Comparison between *Case A* and *Case B* shows that *Case A* can only accommodate monotonically increasing values of Δk_i, all increases weighted equally; physically this implies that the reactivity increases as the carbon number increases and the ks are spaced following the same increasing rule (see Eq. 3.6). *Case B*, on the other hand, gives the flexibility to accommodate the possibility that components have reactivity not uniformly spaced along the k-axis. In the case of hydrocracking, the *Case B* can still be used provided that the parameters are chosen in a way that the reaction-type function becomes an exponential distribution. It is also noted later that, if the *Case B* is adopted, the larger number of parameters gives a better fitting of the experimental data, as to be expected.

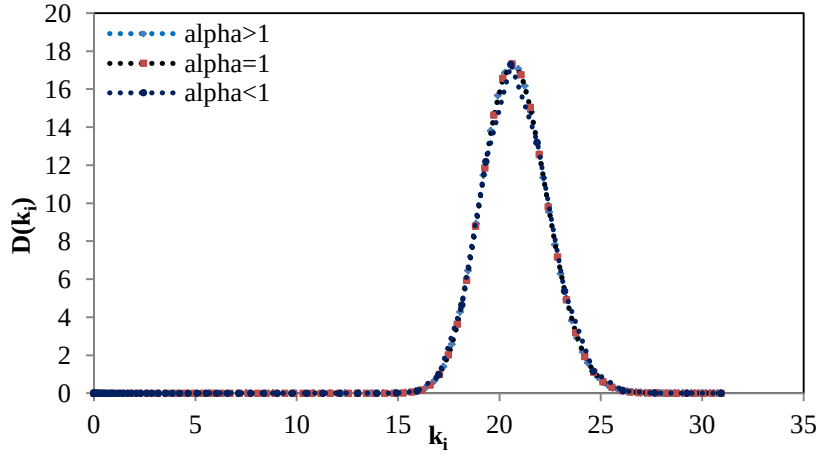

Figure 3.10. The reaction type distribution as a function of the reactivity (*Case B*).

3.3.3 The yield function $p(k, K)$

The assumption made in the present study is that the reactants undergo cracking only. Each component can then be formed, in principle, by the cracking of all the components having a larger chain length (molecular weight). The distribution function $p(k, K)$ then represents the yield distribution function for the formation of the component having reactivity k from the components of reactivity ($with\ K > k$). The properties of $p(k, K)$ are readily obtained by considering its physical meaning:

- The value of $p(k, K)$ has to be zero when $k = K$ (the species of reactivity k cannot yield to itself upon cracking).
- $P(k, K) = 0$ for $k > K$ since dimerisation is not significant in hydrocracking.
- $P(k, K)$ has to satisfy a material balance, namely $\int_0^K p(k, K).D(k)dk = 1$.
- $P(k, K)$ should always be positive.

Although it is extremely difficult to determine experimentally the primary yield distribution of a model compound, one can follow some guidance on the functional form of $p(k, K)$ based on information gained from experimental data from the hydrocracking of various paraffinic, olefinic and aromatics model compounds. Ancheyta et al (2005) analysed a large number of experimental data reported in the literature and then decided to assume for $p(k, K)$ a skewed Gaussian-type distribution function (to represent the yield distribution), as already obtained by Laxminarasimhan et al (1996). The same distribution is adopted in this study.

As it will be seen later, when the model for the hydrocracking will be presented, the expression of the yield function, $p(k, K)$, is fundamental in the treatment of the problem, since it contains most of the hypotheses that make the problem solvable. The expression for $p(k, K)$ was determined based on physical considerations and experimental evidence. Experiments show that the peak of the yield corresponds to species that have reactivity lower than k_{max}. This is a consequence of the fact that the product of the primary cracking would have a reactivity immediately smaller with respect to the reactivity of the crackate (Laxminarasimhan et al, 1996). The peak should be closer to the component characterised by k_{max} (in other words the distribution

should be skewed towards the components with longer chains). Each species is characterised by a different value of the yield resulting in a distribution function. Four parameters are needed for the function $p(k, K)$ to depict all the properties illustrated; those parameters are a_0, a_1, α, and δ. The parameters depend on the reacting species and on the catalyst used, in other words they are "system" dependent: if the reactants and/or the catalyst change, the parameters should change as well. However, it has been shown in a number of previous works (e.g. Laxminarasimhan et al, 1996) that those parameters depend mainly on the catalyst. The parameters are obtained from experimental data, by requiring that the results obtained through the model match the experimental result; in other words the distribution parameters are used as tuning parameters.

The specific expression used for the yield distribution function in both cases is:

$$p(k,K) = \frac{1}{S_0 \cdot \sqrt{2.\pi}}[exp - [\{\left(\frac{k}{K}\right)^{a_0} - 0.5\}/a_1\,]^2\text{-A+B}] \tag{3.14}$$

where

$$A = exp - (\frac{0.5}{a_1})^2 \tag{3.15}$$

$$B = \delta.(1 - \left(\frac{k}{K}\right)) \tag{3.16}$$

$$S_0 = \int_0^K \left[\frac{1}{\sqrt{2.\pi}}.\left(exp - \left[\frac{\left\{\left(\frac{k}{K}\right)^{a_0} - 05\right\}}{a_1}\right]^2 - A + B\right)\right].D(k)dk \tag{3.17}$$

The values of parameters a_0 and a_1 determine the location of the peak in the interval $k\epsilon(0, K)$; δ is a small finite quantity that accounts for the possibility that $p(k, K)$ could take a small finite value when $k = 0$. In many practical cases, one can make the assumption that $p(k, K) = 0$ when $k = 0$. It has been found experimentally that the smallest reactivity components can be formed in traces; therefore a small arbitrary value of δ is justified. However, if the assumption is made that the amount of the smallest reactivity components produced can be neglected, δ can be assumed to be

null. The parameters a_0, a_1 and δ are system dependent and in principle can change when the operating conditions change. However, within the range of operating conditions considered, it is expected that their variation is not significant (Laxminarasimhan et al, 1996).

Fig. 3.11 shows how the yield distribution function depends on reactivity (k_i). Fig. 3.11 is obtained when *Case A* is employed. It is noted that the function is approximated with a skewed Gaussian distribution function and it is mainly based on experimental data (Laxminarasimhan and Verma, 1996; Chou and Ho, 1989; El-Kady, 1979). The three parameters determine the peak location and constrain the distribution to verify the total mass balance.

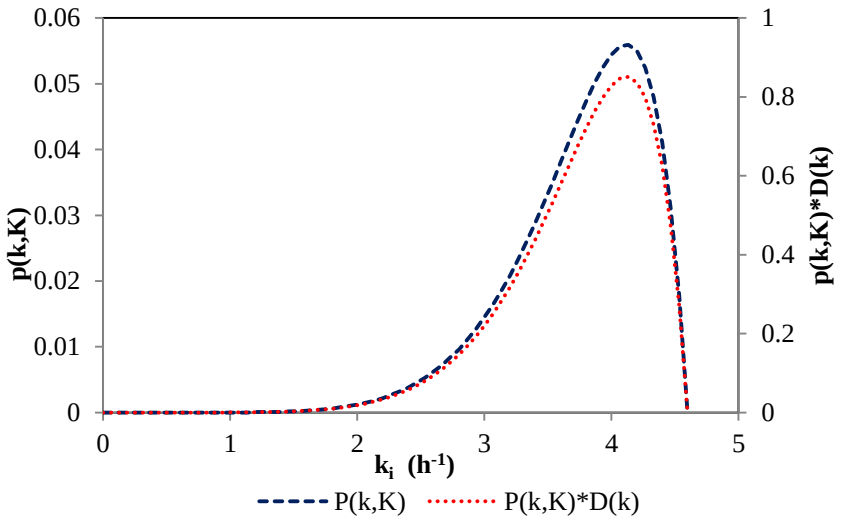

Figure 3.11. The dependence of the yield function upon the reactivity. The values of the parameters used are: $\boldsymbol{a_0 = 3.67}$, $\boldsymbol{a_1 = 22.86}$, $\boldsymbol{\delta = 0.77 \times 10^{-9}}$, $\boldsymbol{\alpha = 0.77}$ and $\boldsymbol{k_{max} = 4.6\ h^{-1}}$

3.3.4 Model assumption

As mention previously, the assumption made in this study is that the reactants undergo cracking only. Although the model is unable to account for isomerisation, it is able to describe the formation of MD deriving from the hydrocracking of higher molecular weight components. It is worth noting that the model presented here, as all models, is able to describe only the features that are modelled and can be used only to

investigate the kinetics of hydrocracking. Each component can be formed by the cracking of all the components having a higher molecular weight.

- The model assumes that the kinetics is first-order. This has been shown to work well in the continuous lumping approach of hydrocracking. A number of authors, e.g. Laxminarimham et al (1996); Basak et al. (2004), made successfully such an assumption which has recently been confirmed also in industry by Ho (2008) using two different types of catalysts.
- The yield function, $p(k, K)$, is assumed to be a skewed Gaussian characterised by three parameters, a_0, a_1, and δ. Those parameters are assumed to depend on the operating conditions, assuming that the operating conditions affect the catalyst behaviour. a_0 and a_1 define the location of the maximum of the Gaussian distribution. The maximum corresponds to the component which has the highest yield probability.
- The parameters a_0, a_1, k_{max}, α, δ, η, and ξ are system specific. This means that the parameters depend on the system scrutiny (constitutive parameters); specifically, they could depend on the catalyst, the activity and the impurity present in the feed. Those parameters are used as tuning parameters of the model and obtained by the experimental data.

3.3.5 Numerical procedures

In the following, the model considers that all components have the same molecular weight as a single lump. The balance equation, for each species, in a plug flow reactor, is then expressed by an integro-differential equation (Eq. 3.7), which is solved numerically. Considering the totality of species, a system of integro-differential equations must be solved at each time. The integration space is the (c, t) plane which is represented schematically in Fig. 3.12. The integration is particularly demanding since the integral in Eq. 3.7 must be solved "backwards". Consider, as an example, the generic component i (of reactivity k_i): at a given time t, the integral appearing in Eq. 3.7 must be solved by considering all the components with a chain length longer than i, namely it must be solved over the interval $[c_{i+1}, c_N]$ (see arrow in Fig. 3.12). However, the actual value (at time t) of those components (greater than i) is not known yet. To solve this problem, integration needs to be carried out backwards, starting from the

component N with the largest chain length. Indeed, the component N is not formed by any other component and therefore the integral representing the "production" of that component (see Eq.3.7) becomes null for $n = N = 70$. Once the composition c_N of N is found, then the concentration of the component $N - 1$ can be obtained through Eq. 3.7. The integration can then proceed backwards to $c_{(N-2)}$ and so forth till the concentration of the generic component i is calculated. This procedure must be repeated at each time step. Given the inherent complexity of the backward calculation, an alternative method has been proposed, checked and implemented. The method is based on the assumption that, if the time step is extremely small, then the evaluation of the "production" term, based on the concentrations at the previous time, does not give significant and appreciable deviation from the "production" calculated through the backward method. Consequently, the final numerical programme has been implemented adopting the "small time step" method.

A quadrature algorithm method was used to evaluate the integral part in the main equation (Eq. 3.7) and the differential equation was solved by using the Runge-Kutta method. At $t = t_0 = 0$ the component distribution corresponds to the feed distribution and, by using it as the input, the component concentration at $t = t_1$ is obtained. The experimental feed distribution is used. At $t = t_2$ the output is obtained by using the results at t_1 as the new "feed". Because of the numerical approximation employed, renormalisation is needed at each step to make sure that the percentage of the various components rightly furnishes the total mass. The procedure is continued until the numerical time corresponds to the real time that the mixture has spent in the reactor.

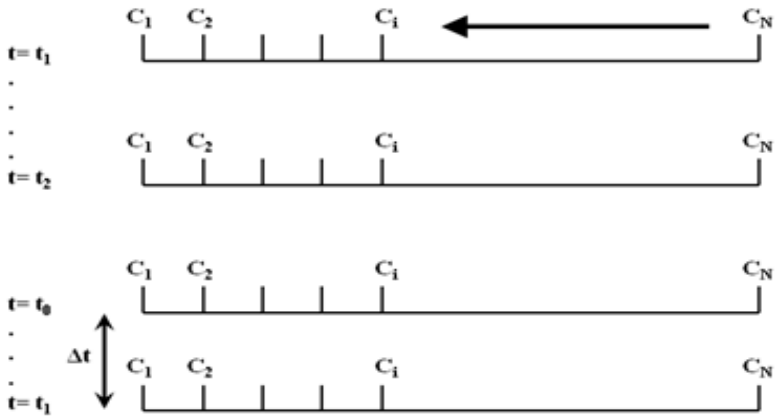

Figure 3.12. Schematic of the model solution. The arrow indicate that the concentration of the component of index higher than ***i*** must be employed to calculate the concentration of the ***i*** component

The simple procedure for calculating is summarised by flowchart diagram that is shown in Fig. 3.13. An optimisation Toolbox in Matlab program was used to determine the minimum of the objective function which depends on the values of seven model parameters in *Case B* and five model parameters in *Case A*. The Levenberg-Marquardt algorithm (*lsqcurvefit*) was applied to get the local optimal set of the model parameters. The objective function which used in the Levenberg-Marquardt algorithm is expressed as the sum of the square difference between the experimental and the computed weight percents:

$$Min\left[J\left(c(t)\right)\right] = 1/2\sum_{i=1}^{N}[c(t)_{exp} - c(t)_{model}]^2 \qquad (3.18)$$

where c(t) is the weight percent for the experiment and model calculation.

Fig. 3.14 illustrates the number of iterations with step sizes, function value, and the residual of the objective function required to reach the optimal value of the model variables. Also it illustrates the number of model variables with the current result. Matlab codes for the *Case A* and *Case B* can be found in Appendix (1).

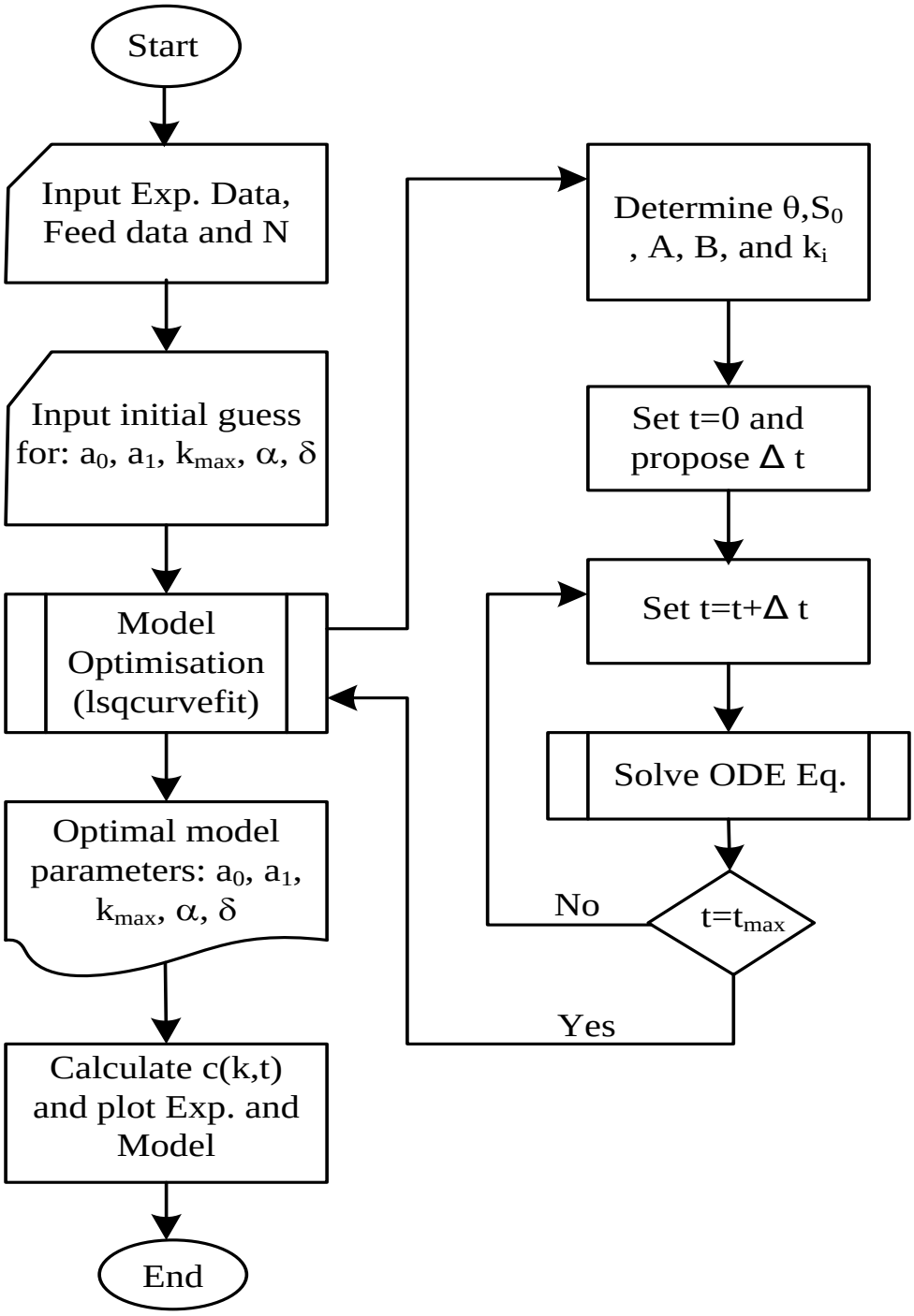

Figure 3.13. Calculation procedures for getting the best set of the parameters.

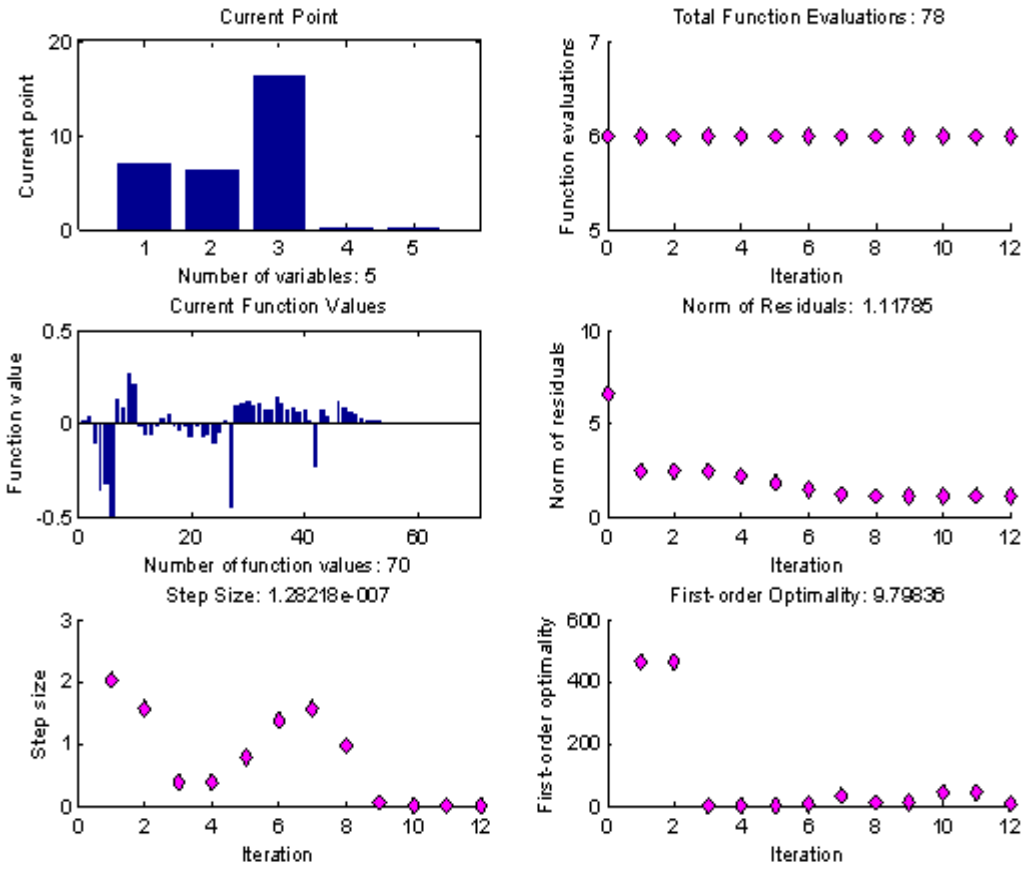

Figure 3.14. Analysis model parameters in the toolbox window.

3.4 Experimental

The capabilities of the model are studied in relation to the hydrocracking tests for Fischer-Tropsch waxes carried out by colleagues at the ENI laboratories in San Donato, Milan, Italy. The data were used for three different purposes: i) to tune the model parameters; ii) to determine the correspondence between the numerical time and the experimental time; and iii) to study the predictive capability of the model.

The experiments (hydrocracking tests) were carried out in a bench scale trickle bed reactor (ID=16mm) opened in down flow mode as shown in Fig. 3.15. The reactor was filled with 9 g of platinum (0.6%) supported on amorphous silica-alumina (SiO_2-Al_2O_3) catalyst which crushed previously and sieved to 0.625 mm average particle size. The catalyst pellet diameter was reduced in order to approximate plug flow behaviour. The feed used throughout the tests was a Fischer-Tropsch wax whose composition is given in Fig. 3.16: a mixture normal parafins ranging from C_5 up to C_{70}. The effects of

operating conditions (temperature, pressure, H_2/wax ratio and weight hourly space velocity (WHSV)) were investigated by a second order factorial design, the so called Central Composite Design (CCD) (Calemma et al. 2005). CCD consists of a complete 2^k factorial design with level coded to the -1, -0.5, 0, +0.5, +1, level; repeated central point (n_0) that in our case were 4; two axial point on the axis of each variable at distance β from the design centre. The operating range of the conditions was the following: temperature (324-354°C), pressure (40-60 bar), H_2/feed ratio (0.06-0.15 kg/kg), and WHSV (1-3 h^{-1}). Experiments carried out according to a factorial design allow to esteem in the most correct way the influence of each single factor (i.e.: temperature, WHSV, pressure and H_2/waxes ratio) on the response (i.e.: conversion, isomer concentration, etc.) minimising the influence of others factors and to evaluate the possible effect due to the interaction of variables. Fig. 3.17 gives a graphic view for three variables CCD.

Gas and liquid products were both analysis by Gas Chromatography (GC). Liquid produced was analysed by GC HP-5890 II equipped with a column injection system, electronic pressure control, and FID (Flame Ionization Detector) detector. The column used was a SPB-1 (Supelco) with a length 15m, internal diameter 0.53 mm and film thickness of 0.1 μm. The programme of the oven temperature was: 1 min at 0 °C then up to 315 °C, with a liner rise rate 5 °C/min and 37 min holding time at the final temperature. And the temperature programming of injector was: 1 min at 50 °C then up to 330 °C with a liner ramp rate of 5 °C/min and 37 min holding time at the final temperature.

Gaseous fraction of products was analysed by a GC HP 5890 II equipped with a FID detector and automatic sampling loop and the column used was a HP PONA (cross-linked methyl silossane) with a 50 m length, 0.2 mm internal diameter, and film thickness 0.5 μm. The temperature programming of the oven was: 7.5 min at 35°C, then up to 70 °C with a linear rise rate 3 °C/min, increase up to 220 °C at 7.5 °C/min and holding the final temperature for 45 min.

The carrier gas used for both analyses was helium. The total composition of hydrocracking products was obtained by summing tighter liquid and gas products

analyses according to their weight fraction. The experimental results for different operating conditions included in Appendix (2)

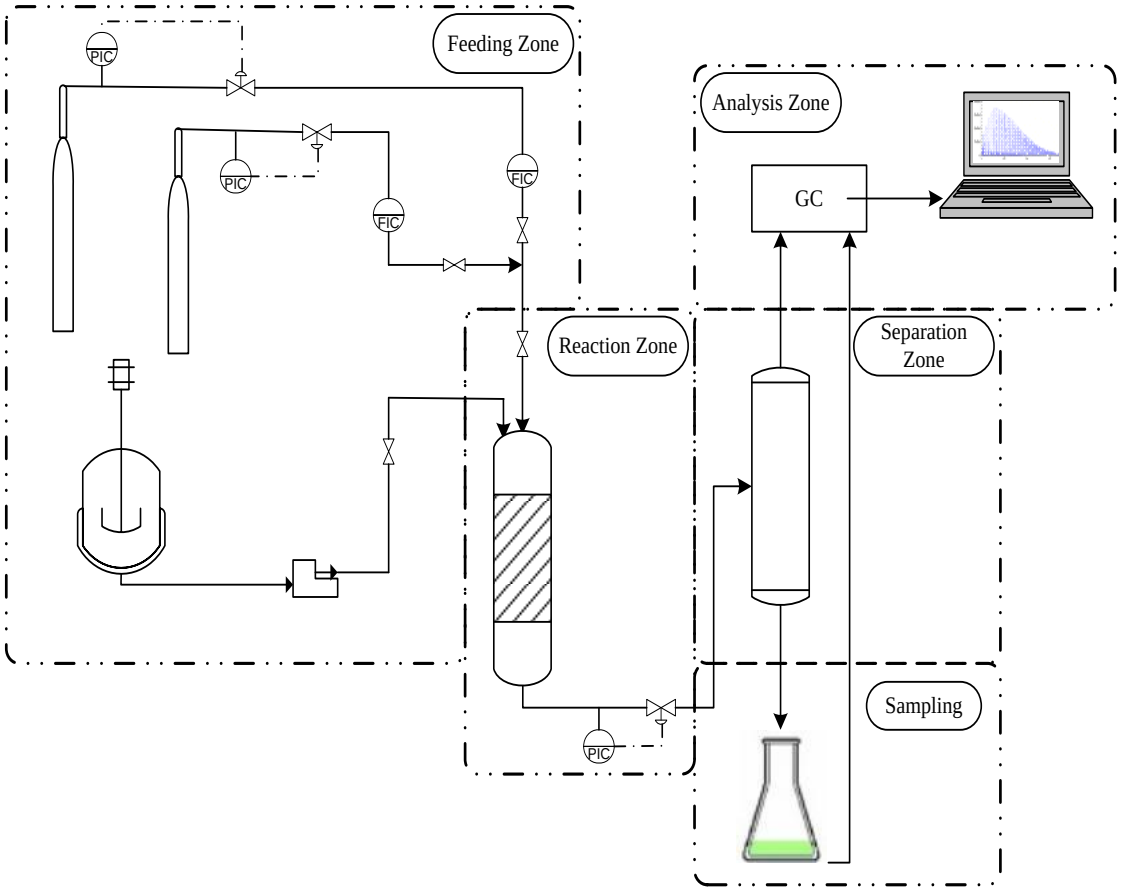

Figure 3.15. Simple schema for representation set-up of the experimental

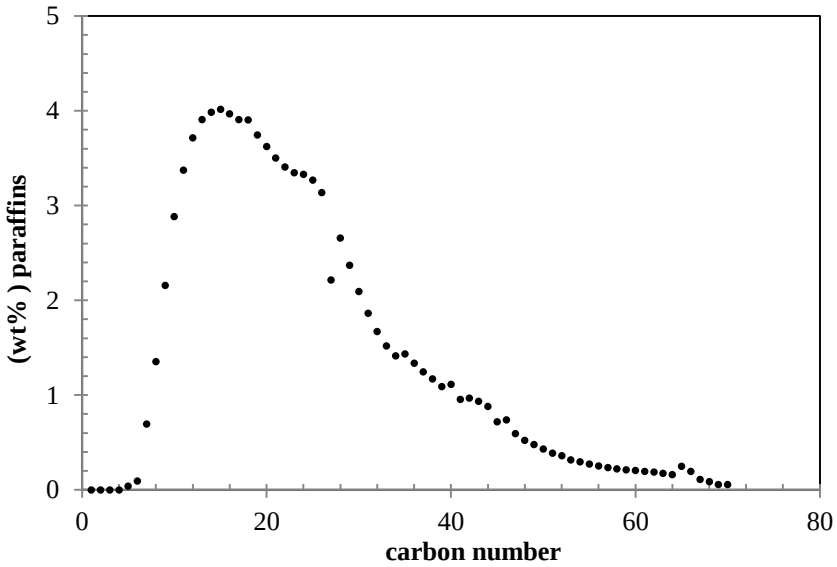

Figure 3.16. Feedstock composition

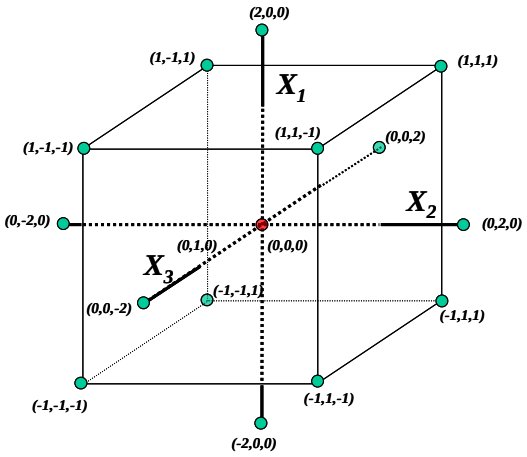

Figure 3.17. Central composite design in k=3 variables

3.5 Model simulation results and discussion

There are five factors affecting the cracking of n-paraffins, namely, temperature, hydrogen and paraffin ratio, space velocity (residence time), catalyst type, and the average carbon chain length. Therefore, the model estimated parameters must include all these factors to get a good result. The model has been applied to the twelve sets of experimental data. Experimental data reported in Appendix 2 were used for obtaining the optimal values of the model parameters. The model contains a number of parameters which have been tuned through an optimisation procedure. A sensitivity analysis study has been undertaken to determine how the various parameters change with the operating conditions. The methodology that has been followed furnishes the variability of the parameters with the chosen variable; such relations can be inserted into numerical programmes to calculate the parameters for a value of the operating variables different from the one attempted in the experimental runs. On every operating condition has done a separate optimisation for the modelling parameters. In the following the influence of temperature, WHSV, pressure, and H_2/feed ratio on product composition are explored.

3.5.1 The effect of temperature

Previous studies have shown that the temperature plays a role in the value of the reactivity. Consequently, the model was investigated (both for tuning and validation purposes) at three different experimental temperatures. For investigation of the effect of the temperature, the parameter α, which is introduced with the kinetic constants (or

equivalently with $D(k)$), separated from the parameters a_0 and a_1 that are introduced with the yield distribution. If the Arrhenius relation is assumed to be valid for kinetic constants, then, for each single species one can write:

$$k = k_0 e^{\frac{-E}{RT}} \tag{3.19}$$

where k_0 is the pre-exponential factor (independent of T), and E is the activation energy. Various expressions have been proposed for kinetic constants as a function of carbon number in hydrocracking process (e.g. Pllegrini et al, 2008). The following expressions have been introduced by Gambaro et al (2011):

$$k_{i0} = 2.5 \times 10^{-4} C_i^5 \tag{3.20}$$

$$E_i = 4 \times 10^4 C_i^{0.5} \tag{3.21}$$

where C_i is the carbon number of the species with pre-exponential factor k_{i0} and activation energy E_i. These expressions can be used in Eq. 3.6 and the corresponding value of α can be evaluated; its dependence on the temperature can be investigated as well.

To study the effect of temperature on the paraffin conversion and product distribution, the simulations have been carried out at three different temperatures (T=324 °C, 342 °C, and 354 °C) whilst the other operating conditions are kept constant (WHSV=2h^{-1}, pressure= 47.5 bar, and H_2/feed ratio=0.105 kg/kg). The comparison between trend of experimental data and modelling results in diagrams reporting weight fraction in the outlet stream vs. number of carbon is done for *Case A* and *Case B* and they are illustrated in Figs 3.18 and 3.19 respectively. As the temperature is increased, the general observed trend shows that the concentration of all components with longer chains decreases whilst the concentration of the components with shorter chain length increases. At low temperature, only components with long chains undergo cracking but at high temperature the selectivity of the reaction changes towards light components. A higher temperature results in higher rates of hydrocracking. The parafins experimental

and modelled conversion is shown in Fig. 3.20. The conversion increases approximately by 26% when the temperature increases by 22 °C, in agreement with evidence reported in the literature (Weismantel, 1992).

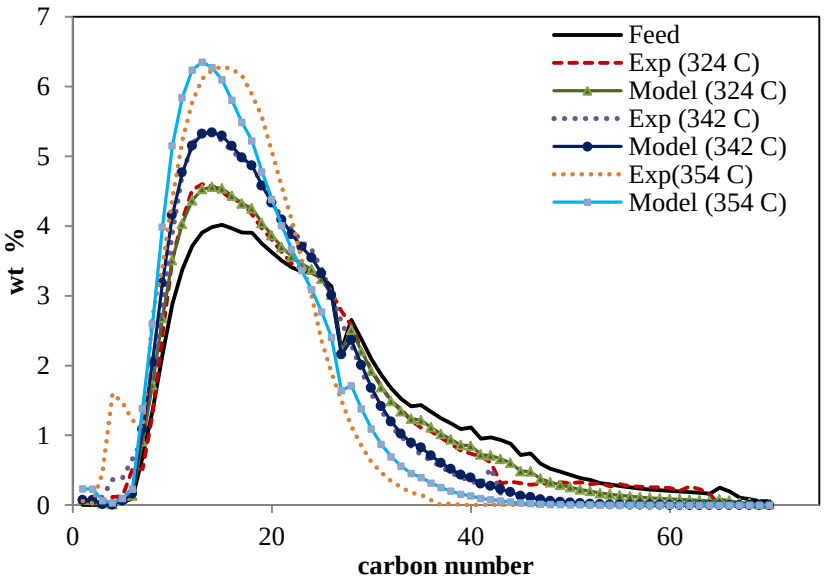

Figure 3.17. *Case A*- results for a given tests run, distribution of parafins.

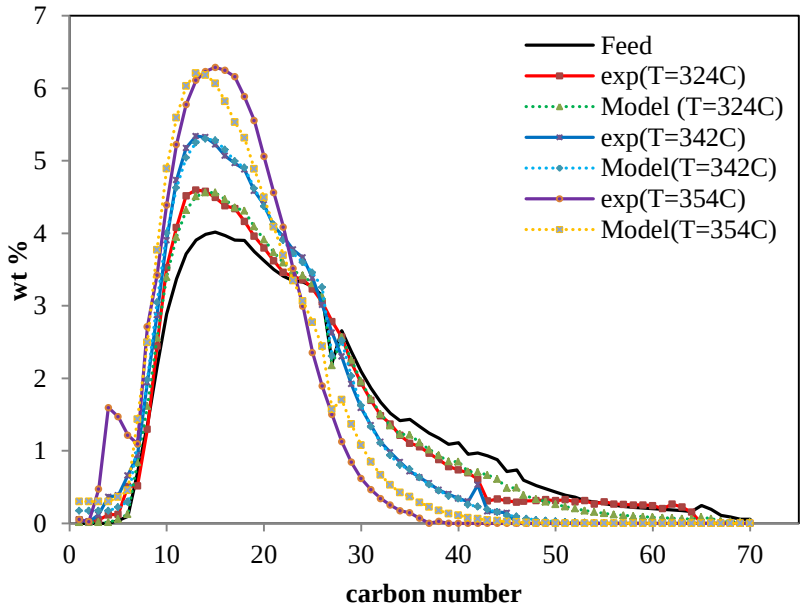

Figure 3.18. *Case B*- results for a given tests run, distribution of paraffins.

The hydrocracking conversion is defined according to the following equation:

$$\%C_{22+}(conv) = \left(\frac{\%wtC_{22+}in - \%C_{22+}out}{\%wt\ C_{22+}\ in}\right) \times 100 \qquad (3.22)$$

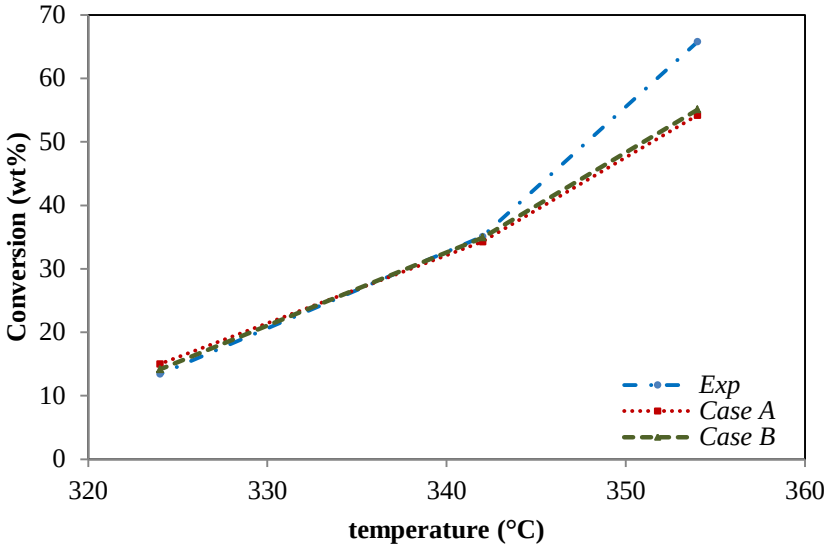

Figure 3.19. Effect of reactor temperature on conversion

The optimised model parameters at each temperature for *Case A* and *Case B* are presented in Table 3.1. *Case A* has five independent parameters and two additional parameters are required for *Case B*. These parameters were used to predict the yield distribution curve of the products. Both cases were used to determine the weight percent of species in the product which are compared with the experimental data.

	Model Parameters							
	Temperature (°C)	**a_0**	**a_1**	**k_{max}**	**α**	**δ**	**η**	**ζ**
	324	8.14	4.68	2.64	0.35	7.05E-07	--	--
Case A	342	6.00	3.80	8.08	0.40	9.05E-07	--	--
	354	5.82	3.60	32.08	0.314	7.05E-07	--	--
	324	9.66	2.78	2.860	0.500	1.28E-01	65.64	39.8
Case B	342	8.66	3.46	18.28	0.310	1.78E-02	40.64	44.8
	354	5.66	2.48	29.28	0.340	8.08E-01	40.64	40.8

Table 3.1. Predict parameters for the model at different temperatures.

The cumulative weights for feed, the experiments, and model predictions are reported in Fig. 3.21 and 3.22, for cases *A* and *B*, respectively. The hydrocracking of high molecular weight into low molecular weight causes shifts to the left of the distillation curves. It can be seen that the experimental data and the result from the model are practically indistinguishable for both cases at temperature 324 °C and 342 °C but when the temperature is increased to 354 °C , predicts are less good, especially for *Case A*.

Comparisons between experimental data and model calculations are shown in Fig. 3.23 and 3.24 for *Case A* and *Case B*, respectively. It can be seen that the comparison is very good. The parity plot of the product at different temperatures is presented in Fig 3.25 and 3.26. The results give a good indication of which components in the mixtures are described with less accuracy. The higher temperature seems to give less good results, especially in correspondence of low and middle length chain components. On the contrary, the very large chain components are described well at high temperature. Indeed, when the temperature is high the reactivity of the longest chain components should be higher; when the temperature increases, the longer chain components start cracking faster than what is observed through the model. At high temperature, the cracking of the components with longer chain is likely to produce more components with middle length chain (from C_{15} to C_{22}) than components with low length chain (from C_1 to C_{14}); however the opposite is observed from the model results. It means that increasing the reactor temperature decreases formation of hydrocarbons with short-chain and, therefore, reduces the number of secondary cracking reactions (Moller 2009).

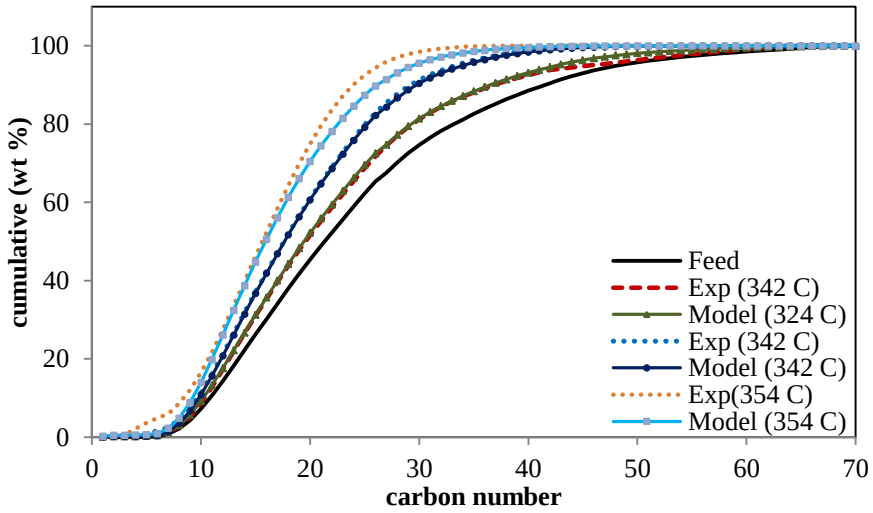

Figure 3.20. *Case A*- Cumulative predictions at different operating temperatures.

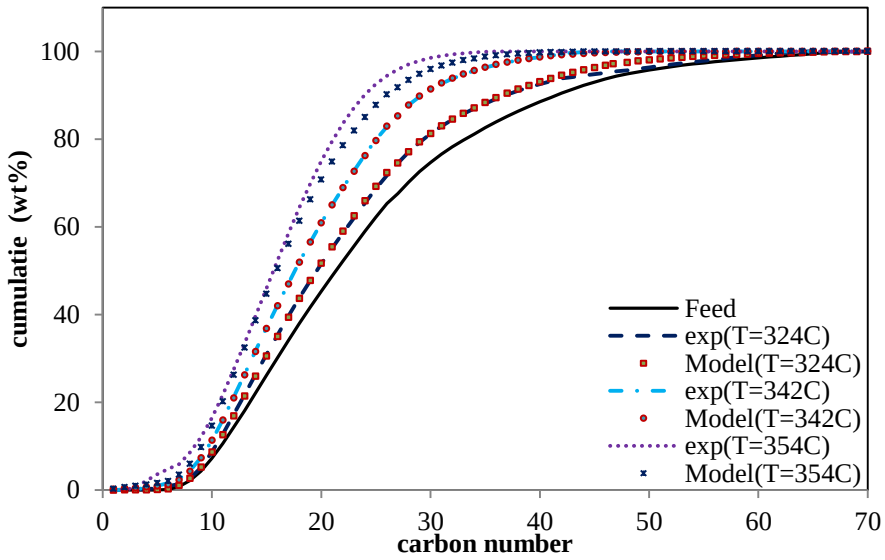

Figure 3.21. *Case B*-Cumulative predictions at different operating temperatures.

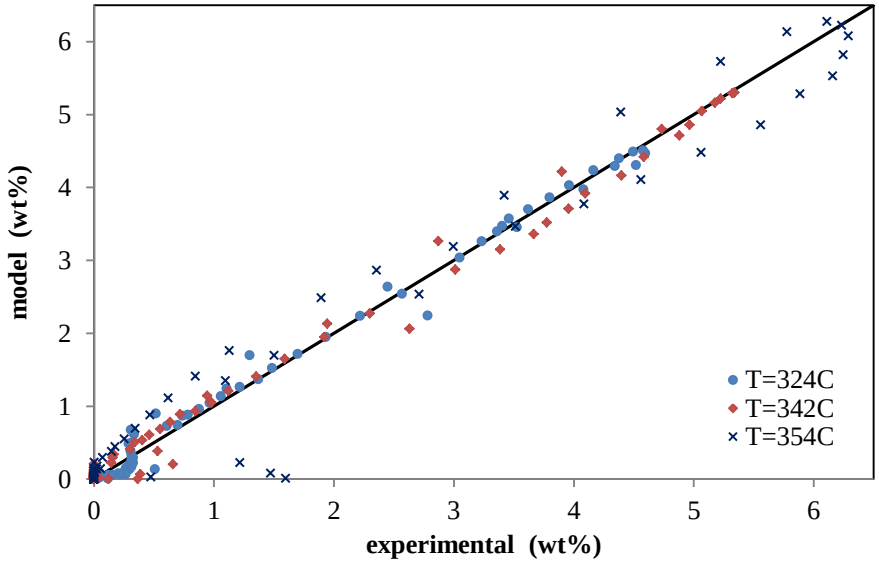

Figure 3.22. Parity plot between model calculation and experimental data for *Case A*

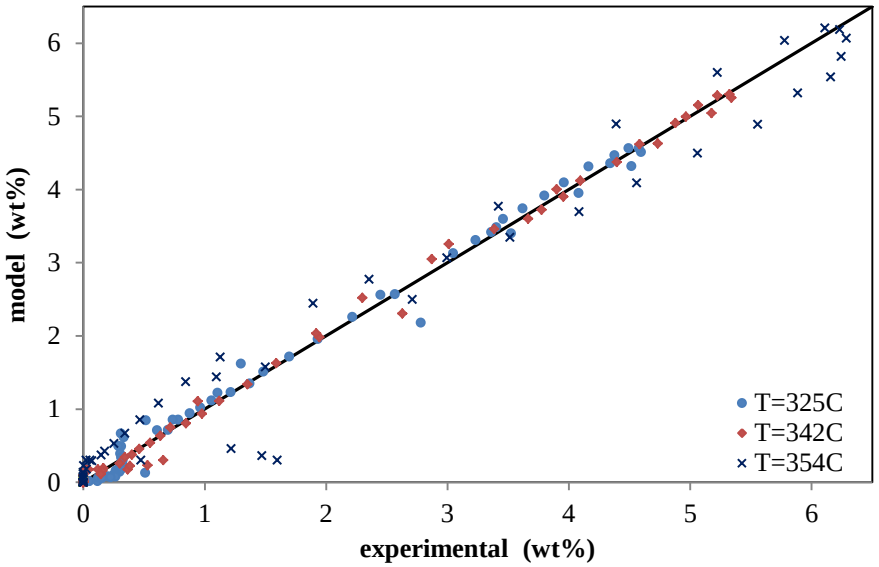

Figure 3.23. Parity plot between model calculation and experimental data for *Case B*

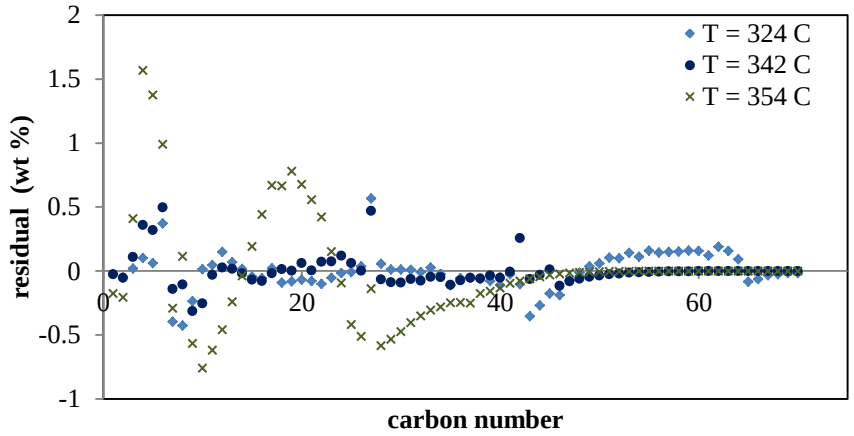

Figure 3.24. *Case A*- The residual values for the model product.

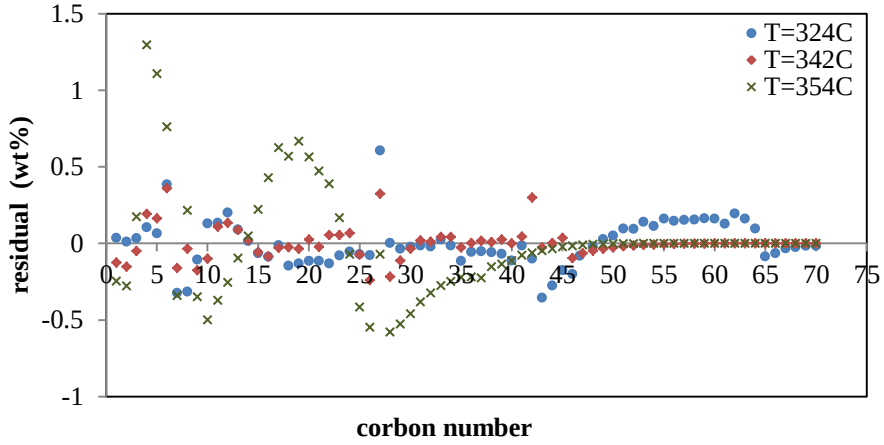

Figure 3.25. *Case B*- The residual values for the model product.

3.5.2 The effect of weight hourly space velocity (WHSV)

The residence time is an important variable which needs to be related to the numerical time. Indeed, if the model has to be used as a predictive tool, then one has to establish how long the model must run to mimic a given residence time. The residence time is the inverse of the weight hourly space velocity (WHSV) [$t = \frac{1}{WHSV}$]. The results in Fig. 3.27 and 3.28 for *Case A* and *Case B* respectively show the comparisons between model calculation and experiments data for three different WHSVs while the other common parameters (temperature, pressure, and H_2/feed ratio) are constant. It can be seen from these figures that more cracking occurs for the components which have heavier molecular weight with reducing the WHSV. It means that about a 48% increase in C_{22+} conversion occurs by reducing the WHSV from 3 h^{-1} to 1 h^{-1} (see Fig. 3.29).

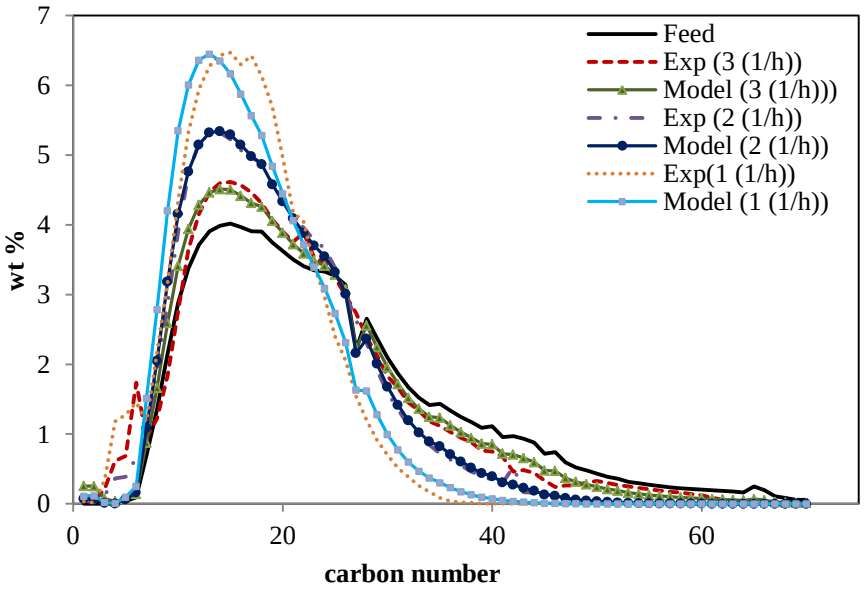

Figure 3.26. *Case A*- predictions at different operating WHSVs.

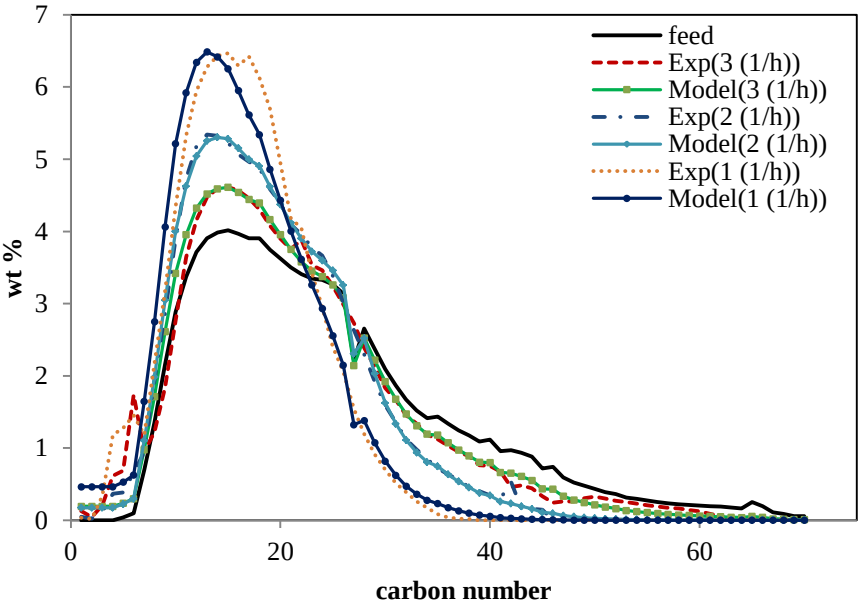

Figure 3.27. *Case B*- predictions at different operating WHSVs.

The model parameters which have been chosen to fit the experimental data for both cases are presented in Table 3.2. It can be seen that the reactivity (k) of the components, which have higher molecular weight, increase with decreasing WHSV. A good agreement between experiment data and model results can be noted as shown in Fig. 3.30 and 3.31. Although the *Case B* gives less error than *Case A* the error reduces with increasing the WHSV. The error could be due to the simultaneous cracking and dimerisation between low molecular weight components in the reactor at low space

velocity. Results of residuals for both cases are depicted in Fig. 3.32 and 3.33. The residuals vary in the range of 0.6 wt% to -0.7 wt% for both cases when the WHSV equals 3 h^{-1} but this range increases to 1.16 wt% to -1.13 wt% for *Case A* and 0.83 wt% to -0.87 wt% for *Case B* when the WHSV is reduced to 1 h^{-1}. The highest errors in both cases are shown in the carbon range between C_1 and C_{10} which form the gas part.

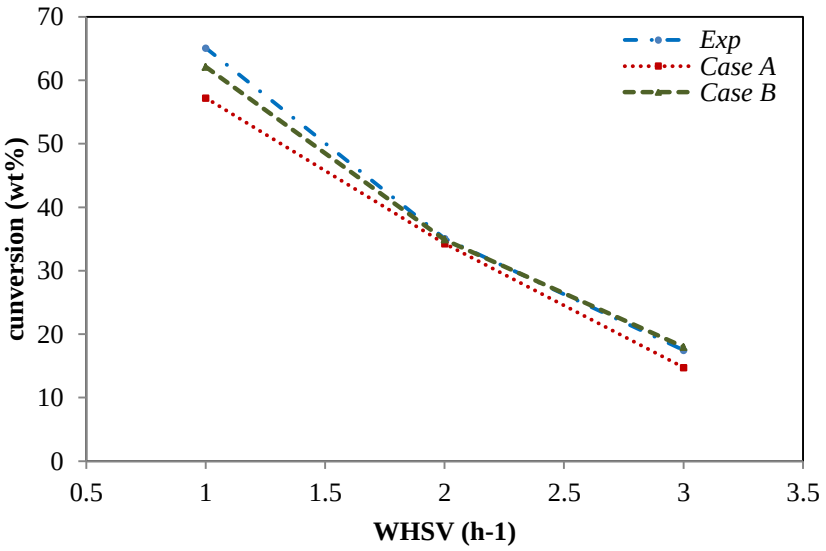

Figure 3.28. Effect of WHSV on conversion of C_{22+}.

		Model Parameters						
	WHSV (h^{-1})	**a_0**	**a_1**	**k_{max}**	**α**	**δ**	**η**	**ζ**
	1	6.84	23.9	21.05	0.2892	1.91E-09	--	--
Case A	2	6.00	3.80	8.08	0.40	9.05-07	--	--
	3	7.66	10.2	4.66	0.362	1.05E-09	--	--
	1	20.6	3.18	18.88	0.34	1.80E-01	35.64	40.8
Case B	2	8.66	3.46	18.28	0.310	1.78E-02	40.64	44.8
	3	5.66	5.18	6.02	0.380	1.78E-02	6.64	36.8

Table 3.2. Predict parameters for the model at different WHSVs.

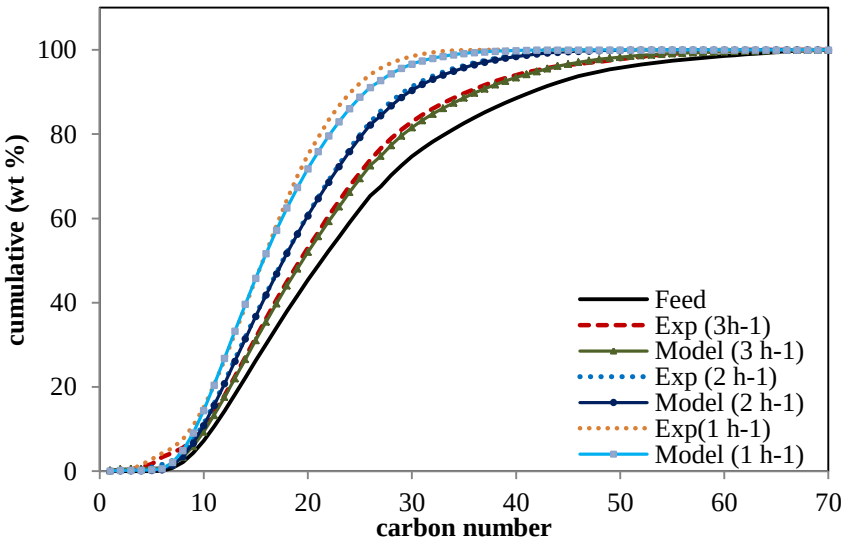

Figure 3.29. *Case A*- Cumulative predictions at different operating WHSVs.

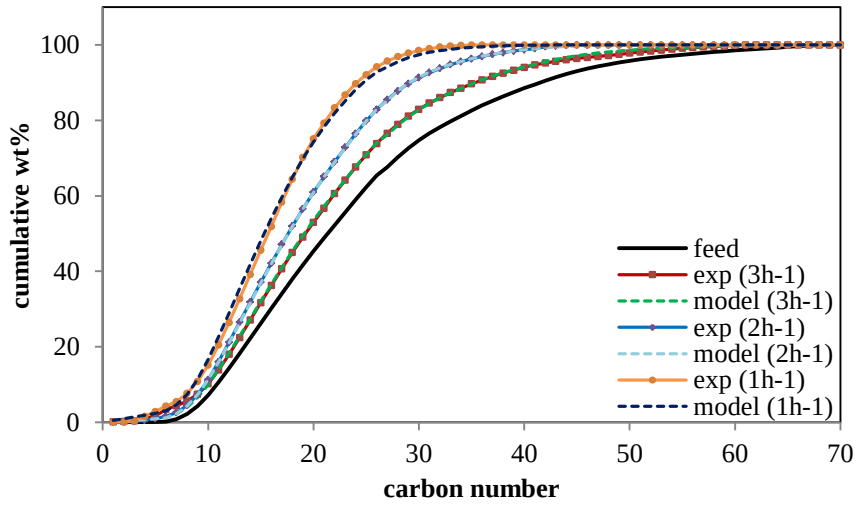

Figure 3.30. *Case B*- Cumulative predictions at different operating WHSVs.

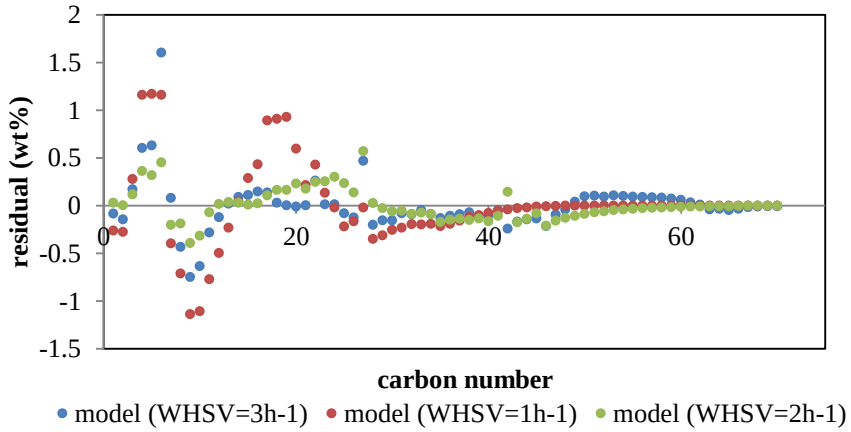

Figure 3.31. *Case A*- The residual value for the experimental runs.

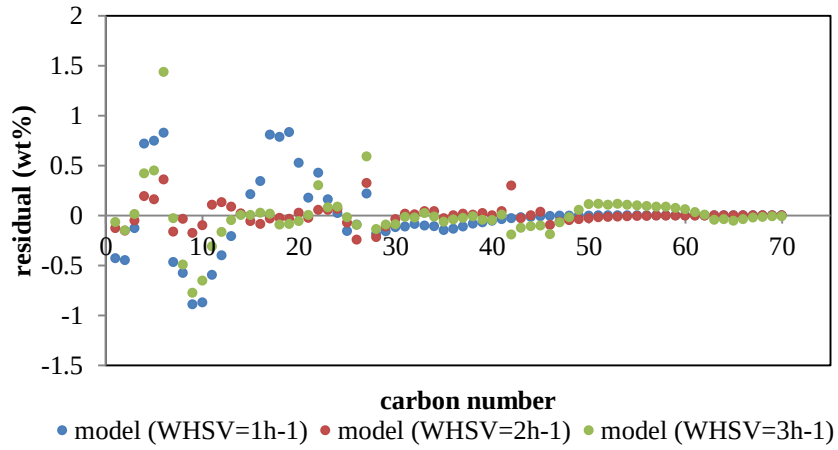

Figure 3.32. *Case B*- The residual value for the experimental runs.

3.5.3 The effect of pressure

The effect of total pressure at a constant temperature (342 °C), WHSV (2 h^{-1}), and H_2/feed ratio (0.105 kg/kg) has been simulated for three different reactor pressures (40 bar, 47.5 bar, and 60 bar). The experimental and model results are showed in Fig 3.34 and 3.35 for both cases respectively.

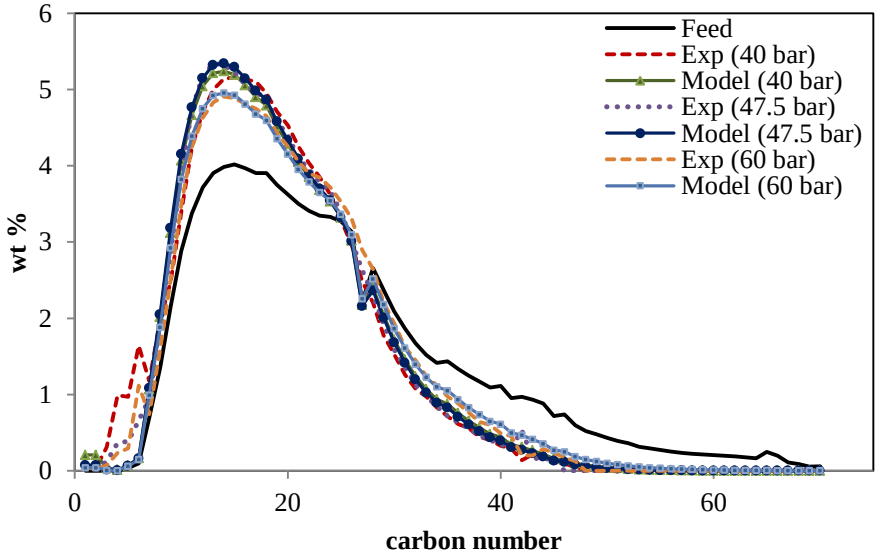

Figure 3.33. *Case A*- Calculated weight percent distributions at different operation pressure (bar).

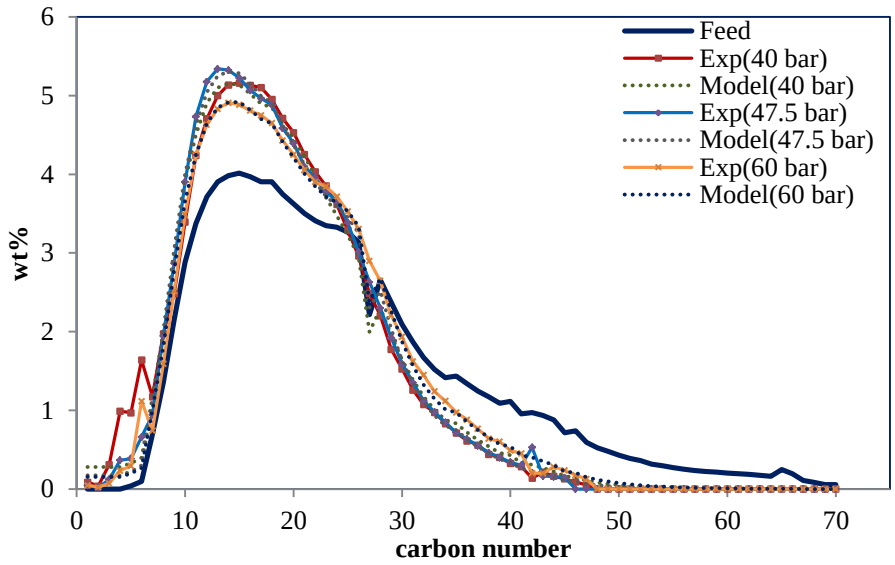

Figure 3.34. *Case B*- Calculated weight percent distributions at different operating pressure (bar).

As the pressure is increased, the concentration of the hydrogen in the liquid phase increases which in turn increases the rate of hydrogenation rather than increasing the rate of cracking. On the other hand, when the pressure reduces; the concentration of the lighter components increases making such components susceptible to crack again. This means that components having length chain between C_{15} and C_{22} are cracking again to produce components with lower length chain. The conversion of C_{22+} decreases with increasing the pressure due to the increase of the fugacity of hydrogen that affects negatively the dehydrogenation equilibrium of the feed (Gamba et al. 2009). In other words, the total conversion decreases because increased hydrogen fugacity that decreases the rate of dehydrogenation of the paraffin (Kumar and Froment, 2007). At high pressure, a low percent conversion was observed, while low pressure resulted in a high percent conversion. In other words, hydrocracking conversion is inversely related to the hydrogen pressure. The comparison between the experimental and modelling conversion is showed in Fig. 3.36. From the graph it can be seen that the *Case A* has the higher error at the pressure 40 reach to 12% compared to the *Case B* which is only 6 %. The error in both cases may come from the change the experimental peak in Fig. 3.34 and Fig. 3.35 when the experiment run at pressure equal to 40 bar. The cumulative comparison of model results and experimental data, at three different values of pressure for both *Case A* and *Case B* is shown in Fig. 3.37 and 3.38, respectively. The model results are in good agreement with the experimental data. The model parameters used are reported in Table 3.3 for each experimental run.

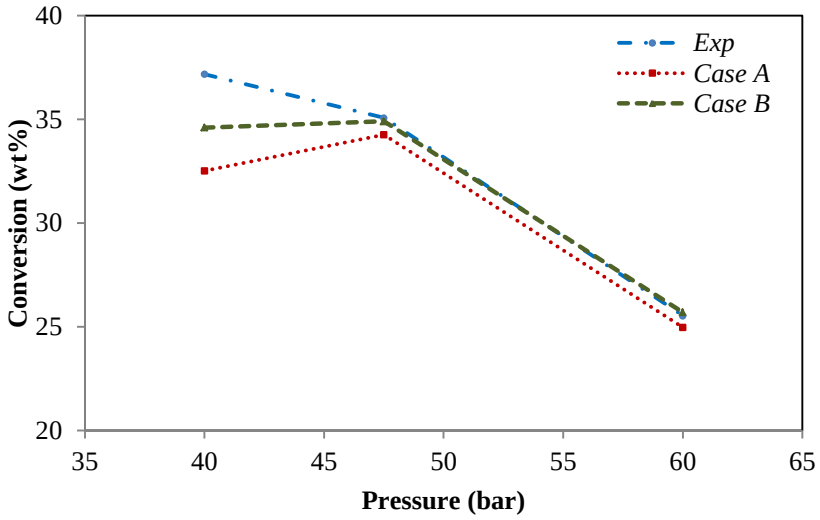

Figure 3.35. Effect of total pressure on the conversion of C_{22+}.

	Model Parameters							
	Pressure (bar)	**a_0**	**a_1**	**k_{max}**	**α**	**δ**	**η**	**ζ**
Case A	40	6.20	3.60	9.08	0.34	9.91E-07	--	--
	47.5	6.00	3.80	8.08	0.40	9.05E-07	--	--
	60	6.40	1.60	7.48	0.324	1.01E-06	--	--
Case B	40	4.66	4.88	13.88	0.33	1.78E-01	15.64	38.8
	47.5	8.66	3.46	18.28	0.310	1.78E-02	40.64	44.8
	60	4.66	4.88	11.46	0.31	1.78E-02	25.64	40.8

Table 3.3. Predict parameters for the model at different values of pressure.

Dividing the components into groups based again on the carbon number, namely C_1-C_4 (fuel gas), C_5-C_9 (naphtha), C_{10}-C_{14} (kerosene), C_{15}-C_{22} (diesel), and C_{23+} (residue) gives a better understanding of the behaviour of the mixture with change in total the pressure. The influence of the total pressure on the weight fraction of the outlet groups is shown in Fig. 3.39. It can be seen that the model has a good agreement with the experimental data. The middle distillate (kerosene and diesel) yield increased up to 60 wt% along with C22+ fraction conversion at pressure 40 bar but this value is reduced to 57 wt% by increasing the pressure to 60 bar. Fuel gas and naphtha reach maximum yields of 1.6 wt% and 8 wt% at 40 bar but are reduced to 0.6 wt% and 6 wt% when the pressure is increased to 60 bar, respectively. And the residual is increased from 30 wt% to 36 wt % by increasing the pressure from 40 bar to 60 bar.

It should be noted that, in contrast with what happens for temperature, changes in pressure do not have an appreciable effect on the results, at least for the range of values considered in this study. It means increasing pressure in the reactor has little effect on the conversion. Increasing the pressure may increase coke yield in the reactor that is not studied by this model.

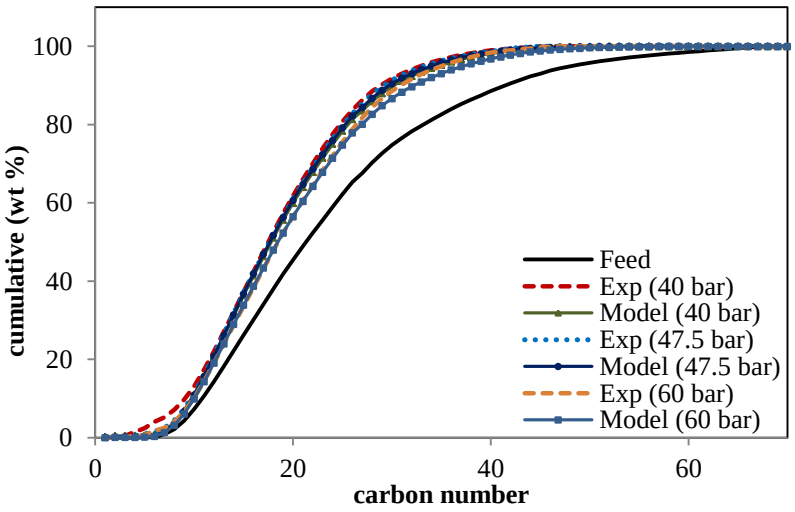

Figure 3.36. *Case A*- Comparison of predicted and experimental data of cumulative weight percent.

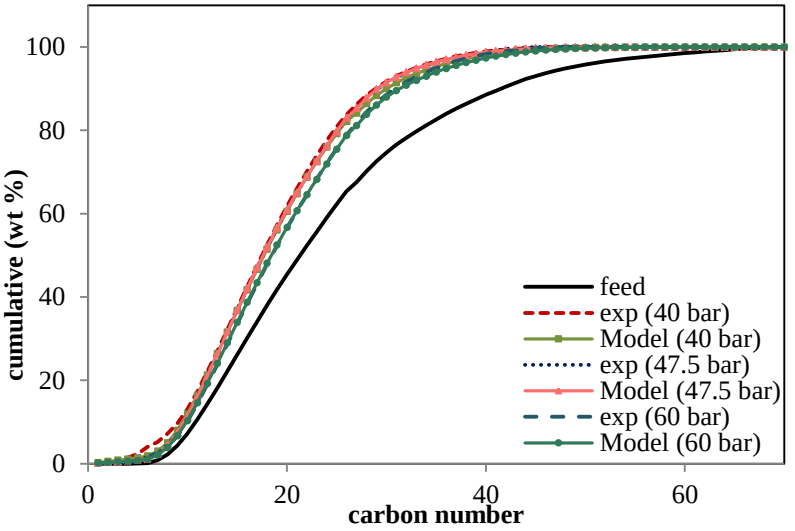

Figure 3.37. *Case B*- Comparison of predicted and experimental data of cumulative weight percent.

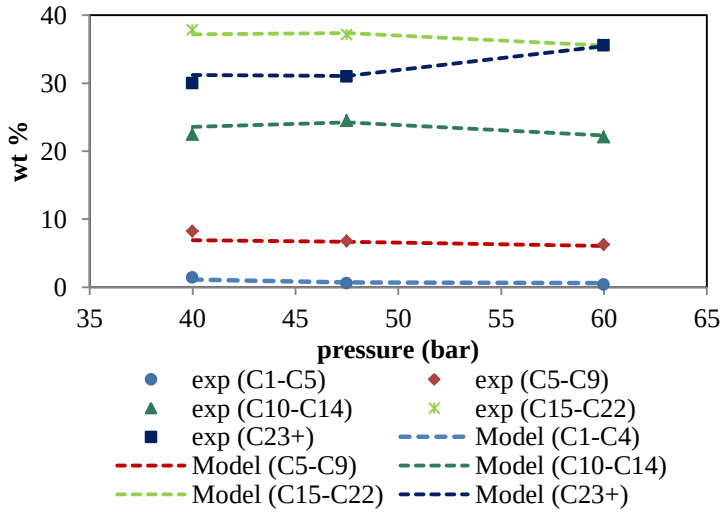

Figure 3.38. Pressure effect on the weight percentage of outlet groups (*Case B*).

3.5.4 The effect of H_2/feed ratio

Typical model results for given different values of H_2/Feed ratio (0.06, 0.105, and 0.15 kg/kg) and the other operating parameters kept constant (temperature = 342 °C, pressure = 47.5 bar, and WHSV = 2 h^{-1}) for both cases are shown in Fig. 3.40 and 3.41, respectively. The optimal estimated model parameters were used to predict the distillation curve of hydrocracking product to compare with the experimental data. The variations of the model parameters, when the H_2/Feed ratio is changed, are reported in Table 3.4 for both cases.

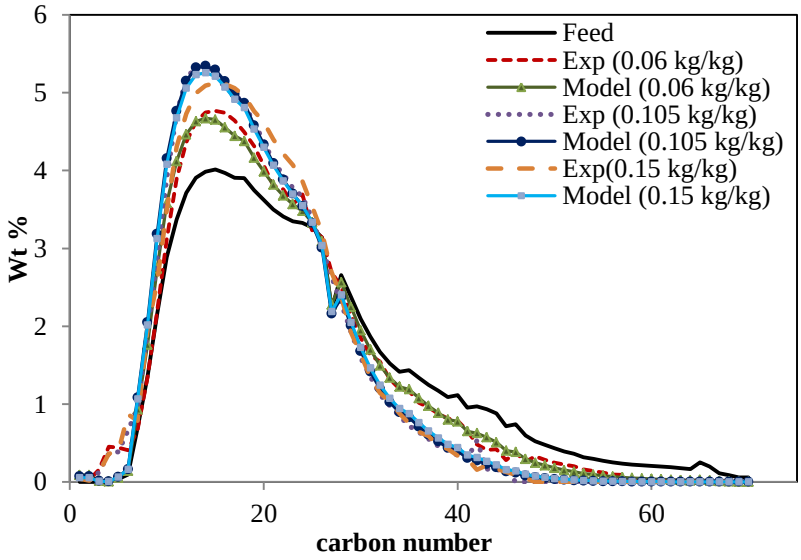

Figure 3.39. *Case A*- Comparison between calculated and experimental data at different values of H_2/Feed ratio (kg/kg).

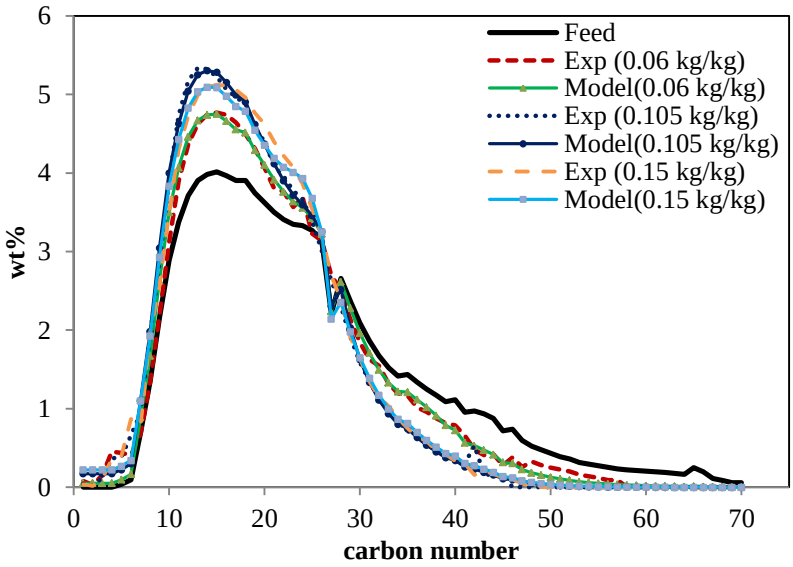

Figure 3.40. *Case B*- Comparison between calculated and experimental data at different values of H_2/Feed ratio (kg/kg).

The reactivity of the components with longer chain increases as the hydrogen-to-hydrocarbon ratio increases. The most obvious effect of increasing the H_2/Feed ratio was the increase in C_{22+} cracking conversion. At the H_2/Feed ratio 0.06 kg/kg the cracking conversion was 18% and this conversion goes up to 35% when the H_2/Feed ratio increased to 0.105 kg/kg. The hydrogen-to-wax ratio has the lowest impact on the wax conversion compared with the other parameters (temperature, WHSV, and pressure). Increasing the hydrogen-to-wax ratio has a great effect on the hydrocarbon distribution between the liquid and gas phases and works as a stripping agent to deplete the lightest hydrocarbons in the liquid phase (Camba et al, 2010). Moreover, the hydrogen-to-wax ratio affects equilibrium more than the other operating variable (Pellegrini et al., 2008).

Fig. 3.42 shows the effect of increasing the hydrogen to wax ratio on the conversion when the yield is divided into five lumps for *Case A*. It can be seen that, with increasing hydrogen-to-wax ratio the weight percent of fuel gas reduced from 0.716% to 0.533% and the residual lump is reduced from 38.9% to 32%. However, the other lumps (naphtha, kerosene, and diesel) have a limited increase when increasing the hydrogen-to-wax ratio from 0.06 to 0.15 kg/kg. Both cases give a good agreement with the experimental data with error in the conversion less than 5%.

	Model Parameters							
	H_2/Feed ratio kg/kg	a_0	a_1	k_{max}	α	δ	η	ζ
	0.06	5.20	1.80	4.284	0.358	1.11E-07	--	--
Case A	0.105	6.00	3.80	8.08	0.40	9.05E-07	--	--
	0.15	6.20	3.60	8.88	0.30	2.01E-07	--	--
	0.06	4.66	4.88	13.88	0.33	1.78E-01	15.64	38.8
Case B	0.105	8.66	3.46	18.28	0.310	1.78E-02	40.64	44.8
	0.5	4.66	4.88	11.46	0.31	1.78E-02	25.64	40.8

Table 3.4. Predict parameters for the model at different values of H_2/Feed ratio.

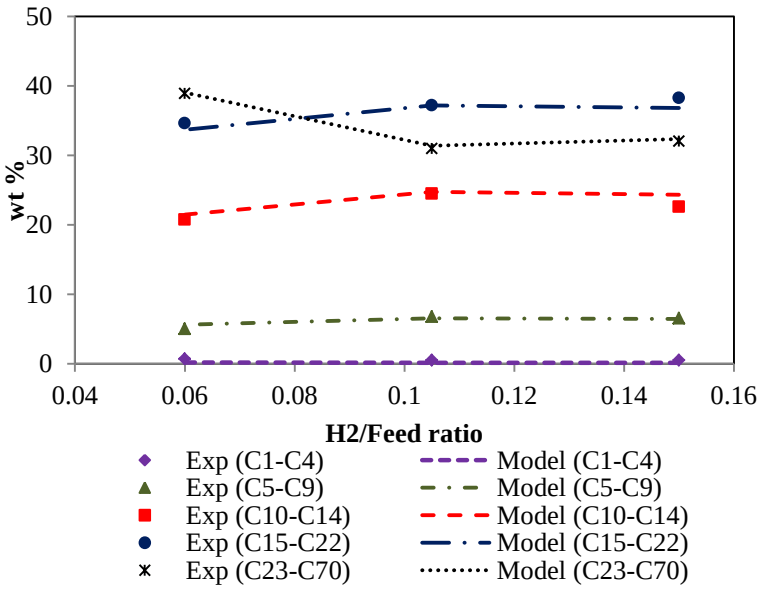

Figure 3.41. *Case A*- Comparison between calculated and experimental data for 5 lumps analysis at different values of hydrogen-to-wax ratio

3.5.5 The reactivity of the species

Fig. 3.43 shows the relationship between reactivity of species against the operating conditions, where it is worth-noting that the reactivity of species of higher molecular weight can be more affected by changing temperature and WHSV compared to that at different conditions of pressure change and H_2 feed ratio. It means that, a conversion of components possessing high molecular weight increases to produce components of low molecular with increasing the temperature or residence time. While the effect of the pressure and the H_2 feed ratio are less on the overall conversion.

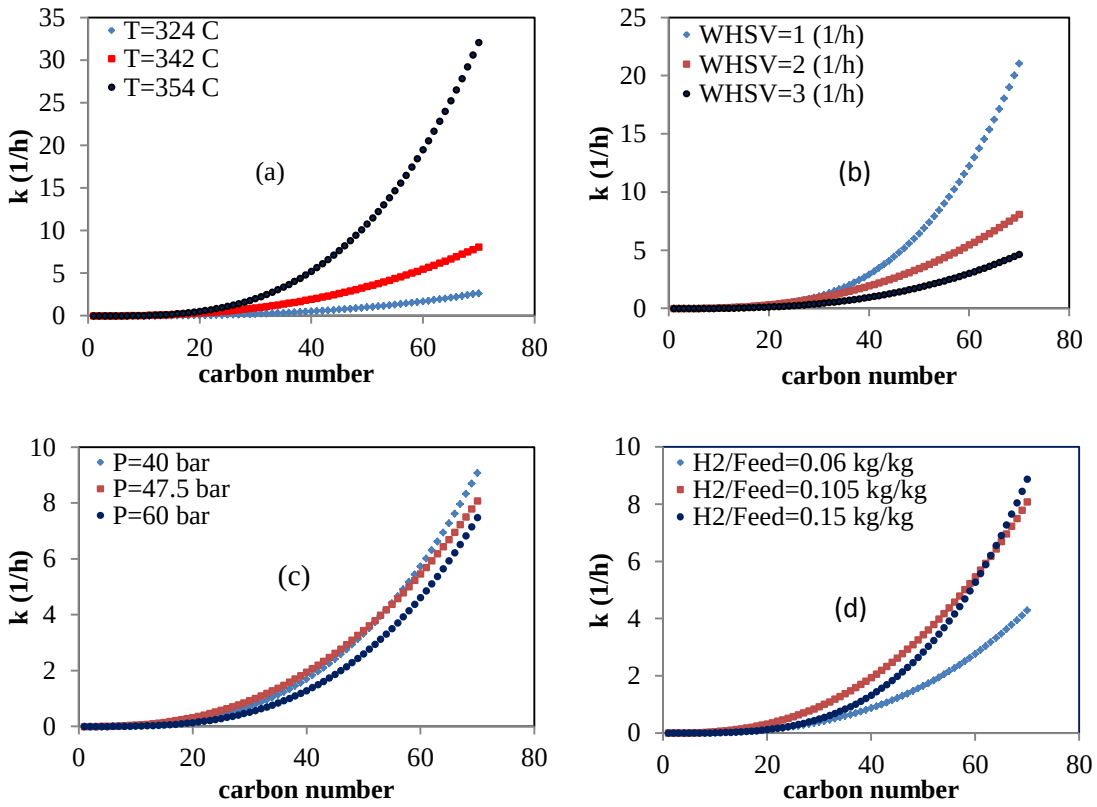

Figure 3.42. Changing reactivity of species with changing the operating condition: (a) changing temperatures, (b) changing WHSV, (c) changing pressures and (d) changing H_2 feed ratio.

3.5.6 Model parameters

The operating variables such as temperature, pressure, space velocity, and hydrogen-to-wax ratio have different effects on the hydrocracking reactions and conversion and also have different effects on the model parameters. The effect of temperature on continuum lumping model parameters has been observed by Khorasheh et al. 2005 and Elizalde et al 2009. A linear dependence has been proposed for $a_0, a_1, \alpha, and\ \delta$ parameters as following:

$$a_0\,, a_1\,, \alpha, and\ \delta\ =\ b + \ m \times T \tag{3.23}$$

where T is a temperature in (°C). Whereas k_{max} has been correlated with the temperature by using the Arrhenius relationship as follows:

$$\ln(k_{max}) = b + \frac{m}{T} \tag{3.24}$$

where T is in Kelvin (K).

Fig. 3.44 demonstrates the effect of the variation temperature on the model parameters for *Case A*. It can be observed that within the range of temperature (324-354 °C) this dependence is linear. The correlations developed for temperature parameters ($a_0,\ a_1,\ k_{max},\ \alpha,\ and\ \delta$) are reported in Table 3.5. The frequency factor and activation energy of the n-paraffins (waxes) hydrocracking reaction are obtained from slope and intercepts of the straight line from a plot of the values of $1/T$ vs. $ln(k)$ and are given in Table 3.6. From the Table it can be seen that both cases almost give the same activation energy and frequency factor.

Model parameters (y)	Temperature dependent variable (x)	$y = b_i + m_i * x$	
		b_i	m_i
a_0	T	34.062	-0.0806
a_1	T	16.613	-0.037
k_{max}	$1/T$	51.811	-30.414×10^3
α	T	0.6559	-0.0009
δ	T	5×10^{-7}	9×10^{-10}

Table 3.5. Constants for Eqs. (3.23) & (3.24) at pressure = 47.5 bar, WHSV= 2 h^{-1} and temperature range (324-354 °C)

	Case A		***Case B***	
	A_0 (h^{-1})	E (J/mol.K)	A_0 (h^{-1})	E (J/mol.K)
	3.17E+22	252.88	1.5498E+22	247.8624

Table 3.6. Activation energy and frequency factor for hydrocracking waxes.

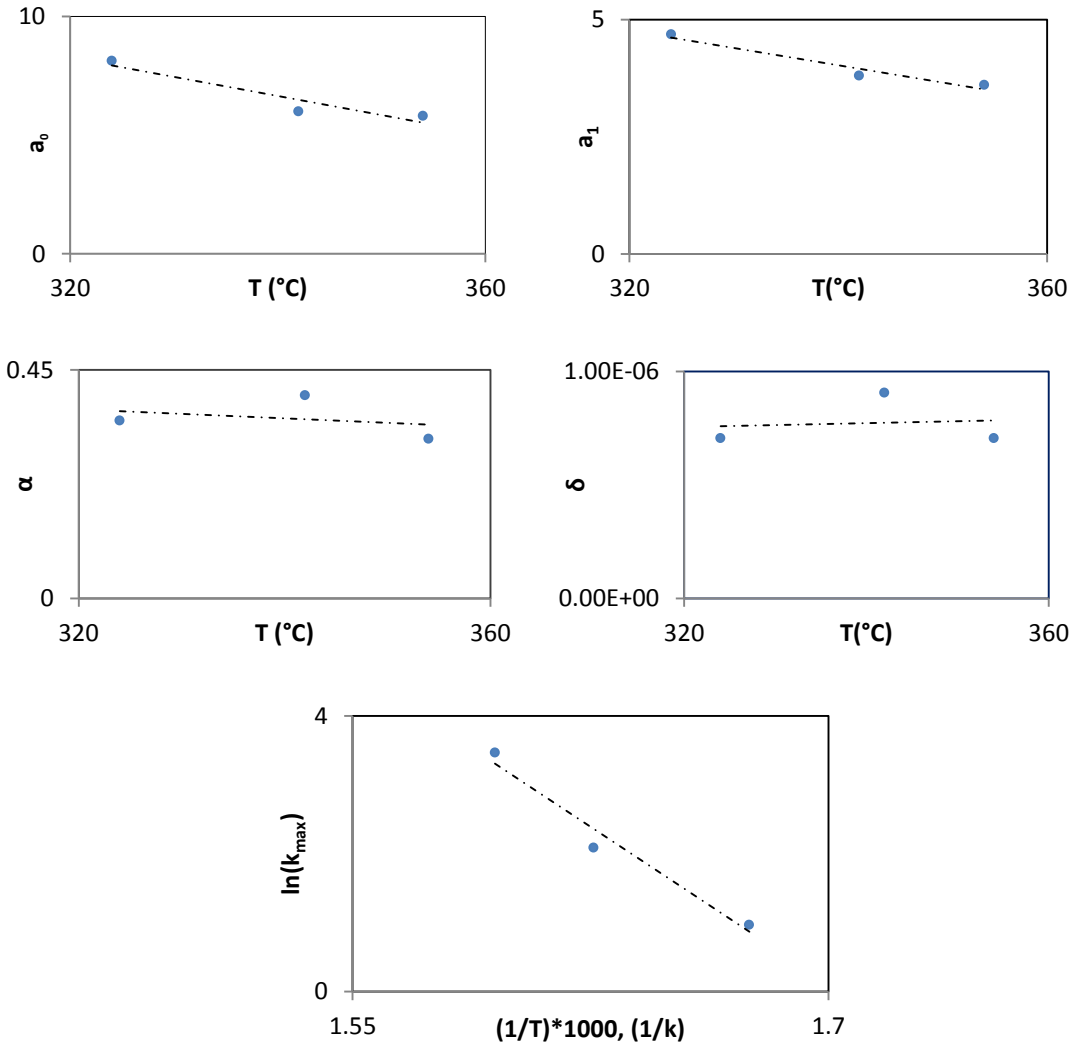

Figure 3.43. *Case A*- Variation of optimized values of parameters with temperature.

The effect of both pressure and temperature on the rate constant for the hydrocracking of n-paraffins can be determined by using the modified Arrhenius equation as follows (Sanchez, et al 2007 and Elizalde et al. 2010):

$$k = A_0 \exp(-\frac{E}{R.T})(\frac{P}{P_0})^{\beta} \tag{3.25}$$

where P_0 is a reference pressure, β is a pressure dependent parameter, and R a gas constant. According to Eq. 3.25 the dependence of k_{max} with temperature and pressure can be expressed as:

$$\ln(k_{max}) = \mathrm{A} + \frac{B}{T} + C\ln(\frac{P}{P_0}) \tag{3.26}$$

The terms A and B account for the effect of temperature and term C accounts for the effect of the pressure on the model parameters. The other model parameters $(a_0, a_1, \alpha, and\ \delta)$ can be correlated by the following correlation:

$$a_0, a_0, \alpha, and\ \delta = A + B\left(\frac{T}{T_0}\right) + C\left(\frac{P}{P_0}\right) + D\left(\frac{P}{P_0}\right)\left(\frac{T}{T_0}\right) \tag{3.27}$$

where the T_0 and P_0 are the reference temperature and pressure respectively. They have been considered to be the lowest experimental parameter in this study that is 330 °C and 40 bar. And D is a constant for accounting for the combined effect of temperature and pressure on model parameters. The constant values of the Eq. 3.26 and 3.27 are reported in Table 3.7. Note: (T and T_0 in K; P and P_0 in MPa) in both equations 3.26 and 3.27.

Model parameters (y)	y= Eq. 3.26 or Eq. 3.27			
	A	B	C	D
a_0	322.0415	-308.6754	-265.3163	259.136
a_1	2.0849E03	-2.0420E03	-1.6750E03	1.6436E03
k_{amx}	32.2095	-1.8397E-04	0.9707	0
α	-31.8842	31.2861	28.2374	-27.3771
δ	-2.0163E-04	1.9915E-04	1.4992E-04	-1.4747E-04

Table 3.7. Constants of the Eq. 3.26 and 3.27.

3.6 Conclusions

A continuous model with two types of formulation for species-type distribution function has been presented in this chapter. Two different expressions for the reactant-type distribution function have been considered, namely a power-law distribution (*Case A*) and a gamma distribution (*Case B*). The model was applied to the catalytic hydrocracking of Fischer-Tropsch wax (normal paraffin) which consists from C_5 to C_{70}. The effects of operating parameters such as temperature, pressure, hydrogen-wax ratio,

and weight hourly space velocity (WHSV) on model parameters have been investigated. The kinetics and product distribution parameters for both cases were fine-tuned by using experimental data to calculate the weight percent of the products. The reactivity of the heavy species increases with increasing temperature and WHSV but decreases with increasing the pressure. The error percentage of the model increases with increasing the conversion due to our assumption that all components in the mixture will crack whereas in reality cracking may happen only to the components that have high molecular weight. Or another reason for the error is due to the first order kinetics assumed in the model.

CHAPTER 4.

Case (II) – Lumping Kinetics Modelling of Pyrolysis of Lignin

In this chapter, a study is undertaken to assess the suitability of the lumping approach to describe the kinetics of pyrolysis of Kraft lignin. The model is then validated against experimental data obtained in a fluidised bed pyrolyser. Two discrete lumping models have been developed to describe the kinetics of primary and primary and secondary reactions of lignin pyrolysis. A reaction scheme of a set of three parallel reactions to predict the pyrolysis yields (tar, gas, and char) has been used in the first model, whereas the second model used a reaction scheme of a set of three parallel reactions followed by a one parallel reaction to describe the primary and secondary reactions of lignin pyrolysis. A first order kinetic reaction has been applied for all reactions to predict the product yields. Subsequently, a continuum model, developed in chapter three, is applied to describe the upgrading (fractionation) of the produced tar. The aim here is to present models that consider only the (lumped) reactions. The two discrete lumping models for the primary and secondary pyrolysis are introduced with the aim of providing the formation route for the lump (i.e. tar) that will be subsequently fractionated.

4.1 Introduction

Utilisation of renewable resources for fuels and chemicals is one of the ways to reduce a greenhouse gas emission. Biomass has been identified as a source of organic material that can be converted into fuel liquid (Huber et al., 2006). Biomass consists of three major components: cellulose, hemicelluloses and lignin. Every component has different characteristics through its thermal decomposition. There are many methods that are used to extract the energy from biomass, for example, gasification, direct combustion and pyrolysis. Interest in the pyrolysis process has surged recently since pyrolysis converts the solid biomass into liquid, which can be successfully used for

product heat and chemicals, char and gas with reduction in CO_2 emission compared with combustion, thus making biomass to energy a clean and green technology.

4.1.1 Lignin structure

Lignin is an organic polymer and it is, after cellulose, the second most abundant renewable carbon source, accounting for approximately 30% in the biosphere (Whetten et al. 1995 and Saiz-Jimenez et al. 1986). Lignin is not one compound, but a co-polymer of three hydroxycynnamly alcohol monomers (usually referred to as phenyl propane monomers) differing in their degree of methoxylation: p-coumaryl, coniferyl, and sinaply alcohols (Boerjan et al. 2003). Their molecular weights may reach 15000 kg/kg.mol or more in their natural form. Given its abundance and structure, exploitation of lignin as a source of bio-oil is of importance especially because it can lead to the production of interesting aromatic products. The lignin structures can be divided into three different structures. These structures are designated as Lig-C, Lig-O, and Lig-H as shown in Fig. 4.1 (Faravelli et al. 2010). The structure of lignin varies depending on their plant source and on the isolation method used (Lora et al. 2002). More details about lignin structures can be found in the literature such as (Ikeda et al. 2002) and (Guerra et al. 2006). Kumar (2009) gave some factors that control the properties and functionality of lignin preparations:

- Source of lignin. For example the typical carbon contents of softwood lignin and hardwood lignin are 64% and 60% respectively.
- Methods used to remove lignin from plant. There are different methods for obtaining lignins such as krait process, enzymatic treatment, alkaline treatment, and steam explosion.
- Method(s) used for lignin purification. The Lignins obtained by industrial processes are usually contaminated with cellulose, hemicelluloses and other inorganic impurities. So any method used will give different of lignin structures.
- The nature of the chemical modification of the lignin.

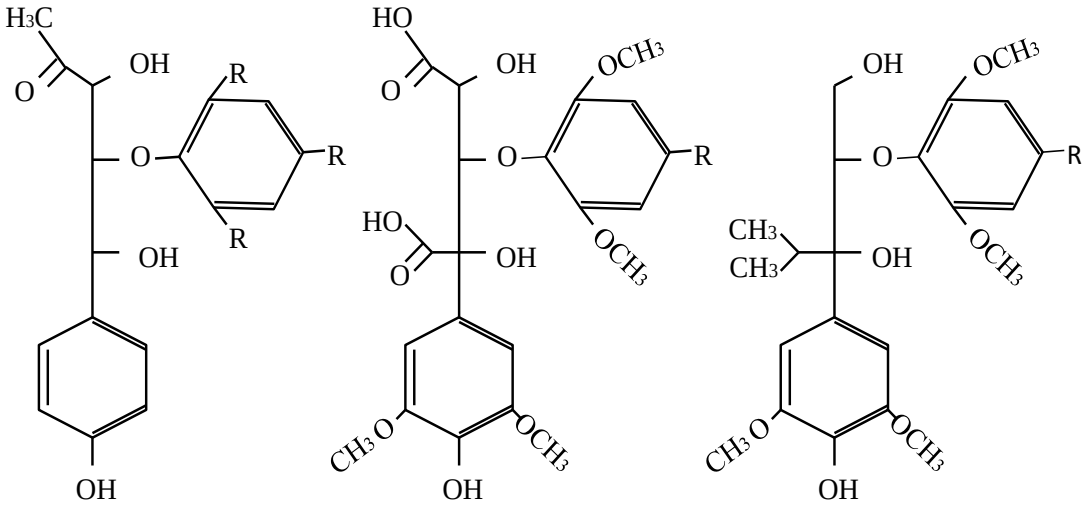

LIG-C $C_{17}H_{15}O_5$ (68.5%C, 4.7%H, 26.8%O

LIG-O $C_{17}H_{10}O_8(OCH_3)_4$ (54.0%C, 4.7%H, 41.3%O

LIG-H $C_{18}H_{18}O_4(OCH_3)_4$ (62.8%C, 6.7%H, 30.5%O

Figure 4.1. The structure of the three main components in lignin composition.

4.1.2 Lignin pyrolysis

Large amounts of lignin are produced as a by-product in the production of high-quality cellulose pulps; its extensive future utilisation would rely on the development of an economically favourable technology for converting lignin into useful liquid, gaseous and solid products. Two major thermal processes are used to extract energy from lignin: direct combustion and pyrolysis.

Pyrolysis is the most promising way to convert lignin (biomass) into lower molecular weight liquid and/or gas products. In other words, pyrolysis of lignin is a method to upgrade this material into higher value products. Pyrolysis is a thermal decomposition process, pursued at high temperature in the absence of oxygen, to produce gas, liquid, and solid (char) products. It is an irreversible process and generally produces chemical components in the form of vapours, aerosols and solid. The non-condensable vapours consists of gases species such as CO, CO_2, CH_4 and H_2 while the solid residue obtained from the pyrolysis is called char. The total yields are due to decomposition of the raw material (primary reaction) and to the reaction undergone by the primary volatiles (secondary reactions). The temperature and the residence time of the volatiles in the reactor are the relevant parameters for the secondary reaction (Caballero et al. 1996). There are three types of pyrolysis technology: slow pyrolysis,

fast pyrolysis and flash pyrolysis. In the slow pyrolysis model, low heating rates and long vapour residence times are employed to maximize the char formation while fast pyrolysis can be achieved by rapid heating of biomass with low vapour residence times. The flash pyrolysis utilises high temperature and the major product is gaseous species. Table 4.1 presents the pyrolysis technology, parameters and product distribution (Patwardhan, 2010).

Pyrolysis technology	Process conditions			Products		
	Residence time	Heating rate	Temperature	Char	Tar	Gases
Slow pyrolysis	5-30 min	<50 °C/min	400-600 °C	<35%	<30%	<40%
Fast pyrolysis	<5 sec	~ 1000 °C/s	400-600 °C	<25%	<75%	<20%
Flash pyrolysis	<0.1 sec	~ 1000 °C/s	650-900 °C	<20%	<20%	<70%

Table 4.1. Pyrolysis technology, process parameters and products

The pyrolysis of lignin depends on several factors such as the composition of lignin, the temperature of reaction, the heating rate and the design of the pyrolyser (Ferdous et al., 2002). During the thermal decomposition of lignin, weak bonds break at low temperature whilst strong bonds break at higher temperature. At temperatures higher than 500°C, the aromatic rings rearrange themselves and release H_2, CO and CH_4 with production also increasing with increasing reactor temperature. CO is produced from two types of ether groups; at low temperatures the main source of CO is the ether bridge joining subunits, since this group has a low dissociation energy (60-75 kcal/mol). At higher temperatures, dissociation of diaryl ether causes the additional formation of CO. CH_4 is produced readily from a weakly bonded methoxy group (-OCH_3-) (Sada et al., 1992 and Caballero et al., 1997). A lot of studies have explored a wide range of biomass pyrolysis applications including heat and power, liquid fuels, and carbon mitigation strategies. Fig. 4.2 summarises the major thermochemical processes, products, and where the product is used, as recently published by Pandey and Kim (2011). It can see there are three different types of process to convert the lignin into gas, liquid, char and heat that can be used as fuel and raw material in chemical manufacture. Hydrogenolysis is a thermal treatment in the presence of hydrogen. It is used at lower temperature and, hence, favours higher yields of liquid. Gasification is a process to

convert lignin to gases. The major products of lignin gasification are H_2, CO, CO_2 and CH_4. Oxidation process represents thermal treatment in the presence of oxygen and it is used to convert lignins to aldehydes (Pandey and Kim, 2011).

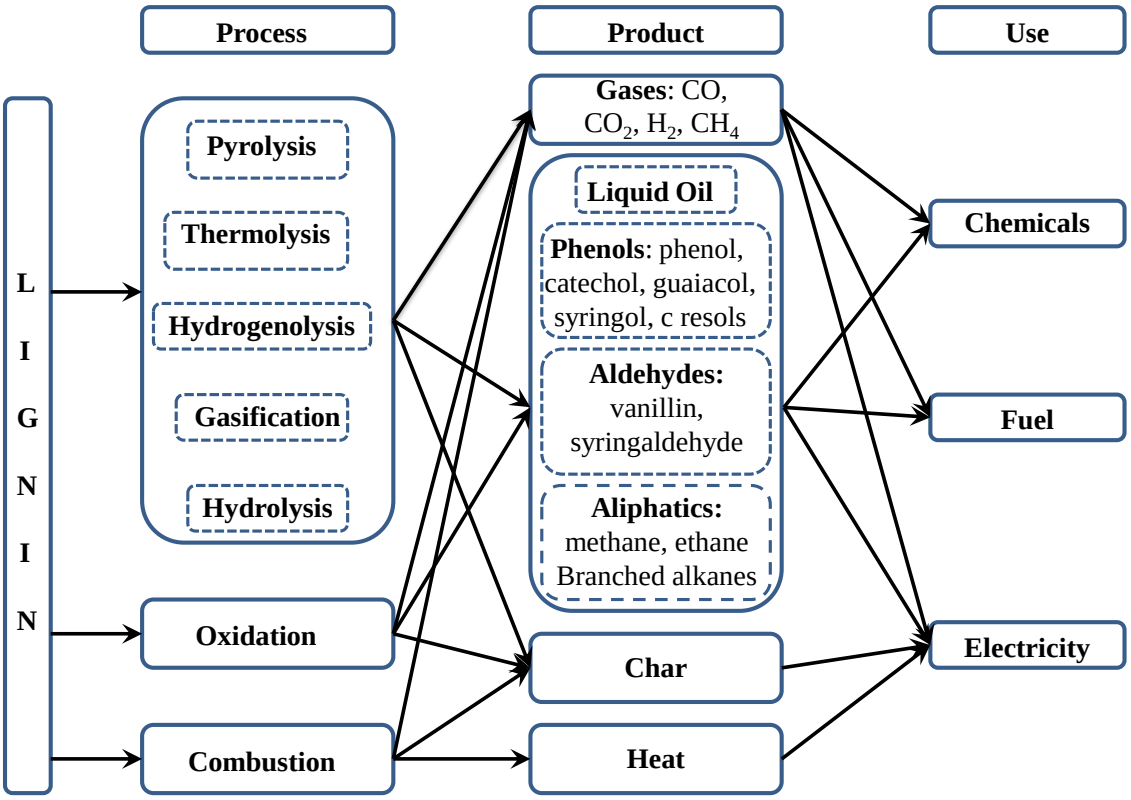

Figure 4.2. Lignin conversion processes and their potential yields (Pandey and Kim, 2011)

To understand the pyrolysis of lignin, it is important to study the independent effects of the reaction conditions such as temperature, pressure, volatiles residence time, heating rate, solid residence time, and rates of production of pyrolysis (gases, liquid, and solid). The complexity of the lignin structure and of the reaction mechanisms during pyrolysis has attracted the attention of a number of researchers and detailed kinetic studies have been undertaken. Many researchers have studied the pyrolysis of lignin and reported weight loss at different reactor temperature and different overall product yields. Iatridis and Gavalas (1979) used a "captive sample" electric screen reactor to investigate the effect of reactor temperature and reaction time on product distribution and weight–loss from the pyrolysis of Kraft lignin without apparent secondary reaction. Nunn et al. (1985) studied the product compositions and kinetics of

milled wood lignin in the temperature range 327 – 1127 °C and a pressure 5 psig of helium in the same type of reactor as that used by Iatridis and Gavalas. They estimated the apparent activation energy and frequency factor by assuming that the pyrolysis occurs following a single first order kinetic reaction (one-stage or one component mechanism). These authors also evaluated the production of gaseous products (CO, CO_2, and hydrocarbons from C_1 to C_3) and liquids. A maximum tar yield of 53 wt% was obtained at 627 °C which declined to 47 wt% at 877 °C.

A model developed for the pyrolysis of coal was modified to simulate the results of lignin pyrolysis by Avni et al. (1985). The model considers the removal of functional groups (e.g. carboxyl group and hydroxyl group) by a parallel independent evaluation of the light gas species in relation to the tar production. The model proved to be successful in simulating seven types of lignin pyrolysed under (i) isothermal conditions in vacuum over a temperature range of 300-1300°C; and (ii) at a constant heating rate of 30 °C/min and pressure of 0.1 MPa over the temperature range of 150-900 °C. It was found that the pyrolysis kinetics is sensitive to the source or extraction process of lignin. Caballero et al. (1995) developed a mathematical kinetic model describing the complexity of Kraft lignin decomposition in the temperature range 150-750 °C, when the residue at very long times depends on the final temperature and not on the heating rate. The model assumes that lignin comprises a large number of "fractions". A given fraction can crack only if the temperature is greater or equal to the characteristic temperature of that fraction. Caballero et al. (1996) employed the same approach to study yields and kinetics of the primary pyrolysis of Kraft lignin at heating rates 20 °C/s over a range of temperature of 450 - 900 °C and different residence times (1-30 s) of the volatiles in a Pyroprobe 1000 pyrolyser. They applied a C function model for primary pyrolysis of thermal decomposition of lignin and derived equations for activation energy (E) and frequency factor (k) as:

$$\ln(k_0) = 14.77 + 0.0208(T_R - 273)s^{-1}\ and$$

$$E = 52.64 + 0.173(T_R - 273)kJ\ mol^{-1}$$

Varhegyi et al. (1997) studied the thermal decomposed of lignocellulosic biomass material and their major components (cellulose, hemicelluloses, and lignin). In this model, complex reaction networks were considered. Thermo-gravimetric and Differential Scanning Calorimeter curves were evaluated by the method of least squares at different heating programmes to develop a pseudo-first order model including all reaction networks. Ferdous et al (2002) obtained kinetic parameters of Alcell and Kraft lignins in a thermo-gravimetric analyser distributed activation energy model, which was originally proposed by Miura (1995) to investigate the kinetic parameters for coal pyrolysis. They observed that at low temperature the conversion to gases and tar at a given temperature was higher at the lowest heating rate than at the highest heating rate. Montane et al. (2005) developed a kinetic model based on thermo-gravimetry and differential thermo-gravimetry data from pyrolysis experiments and assumed that lignin carbonisation proceeds through a set of pseudo-first-order reactions. The model was applied on the pyrolysis of lignin activated with phosphoric acid at low heating rate.

Fushimi et al. (2003) did a study to investigate the effect of heating rate of 1, 10, and 100 Ks^{-1} on pyrolysis of lignin using a thermobalance reactor. They determined the effect of heating rate on Arrhenius parameters by assuming pyrolysis to be a first order reaction. They found that the activity energy of lignin at a heating rate 10 K s^{-1} was 55.7 kJ mol^{-1}, which is slightly higher than the activity energy at the heating rate of 1 K s^{-1} that was 52.8 kJ mol^{-1}. But the activity energy at the heating rate of 100 K s^{-1} was smaller than that at the heating rate 1 K s^{-1}. It is suggested that heat transfer limitations influence the temperature measurement of lignin in the case of 100 K s^{-1}, therefore the value at 100 K s^{-1} was inaccurate. Liu et al. (2008) studied a wood lignin pyrolysis by using a Fourier transform infrared spectrometry (TG-FTIR) and proposed a kinetic model to describe the thermo-degradation behaviour of wood lignin. They observed the main pyrolysis sections and the maximum weight loss rates are different for different wood species. The main pyrolysis process was divided into two stages (at low temperature and at high temperature). The reaction at lower temperature showed activation energy of 70-90 kJ mol^{-1}, while that at higher temperature the activation energy was 135-142 kJ mol^{-1}.

Jegers and Klein (1985) formulated a simple kinetic lumping scheme to predict the production composition from primary and secondary lignin pyrolysis reactions. Pseudo-first-order rate constants for the decomposition of products during lignin pyrolysis were estimated. The model focused mainly on the secondary reaction of lignin. Faravelli et al. (2010) proposed a detailed kinetic model for the pyrolysis of lignin employing the lumping methodology. The detailed kinetic scheme of lignin devolatilisation relies on considering three different classes of components: real species (molecules: H_2, H_2O, CO, CO_2, CH_4, CH_2O,.. and radicals: OH, CH_3, CH_3O,…), heavy species (these components are representative both of the initial lignin structure and of the successive intermediate components inside the evolving structure of polymeric) and functional groups (these groups are linked to the polymer and they decompose to CO and H_2 during the decomposition process). The model assumes that all the heavy species remain in the melt phase with the char residues. The model properly predicted the final residue and the volatilisation rates.

From the description of some the available kinetic studies, it appears evident that the detailed mechanisms for the pyrolysis of lignin are difficult to detect and assumptions are necessary to simplify the rather complex reaction network. Nevertheless, in many practical applications, one is interested in the information of the product yield; thus, knowledge of the apparent reaction kinetics can be sufficient for practical purposes. Therefore a lumping methodology is used in this study to simplify the kinetic reaction for predicting the pyrolysis of lignin.

4.2 Thermal mechanisms of lignin pyrolysis

A kinetic study of lignin pyrolysis is necessary to design properly the reactor and to get an efficient production of fuel gases, chemicals, energy and process correctly. Many investigators have studied the pyrolysis of lignin and reported overall product yields, heat effects, and weight loss at different reactor temperatures. However, very few kinetic data are available on the formation rate of the various pyrolysis products. Numerous methods to study the pyrolysis of lignin are available in the literature, but there is a lack of systematic classification of biomass fuels that are based on method of analysis and general mechanisms to interpret such analysis. These methods are affected by several factors such as biomass species, the age or the specific part of the plant.

Indeed, different experimental conditions and apparatus also cause differences in the results.

Understanding the behaviour of the thermal decomposition during lignin pyrolysis is crucial to control the end product composition but this understanding is difficult due to the complexity of the process during pyrolysis, lignin undergoes several reactions such as depolymerisation, re-polymerisation and dehydration. The products from these reactions undergo secondary reaction depending upon the vapour residence time inside the reactor. As an overall result, the most of chemical compounds that are produced from the pyrolysis have a possibility of condensing into the liquid bio-oil. The pyrolysis process also produce two by-products along with bio-oil: a sold product called "bio-char" and non-condensable gases. To simplify the pyrolysis reaction, in this work the products are lumped into three lumps: solid, liquid and gas; this is quite a popular approach in the literature.

The overall reaction mechanism of pyrolysis of lignin is not understood yet but some simplifying schemes have been assumed for modelling purposes. The pyrolysis of a lignin consists of two types; namely primary and secondary reaction as mention in the previous paragraph. The primary reactions depend only on solid (lignin and bed) temperature and the secondary reactions involve the decomposition product of primary reactions. Fig. 4.3 presents a summary of the reaction mechanisms for the pyrolysis of lignin. From the graph it can be seen that the lignin starts depolymerisation at a temperature of 227 °C to produce gas, tar and nascent char, which it repolymerises to produce char at reaction temperatures <500 °C, all these reactions run in the solid phase. However, the secondary pyrolysis reaction is run in the gas phase at reaction temperatures <550 °C to produce gas and less reactive tar.

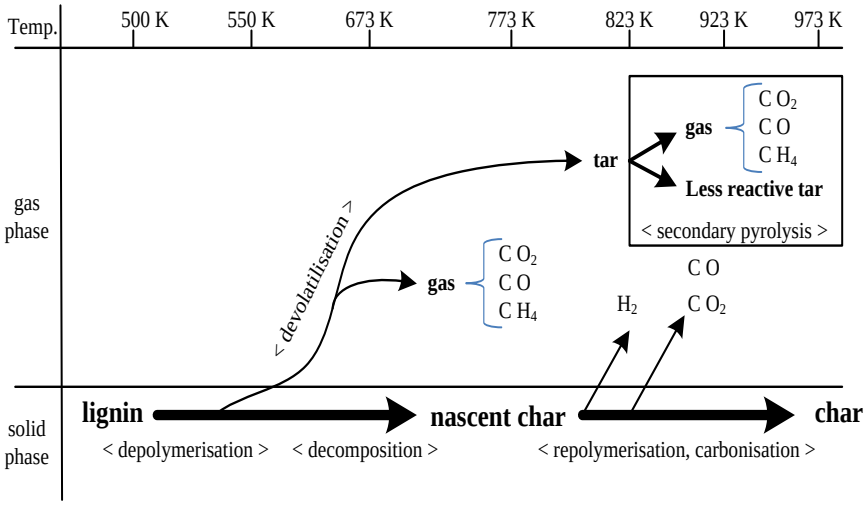

Figure 4.3. Reaction mechanism of pyrolysis of lignin (Fushimi et al 2003).

4.2.1 Kinetic models

The modelling of pyrolysis means the representation of the physical and chemical phenomena in a mathematical form. In other words, pyrolysis is to be introduced as a number of equations which taken together can give a valuable information about the process. The basic equations are those used to describe the chemical kinetics, mass transfer and heat transfer. It is important for the kinetics in pyrolysis of lignin to know the values of kinetics parameters of the lignin under a set of operating conditions.

As mention before in the beginning of this study, the pyrolysis of lignin involves complex reactions resulting in a large number of products; consequently, devising an exact reaction mechanism scheme is very difficult and the associated models carry inevitably a large degree of approximation and assumptions. The lumping approach is one of the ways to simplify the complexity of the lignin degradation. Such a methodology has been successfully used in modelling the kinetics of complex reactive system (e.g. Astarita and Ocone, 1988) and wood pyrolysis (Thurner and Mann, 1981). There are various models of biomass pyrolysis that have appeared in the literature based on the lumping methodology. All models agree that the product of pyrolysis is a mix of char, bio-oil and gas. Fig. 4.4 summarises some of the types of biomass models which have been published in the literature. Koufopanos et al (1991) proposed a two mechanism step scheme for describing the kinetics of the pyrolysis of biomass. The

model indicated that the biomass decomposed to volatiles, gases and char. The gases and volatiles may further react with char to produce different types of volatiles, gases and char where the compositions are different. Di Blasi (1995) introduced two-stage semi-global model to describe the competing primary and secondary reactions for cellulose based on lumping. Sadhukhan et al (2008) developed a model to describe the pyrolysis of a single biomass particle based on the lumping method. The model contain on three elements: primary reaction kinetic model, secondary reaction kinetic model and heat transfer model.

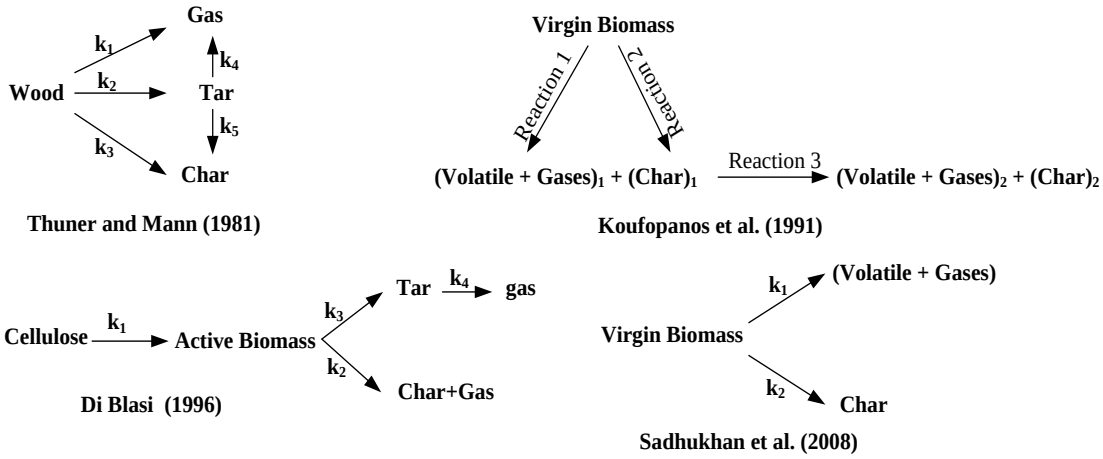

Figure 4.4. Various models proposed for pyrolysis of biomass

The present study looks into the kinetics of pyrolysis of Kraft lignin by employing the discrete lumping methodology to improve the tar composition which is produced from pyrolysis of lignin mathematically by using the continuum lumping methodology. Two different models for the kinetics of pyrolysis of lignin are proposed: "primary reaction kinetics" (PRK) model assumes that lignin pyrolysis into gas, liquid (tar or bio-oil) and solid components; and "primary and secondary reaction kinetics" (PSRK) model assumes that, following the primary reactions, some of the liquid fraction decomposes into gas. Both models are developed for a plug flow reactor reflecting the experimental conditions which, subsequently, will be used to validate the model.

In this research, simplified models of kinetic analysis were used in which it was postulated that the rates of internal heat transfer, external mass transfer and internal

mass transfer were all very fast due to the small size of the lignin particles. When the rates of external and internal mass transfer were very fast, the reaction rate would be independent of position, and the overall controlling factor is the intrinsic reaction kinetics (Pyle and Zaror, 1984).

4.2.1.1 Primary reaction kinetic model (PRK)

A kinetic model is assumed to consist of hypothesised chemical equations as show in Fig. 4.5. The mechanism is based on discrete lumping and divides the different products into three lumps; gases, tar and char. Tar is defined as a mixture of a large number of high molecular weight compounds that are liquid at room temperature. Char is a non-volatile residue with high carbon content left after devolatilisation. The remaining products are gases which have a low molecular weight and have a vapour pressure measurable at room temperature. Thus, the lignin decomposition is described by three parallel reactions. Kinetic rate constants of these three reactions can be determined by measuring the amount of each lump as a function of time. Therefore, all production rates are controlled by their kinetic rate constants. Discrete lumping treats the components of a complex mixture individually or as groups of components with similar characteristics (which are then represented via a pseudo-component), and transforms them on the basis of their reactivity (Okino et al. 1998). When modelling the kinetics of lignin pyrolysis, in a bed reactor, one has to consider that the volatile components are continuously carried out by an inert gas stream which is fed into the reactor.

Assuming that each reaction is first order, a mass balance for each lump is given by:

$$\frac{dw_l(t)}{dt} = -(k_G + k_T + k_C)w_l(t) \tag{4.1}$$

$$\frac{dw_G(t)}{dt} = k_G\, w_l(t) \tag{4.2}$$

$$\frac{dw_T(t)}{dt} = k_T\, w_l(t) \tag{4.3}$$

$$\frac{dw_C(t)}{dt} = k_C\, w_l(t) \tag{4.4}$$

where w_l, w_G, w_T, and w_C are the weight fraction of the feed and the yield of each lump, and t is the reaction time. k_G, k_T and k_C are the rate constans of the gas , tar and char, respectively. These relations are expressed in terms of weight fractions.

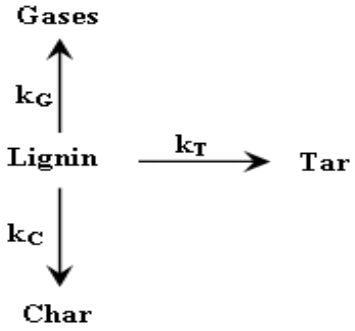

Figure 4.5. Diagram of the kinetic model for primary reaction of the lignin pyrolysis

4.2.1.2 Primary and secondary reactions kinetic model (PSRK)

The PSRK model assumes that, following the primary decomposition of lignin, the bio-oil vapour undergoes a secondary cracking when the temperature in the reactor is high. The secondary tar reactions occur in the gas-phase as well as in the pores of the char particle and on surfaces outside the char particle which are ignored in this study. Secondary reactions of the primary tar vapours are classified as heterogeneous and homogeneous reactions and include processes such as re-polymerisation, cracking, condensation and partial oxidation (Morf et al., 2002). The re-polymerisation of tar vapours to char was ignored due to the fact that the process temperature is not high enough for re-polymerisation and the vapour residence time is low (in our case the vapour resistance time in the reactor is a few seconds). Luo et al. (2005) and Haseli et al. (2011) have studied the vapour tar decomposition for biomass pyrolysis. They assumed the main product of the tar cracking reaction is light gases, and the amount of char yield is negligible. The pyrolysis rate has been simulated by a kinetic scheme involving four reactions as show in Fig. 4.6. Fig. 4.6 shows the primary and secondary reaction scheme of lignin pyrolysis. According to this mechanism, the tar, which is produced from the primary reaction, can be converted rapidly to gases and refractory tar that does not or very slowly, decomposes. This means, with increasing vapour residence time in the reactor, the composition of the liquid is changing from primary tar to refractory tar. Therefore, the quality of the oil product from lignin pyrolysis depends on the vapour residence time in the reactor. Short residence times would be preferred, as

the primary tar would be a better bio-oil constituent than refractory tar. The three parallel reactions (k_G, k_T, and k_C) are called primary reactions, whereas the tar decomposes into gases, with kinetic constant (k_{GT}), is referred to as secondary reaction. Shafizadeh et al. (1977) suggested that all chemical decomposition reactions are of first order; accordingly, the primary and secondary reactions in the present model are assumed to be first-order. The formation or disappearance rate of each lump is given by:

$$\frac{dw_l(t)}{dt} = -(k_G + k_T + k_C)w_l(t) \tag{4.5}$$

$$\frac{dw_G(t)}{dt} = k_G\, w_l(t) + \frac{dw_T(t_v)}{dt_v} \tag{4.6}$$

$$\frac{dw_T(t)}{dt} = k_T\, w_l(t) - \frac{dw_T(t_v)}{dt_v} \tag{4.7}$$

$$\frac{dw_C(t)}{dt} = k_C\, w_l(t) \tag{4.8}$$

$$\frac{dw_T(t_v)}{dt_v} = -k_{GT}\, w_T\,(t_v) \tag{4.9}$$

where k_G, k_T, and k_C are reaction rate constants of the decomposition of lignin pyrolysis and k_{GT} is a rate constant of tar. t is the residence time of the lignin (feed) in the reactor and t_v is the characteristic reaction time of the tar decomposition in the reactor.

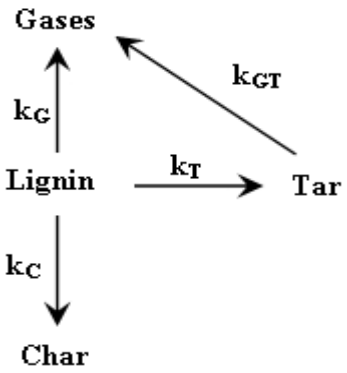

Figure 4.6. Simple primary and secondary reactions scheme of lignin pyrolysis

The mass fraction of the four lumps needs to be known to determine the rate constants of the four lumping reactions. Experimentally, the mass fraction of gases and

tar can be measured, but it is impossible to measure the mass fraction of char or un-reacted lignin separately, because they are both collected together as a solid residue. Here, it is assumed that the lignin is completely converted.

By solving equations 4.1 to 4.4 and 4.5 to 4.8, the theoretical values of the evolution of the mass fraction with time for the four lumps are obtained. The kinetic parameters in the models have been determined by fitting the calculated values to the experimental ones. Programmes have been written in *Matlab* for both the PRK and PRSK models where the set of differential equations have been solved by subroutine *ode45* and optimisation has been carried out by subroutine *lsqcurvefit* for minimising the error between the experimental and calculated values of $W_{G,T,C}$ by searching for the best values of the $k_{G,T,C}$. The solver (*lsqcurvefit)* does not search for the global minimum, but finds the closest minimum to the initial values, which suits the tolerance. To deal with this problem, a range of initial values was taken to calculate the kinetic parameters. A part of the *Matlab* program where the set of initial values is calculated is shown in Fig. 4.7. The model flow chart diagram for optimising the model parameters is presented in Fig. 4.8. In appendix (3) the Matlab program files which are used.

```
%$$$$$ Calculate the Initial Values for Reaction Rate Constants
$$$$$
k_g = 0.02;        % Reaction Rate Constant for Gases
k_T = 0.02;        % Reaction Rate Constant For Tar
k_C = 0.02;        % Reaction Rate Constant for Char
%$$$$$          Loop for Different Initial Values          $$$$$
for k = -9 : 1 : 9
   k_0=[k_g*(10+k)/10
        k_T*(10+k)/10
        k_C*(10+k)/10]
```

Figure 4.7. Initial model parameters (section of the Matlab program code)

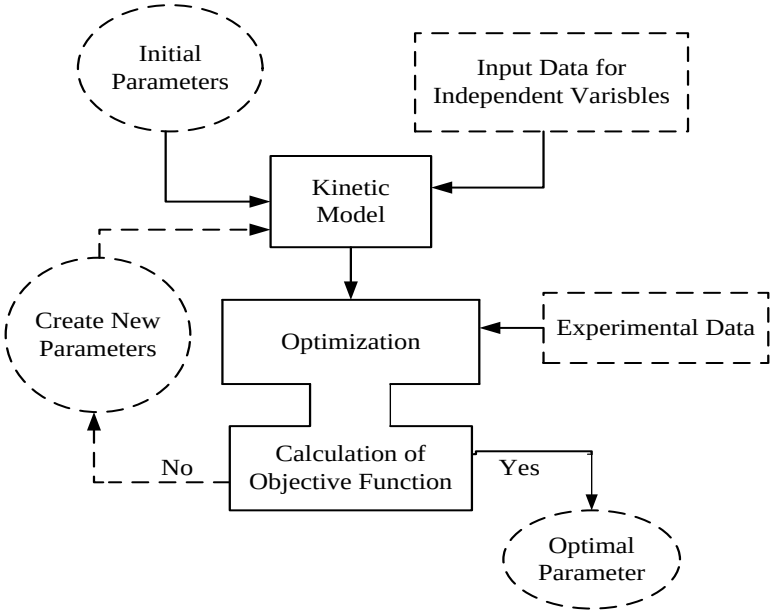

Figure 4.8. Flow diagram for obtaining the best set of parameters of the kinetic lumping model.

4.2.2 Continuum lumping approach

The bio-oil (tar) produced from the pyrolysis is used as chemical or as fuel for turbines, engines and boilers. The tar consists of a very complex mixture of oxygenated hydrocarbons with an appreciable proportion of water and is the main product of the primary pyrolysis reactions. Due to the complexity of the bio-oil mixture, the majority of the previous studies have focused on the effects of parameters such as temperature and vapour residence time on the bio-oil yield rather than its composition. The bio-oil yield can be desirable or undesirable but the cracking kinetics is of major importance for finding optimal operating conditions and an optimal reactor design. The bio-oil cannot be used directly as fuel because of the fuel gas quality requirements. Many processes such as hydrocracking, steam reforming and catalytic cracking have been used by researchers to upgrade tar into transportation fuels. Bridgewater (1994) gave two basic ways to upgrade tar: catalytic (for example dolomite or nickel) and thermal cracking (partial oxidation or direct contact). Therefore, the chemical composition of the tar is a key factor to control the production and cost-effective conversion to transportation fuels.

A model for the tar conversion should provide information about the change in quantity and composition of the tar during the catalytic or the thermal processes. This

can be implemented by describing the tar by means of compound classes having similar thermal behaviour: such classes are denominated lumps. The lumping methodology allows the definition of a simplified model reaction network. Since the cracking (conversion) of the tar implies multiple, parallel and series reactions, employing the lumping methodology would provide an appropriate model concerning the tar conversion mechanisms.

In this study, a continuum lumping model has been formulated to describe the cracking of tar in a catalytic cracking reactor and to show that a continuum lumping model for tar fraction can be, in principle, linked to a discrete lumping model, in a nested fashion. The model mimics the process to improve the composition of the tar to be used as bio-fuel and chemicals. Labelling the reactants represents the starting point for performing the continuum lumping methodology. When the methodology is applied to the problem at hand, namely the fraction of the tar produced via pyrolysis, the tar itself represents the feedstock and needs to be characterised through a label. Since experimentally the tar can be characterised through the molecular weight of its components, the molecular weight is adopted as the component label.

The specific procedure which will be applied here is an extension of the original work of Chapter three. As pointed out, given that any continuous label can be employed in the continuous description, the molecular weight, which is readily available from the experimental analysis (see Fig. 4.12), is adopted here. The normalised molecular weight of each species is defined as:

$$\theta = \frac{W - W_l}{W_h - W_l} \tag{4.10}$$

where W_l and W_h represent the low and high molecular weight in the reaction mixture.

The concentration of the generic component i can then be expressed as:

$$C(t) = C(\theta, t)d\theta \tag{4.11}$$

And, in terms of reactivity, k, as:

$$C(\theta, t)d\theta = c(k, t)D(k)dk \tag{4.12}$$

where $D(k)$ is the species-type distribution function taken as the power-law function. It is regarded as the Jacobian of the $i\ to\ k$ coordinate transformation.

The power law relation is one which has been widely used to transform the k-space to θ-space:

$$\frac{k}{k_{max}} = \theta^{1/\propto} \tag{4.13}$$

where α is a model parameter and k_{max} represents the rate constant for the species with the highest molecular weight. The mass balance equation for the species with reactivity k can be presented by:

$$\frac{dc(k,t)}{dt} = -k.c(k,t) + \int_k^{k_{max}} p(k,K).K.c(K,t).D(K).dK \tag{4.14}$$

In this case study, the power law relation is used for $D(K)$. The details of the numerical solution for the Eq. 4.14 and procedure to determine the model parameters can be found in Chapter three.

4.3 Experimental

Lignin is difficult to pyrolyse due to the very fine particles and the fact that lignin starts melting at low temperature (usually 150-200 °C) and cracks fully at high temperatures. The pyrolysis experiments were performed by colleagues at the Institute for Chemical and Fuel from Alternative Resources (ICFAR) at Western University. A fast pyrolysis pilot plant designed to convert biomass over a temperature range 250-700

°C and under near atmospheric pressure, was employed to pyrolyse lignin. A schematic representation of the fluidised bed pyrolysis pilot plant is shown in Fig. 4.9.

The fluidised bed reactor has a diameter of 0.078 m and a height of 0.52 m with an expanded freeboard section which is made up of a 0.065 m long truncated cone and a 0.124 m long cylindrical section, 0.168 m in diameter. Alternate freeboard sections can be used to allow different vapour residence times without changing the bed hydrodynamics. To prevent the solids from escaping the reactor, a packed hot filter, made of ceramic wool, was installed at the gas outlet. The reactor temperature was measured and controlled by using thermowells type K thermocouples and the reactor is equipped with five taps for measuring absolute and differential pressures. The reactor body is heated with 12 Watlow Mica electric band heaters over all sections of the reactor and its extension. The heaters are independently controlled with Honeywell UDC200 Mini-Pro Digital controllers, which can be used to set the axial temperature profile along the reactor. A National Instrument USB card (USB-6218) is used to monitor when heaters are on and thus estimate the heat provided to the reactor. A perforated distributor plate distributes the fluidization gas (N_2) to the reactor bed.

A pulsed system injects the biomass into the bed, 0.1 m above the fluidization gas distributor plate. A feed injection system (slug injector) is used to feed the reactor as in Fig. 4.10. It uses a special intermittent injection nozzle, which can handle a wide variety of biomass feedstocks, including cohesive powders. The biomass feedstocks (lignin) is fed in a hopper and discharged through a pneumatic valve. The valve opens usually every 4 second for short time (0.5 second) to allow a small amount of the feed to fall into the a horizontal injector pipe. A continuous stream of carrier gas (usually N_2) is used to convey the biomass slug into the reactor. A solenoid valve gives a simultaneous pulse of extra carrier gas (Argon) to avoid any solids settling in the horizontal pipe. A timer is used to control both valves (pneumatic valve and solenoid valve).

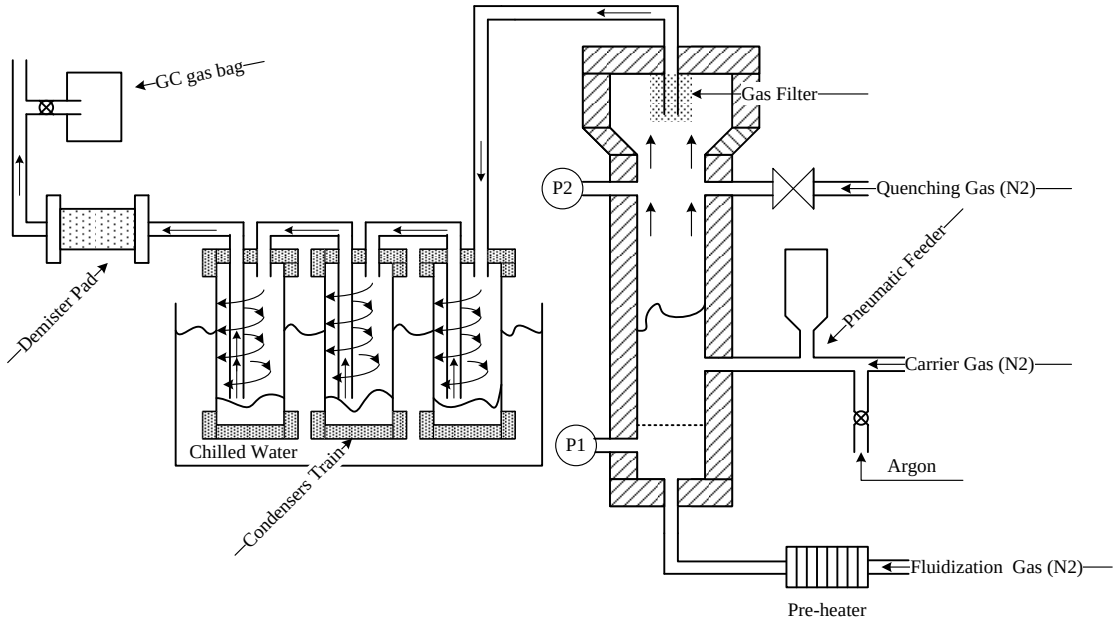

Figure 4.9. Schematic diagram of pyrolysis fluid bed pilot plant

The bio-oil condensing system consists of three steel cyclonic condensers in series immersed into the chilled water. Each condenser is weighed before and after each run to obtain an accurate liquid yield.

Two Gas-Trak Sierra mass flowmeters are used to measure the fluidizing gas and the continuous carrier gas.

Once the feed is injected into the reactor and thermal cracking takes place, the produced vapours exit the top of the reactor through the hot filter section. The filter removes all the solids to avoid contamination of the product vapour by char and sand. The product vapour and carrier gas flow into the condensing system where the bio-oil vapour is rapidly condensed and collected. Persistent aerosols are recovered with an electrostatic demister, while the non-condensable gases flow into a gas-sampling bag.

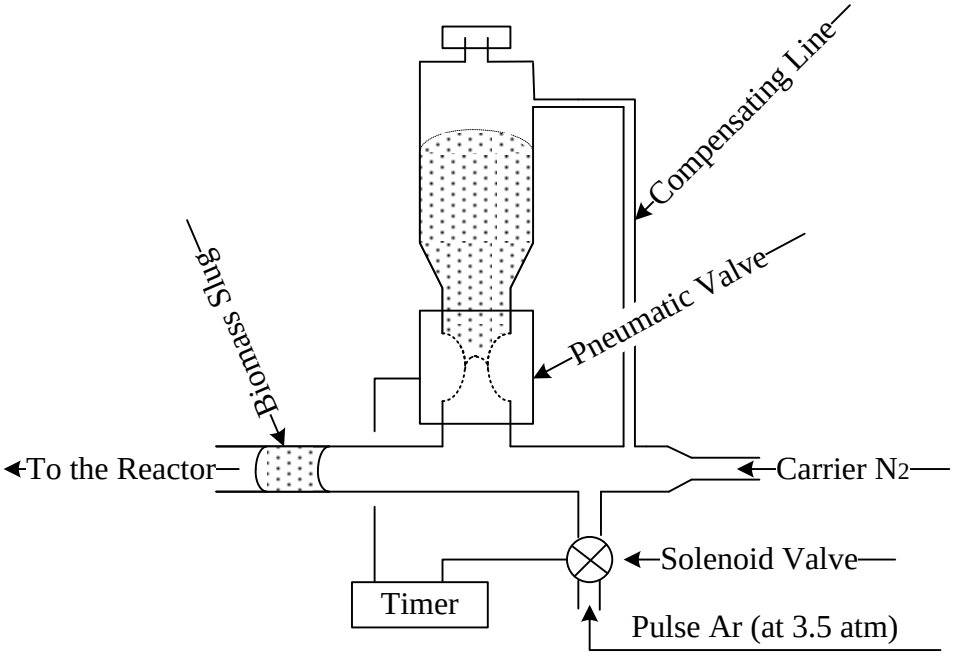

Figure 4.10. Feed injection system.

The feedstock was a Kraft lignin with particles size less than 30 μm and particles density equal to 575 kg/m^3. Inert silica sand with mean diameter 180 μm was used in the fluidized bed. The bed mass was 1.5 kg.

Two types of experiment were carried with the Kraft lignin feedstock: with a mechanical stirrer in the fluidised bed to bring solids from the bed surface down into the bed and without a mechanical stirrer. Fig. 4.11 shows the mechanical stirrer that was used in the fluidised bed reactor. Several runs were carried out at different operating temperatures in the range 400-600°C, as reported in Table 4.2. The average residence of the lignin particles in the reactor was 20 min while the total residence time of the vapour in the hot part of the pilot plant was 0.4 s for the experiments without mechanical mixing (FB) and 1.4 s for experiments with mechanical mixing (FBM). The vapour residence time is calculated as the reactor void volume divided by the sum of the fluidisation gas and carrier gas flow rate at reactor conditions. The total amount of biomass injected for each run was 200 g.

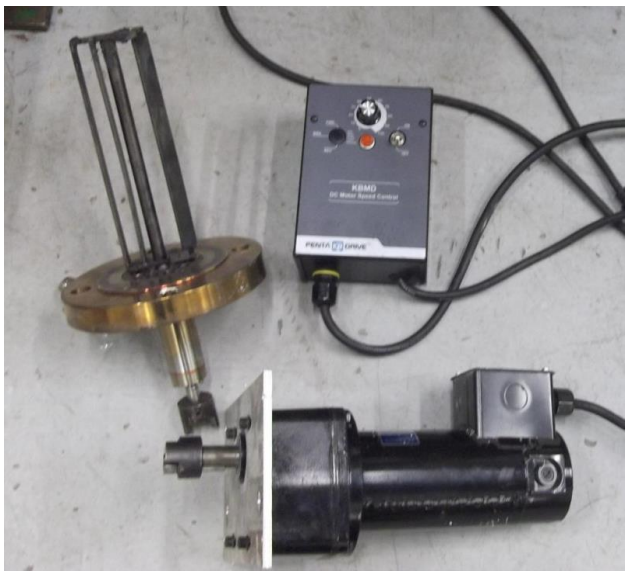

Figure 4.11. Mechanical stirrer.

The net result of the decomposition of lignin is the liquid bio-oil, char and gas. The amount of liquid product (bio-oil) was calculated by weighing both the set of condensers and demister bed before and after each run. The product gases, mainly composed of H_2, CO, CO_2, CH_4, and some low molecular weight hydrocarbons, together with the fluidization gas and carrier gas (N_2), were analysed using a Hewlett Packard 5890 series II GC gas chromatograph provided with a thermal conductivity detector and a Restek Shincarbon Micropacked column that was 2 m long and 1 mm internal diameter, using nitrogen as an internal standard. The amount of residual (solid char) product was calculated from the change of the fluidised bed mass during each run.

A Karl Fischer titrator CL38 was used to determine the moisture content of the bio-oil. Also, the chemical composition of organic chemical contained in the aqueous phase bio-oil was determined with an Agilent 6890 GC/MS by direct injection of the sample through a DB-5 ms (the column was 30 m long, with a 0.25 mm internal diameter and a 0.25 μm film). Results for both types of experiments are illustrated in Table 4.2 while the bio-oil analysis is presented in Fig. 4.12. More details on the feed injection system and the experimental procedure can be obtained from Xu et al. (2009 and 2011).

Reactor	Temperature (°C)	Liquid yield (wt %)	Solid yield (wt %)	Gas yield (wt %) (by difference)
With Mixing	Vapour residence time = **1.4** sec			
	450	25	70	5
	500	30	61	9
	550	31	59	10
Without Mixing	Vapour residence time = **0.4** sec			
	450	38	56	6
	500	41	50	9
	550	48	42	10
	600	45	40	15

Table 4.2. Experimental results.

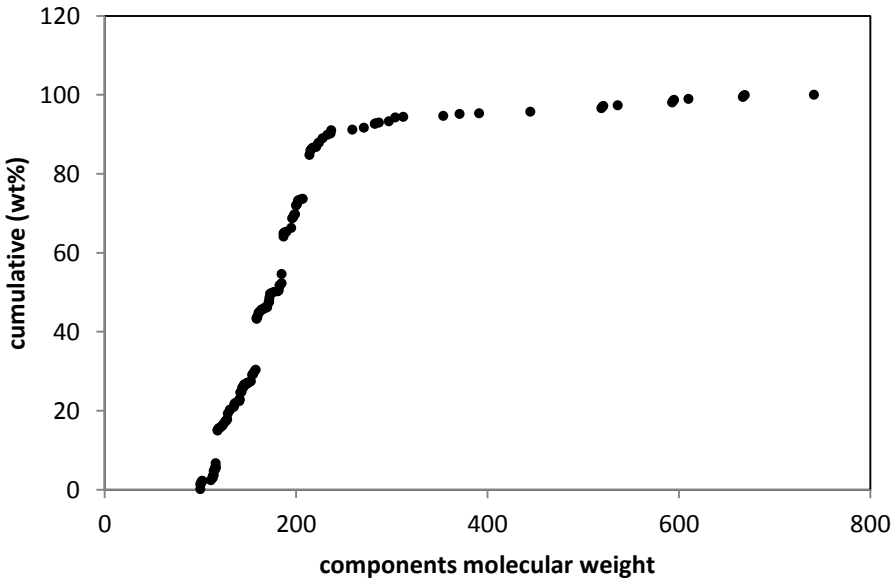

Figure 4.12. Bio-oil analysis (produced at 450 °C).

4.4 Result and discussion

The main objective of using fast pyrolysis in the experiment was to obtain the maximum efficiency and yield of bio-oil (tar). The fast pyrolysis has been used to describe a pyrolysis regime in which vapour production is maximised and the formation of char is minimised, contrasted with slow pyrolysis which is used to maximise the formation of char, because re-polymerisation or recombination reactions are allowed to take place in the slow pyrolysis after the primary reactions have occurred. Shafizadeh

and Chin (1977) reported a typical weight distribution of lignin pyrolysis yields at temperature range 450-550 °C as: 35% liquid, 12% gases and 55% char. From the experimental results in table 4.2 it is observed that the yield distribution in both types of experiment is in the range reported by Shafizadeh and Chin (1977). The maximum yield of bio-oil in both types of the experiment has been obtained when the reactor temperature reached 550 °C. Along with the reaction temperature, the residence time of the pyrolysis vapours in the reactor and the mixing inside the fluidised bed reactor also play an important role in the process. The mixer is used in the reactor to bring solids from the bed surface down into the bed. This method is used to reduce low density foam that forms at the bed surface. Fig. 4.13 shows the foaming layer in the reactor. The fluidised bed reactor is potentially the most efficient reactor for pyrolysis compared with various other reactors (Scott et al., 1999).

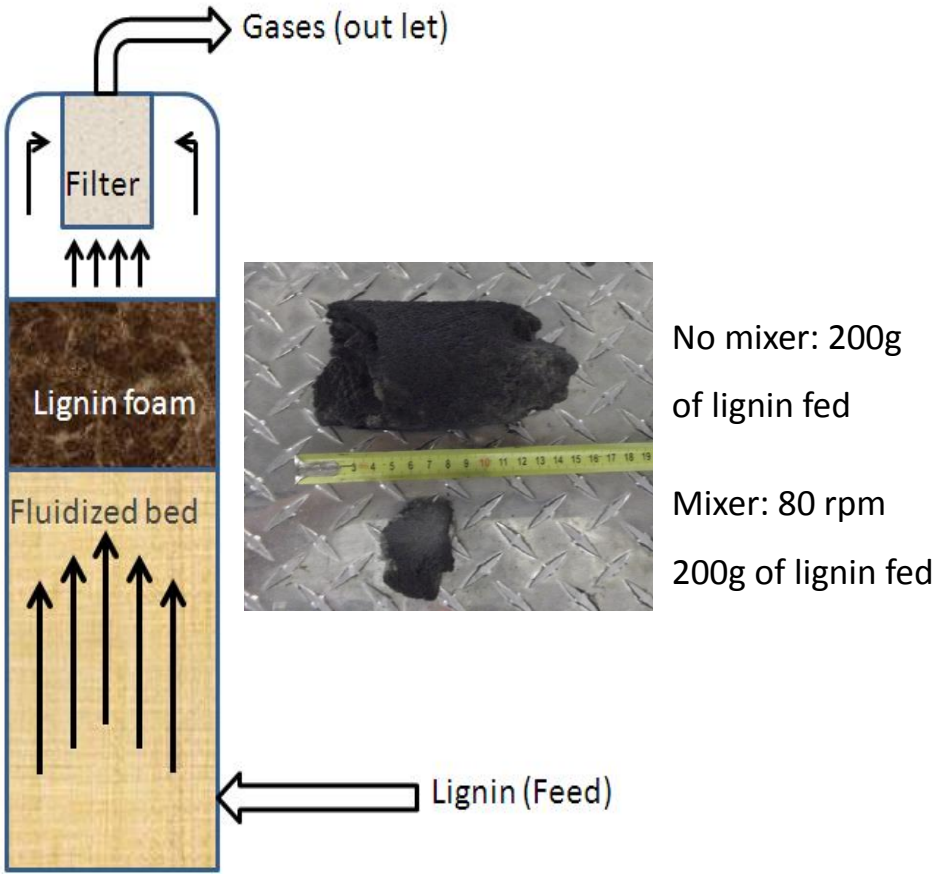

Figure 4.13. Foaming formation in the lignin fluidised bed reactor

The models that were presented in the previous section have been validated using the experimental data taken at ICFAR using the reactors described in Section 4.3.

The effect of the temperature on the yield distribution is shown in Table 4.2. It can be seen that the char yield always decreases with increasing temperature, while the non-condensable gases yield always increases.

Fig. 4.14 and Fig. 4.15 show the experimental results carried out in the FBM and FB reactors, respectively at different temperatures. Those results are compared with model calculations using a primary reaction kinetic (PRK) model and a primary and secondary reaction kinetic (PSRK) model, respectively. The PRK model is employed with the experimental data with mechanical mixing since the experimental data show that the tar and gas product increase with increasing temperature and the char reduces with increasing temperature. The PSRK model is applied with the experimental data from the reactor without mechanical mixing: in this case, the tar and char yields reduced when the temperature reached 600 °C and the gas yield kept increasing. Using the data at the three experimental temperatures, the kinetic constants have been determined by minimising the difference between the model and the experimental data. The first conclusion is that the kinetic scheme is a good representation of the process. When the temperature in the FB reactor reaches 600 °C the secondary reaction appears to take place in the reactor to produce more non-condensable gases. However, in the FBM reactor the yield product (gas, tar and char) seem to be constant when increasing temperature of the reactor more than 500 °C. It means, when the experiment runs by using FBM, the re-polymerisation reaction of the tar may take place in the reactor with increasing temperature.

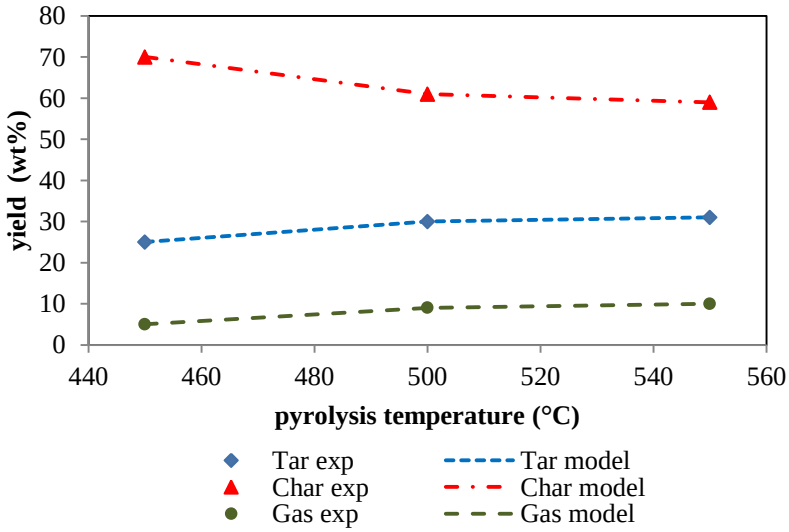

Figure 4.14. Experimental and theoretical results of product lump distribution (primary reaction kinetic model).

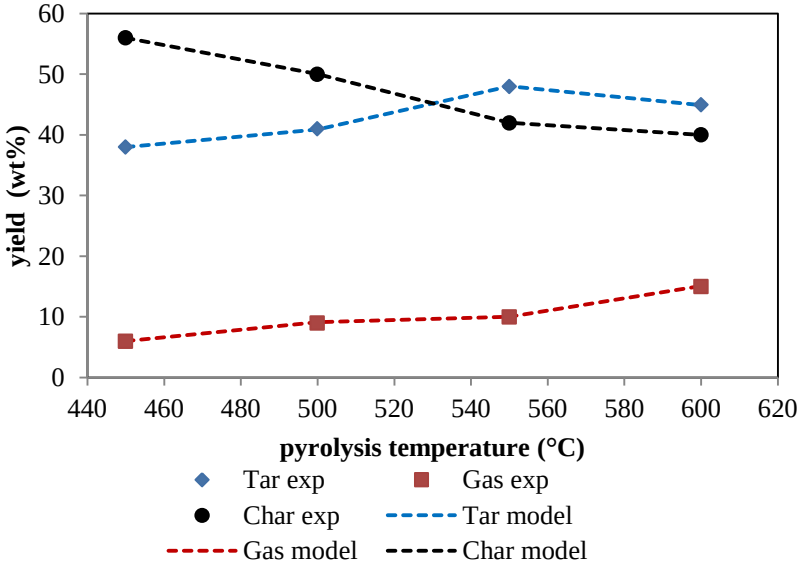

Figure 4.15. Experimental and theoretical results of product lump distribution (primary and secondary reaction kinetic model).

The kinetic parameters for the pyrolysis of lignin were calculated from measurement of the weight fraction of gas, tar, and char as a function of time at different temperature. Fig. 4.16 reports the PRK model calculations at different temperatures and different residence times. Results from the PSRK model are reported in Fig. 4.17 at a fixed temperature of 450 °C. According to the above models, the reaction rate constants of lignin pyrolysis are obtained and reported in Table 4.3. These constants ($k_G, k_T, k_C, and\ k_{GT}$) were determined at three different reaction temperatures for the FBM reactor and four different reaction temperatures for the FB reactor. It can be observed that the rate constant of the gas (k_G) increases with increasing the reactor temperature in both models. However, the rate constant of the tar (k_T) increases with increasing the reactor temperature in the PRK model, while in the PSRK model, (k_T) first increases then decreases as a consequence of the secondary reaction starting at higher reactor temperatures. The kinetic constants of the cracking of feed (lignin) are much higher than the cracking of tar. This indicates that the secondary cracking reaction of tar compared to the total cracking is lower at these temperatures and vapour reaction time; the production of gas from the tar through the secondary cracking is also lower compared to the production of gas obtained through the primary decomposition of lignin.

The Arrhenius plots for all kinetic rate constants are presented in Fig. 4.18 and 4.19 for the two models. The slopes and intercepts were calculated by linear regression. The values of the kinetic parameters, activation energy, as well as frequency factors are summarised in Table 4.4 for both models. The activation energies for the individual decomposed path ways of lignin pyrolysis were in the range of 8-35 kJ/mol for the PRK model and in the range of 6-30 kJ/mol for the PSRK model. The decomposition of lignin towards tar and char happens more quickly than it decomposes to gases in both models. In the PSRK model the reaction of tar towards gases happens faster than lignin to gases and it can be noted that the activation energy for tar-to-gases pyrolysis is higher than that of lignin-to-tar pyrolysis. Consequently, it can be concluded that the amount of gases produced from lignin pyrolysis increases when the reactor temperature increased. The kinetic parameters can be used to predict the yield of the pyrolysis products when running the process with different temperature.

In this study the global devolatilisation reaction constant (k_V) can be calculated by $k_V = k_G + k_L$. As expected in the first model, the activity energy of char formation is lower (8.025 kJ/mol) than that for volatile formation (46.61 kJ/mol) that is, when the reaction temperature is increased the volatile formation is favoured.

There have been a number of studies of kinetic parameters of lignin pyrolysis published in the literature. The majority of studies of the kinetic parameters during lignin pyrolysis used a thermo-gravimetric analysis technique (TGA) and the process was modelled by means of a single-step global reaction to describe the overall rate of devolatilisation from the biomass substrate with first order reaction (Varhegyi et al., 1997; Murugan et al., 2008; Varhegyi et al., 2011). TGA measures the decrease in weight caused by the release of volatiles during thermal decomposition. The considerable difference of the kinetic parameters in the literature can be observed due to several factors such as the experimental methods, operating conditions, data analysis and the chemical composition of the raw materials that were examined in each study (Ghetti et al., 1996). Nunn et al. (1985) reported the activation energy for overall pyrolysis of hardwood lignin was about 82.3 kJ/mol within a temperature range of 327 °C – 1167 °C. Ferdous et al. (2002) studied two types of lignin (Kraft and Alcell lignin) pyrolysis and calculated the activation energy for the Kraft lignin in the range of 80-158

kJ/mol between 234 °C - 503 °C and for Alcell lignin in the range of 129-361 kJ/mol between 272 °C – 532 °C. Murugan et al. (2008) studied pyrolysis of Alcell lignin and obtained the activity energy value to be between 8-68 kJ/mol in temperature range of 71 °C - 259 °C. In this study, when considering the contribution of energies to the total activation energy of the decomposition of lignin, they are in agreement with the above studies. For example, the total activation energy for the PRK model is 54.6 kJ/mol and 64 kJ/mol for the PRSK model.

A comparison between experimental product composition and those calculated by solving equations 4.1 to 4.9, with the reaction rate constant (k) values given in Table 4.3, is shown in Fig. 4.20 for both models. It can be observed that the product composition is well predicted for the different lumps, which is also evidenced by the low value obtained for the objective function (less than 9.88×10^{-6} for both models) which is determined by using the following expression: $J\big(w(t)\big) = \sum_{i=1}^{N}[w(t)^{exp} - w(t)^{pred}\,]^2$.

		Primary reaction kinetic (PRK) model			Primary and secondary reaction kinetic (PSRK) model			
Reaction	Unit	Reaction temperature (°C)						
		450	500	550	450	500	550	600
k_G	min^{-1}	0.0294	0.0534	0.0594	0.0362	0.0539	0.0598	0.0895
k_T	min^{-1}	0.1470	0.1780	0.1842	0.2292	0.2456	0.2867	0.2685
k_C	min^{-1}	0.4116	0.3619	0.3506	0.3378	0.2995	0.2508	0.2386
k_{GT}	min^{-1}	--	--	--	0.0247	0.0249	0.0188	0.0169

Table 4.3. Reaction rate constants of the lignin pyrolysis.

	Primary reaction kinetic (PRK) model		Primary and secondary reaction kinetic (PSRK) model	
Reaction rate constant	Frequency factor (min^{-1})	Activation energy (J/mol)	Frequency factor (min^{-1})	Activation energy (J/mol)
k_G	11.167	35291.57	4.979	29537.96
k_T	0.988	11318.48	0.713	6748.60
k_C	0.107	8025.37	0.040	12864.14
k_{GT}	--	--	0.002	14835.58

Table 4.4. Calculate frequency factors and activation energies for both kinetic models.

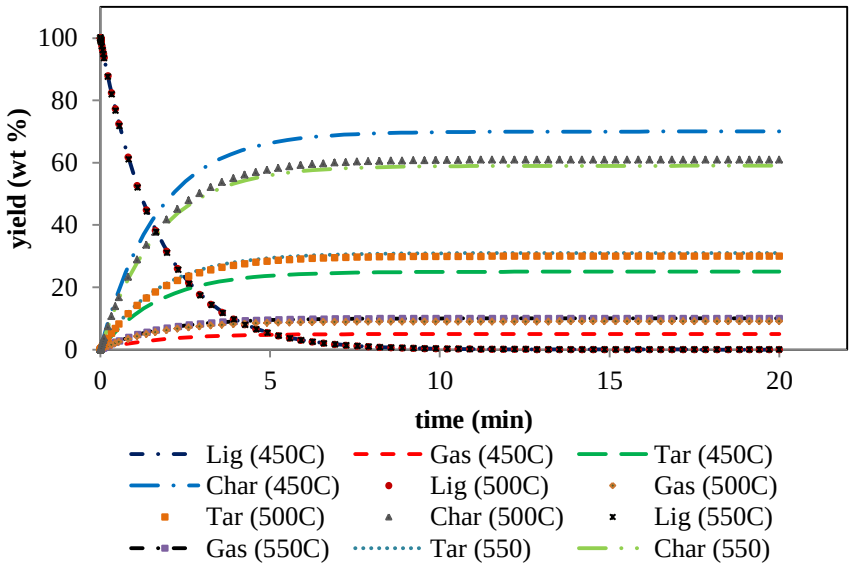

Figure 4.16. Model predictions as a function of time for the primary reaction kinetic model

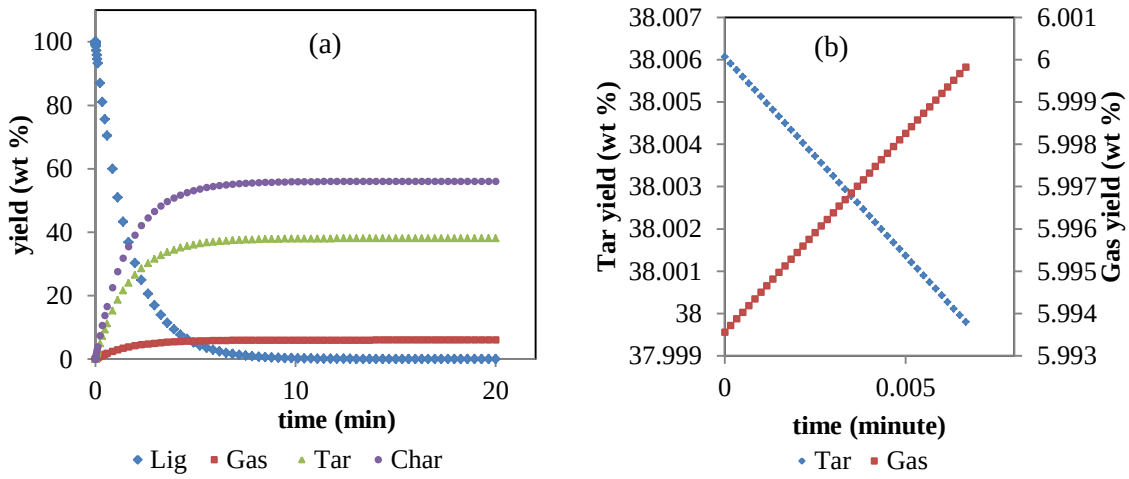

Figure 4.17. Model predictions as a function of time at 450 °C: (a) for the primary and (b) for secondary reaction kinetic model.

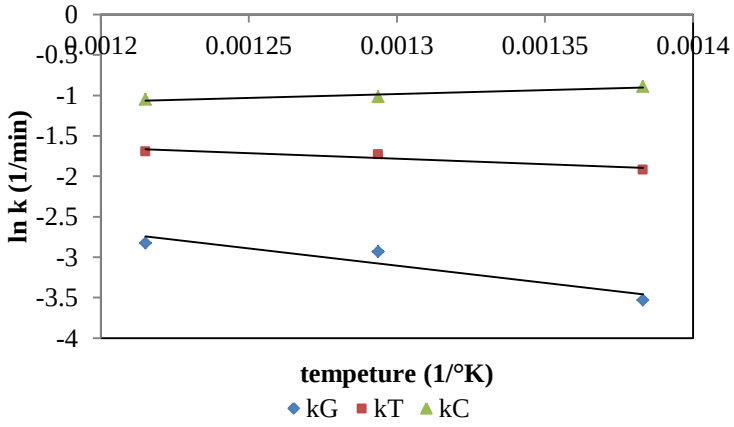

Figure 4.18. Arrhenius plot of reaction rate constants with using PRK model for MFB reactor

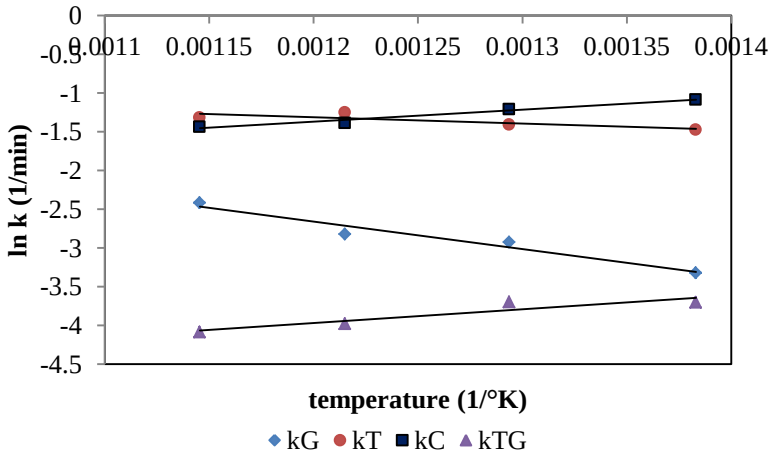

Figure 4.19. Arrhenius plot of reaction rate constants with using PSRK model for FB reactor

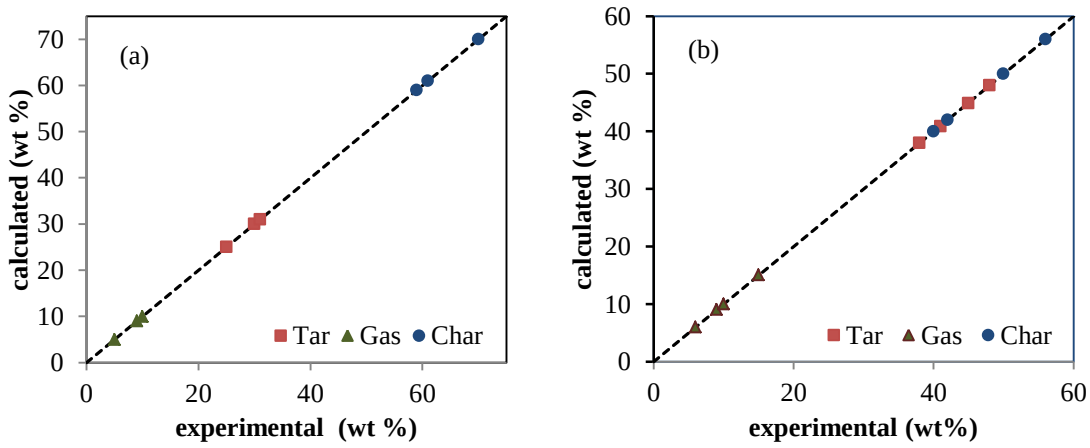

Figure 4.20. Adequacy of the fitting between the experimental and model values of the yields corresponding to three lumps (tar, gas and char): (a) using PRK model and (b) using PSRK model.

By using a kinetic continuous model for the bio-oil (tar) produced from Kraft lignin, simulated results were generated and are plotted in the Fig. 4.21 and Fig. 4.22 for different residence times. The plot illustrates that the proposed continuous lumping model is able to predict the component concentration profiles as a function of the normalised molecular weight, θ. An increase in reaction time results in an increase of the amount of lower molecular weight components and a reduction of the higher molecular weight components. The model has five independent tuning parameters that are presented in Table 4.5 for different residence times of the reaction. And these values are chosen only for computational reasons to study how these parameters affect the prediction model. The model parameters selection was depended on the assumptions for $p(k, K)$ that were introduced in chapter three. The $p(k, K)$ should satisfy the material balance criteria: $\int_0^K p(k, K).D(k).dk = 1$. When the model is applied to a real process, then the parameters would need to be validated against experimental data to get the optimal parameter values. The conversion of the high molecular weight with residence time is illustrated in Fig. 4.23. From the graph it can be seen that as the residence time increases the percentage of conversion of the high molecular weight to tar increases. The conversion is increased from 5 % to 42 % by increasing the residence time from 0.1 to 1.2 h, i.e. the conversion increases more than 35% when the reaction time is increased from 0.1 to 1.2 h. The advantage of applying the continuum lumping model in this study is that it can provide a continuous description of the component concentrations with respect to the normalized molecular weight, and as a function of the reaction time. This allows for a faster treatment of the mixture which does not consider the single components, but rather lumped quantities.

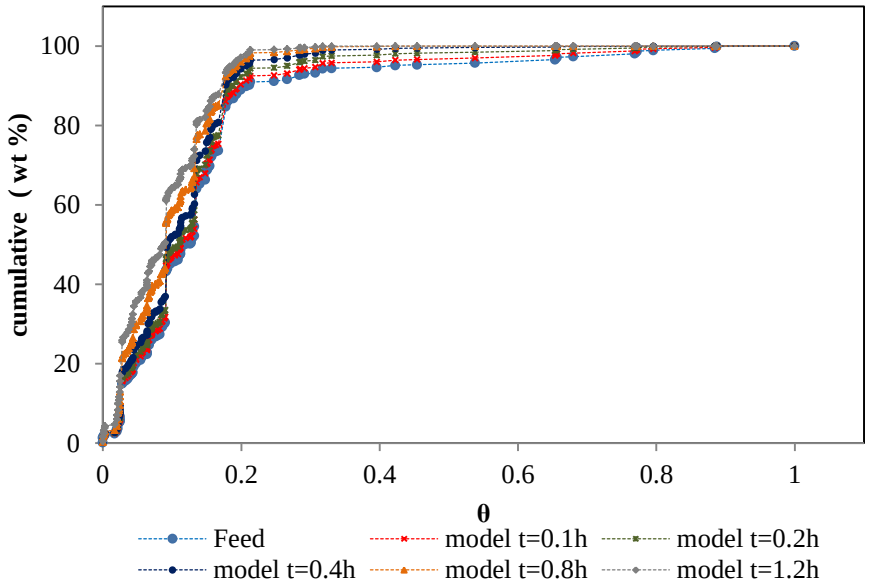

Figure 4.21. Cumulative feed and yield predict from the model for different residence times (t).

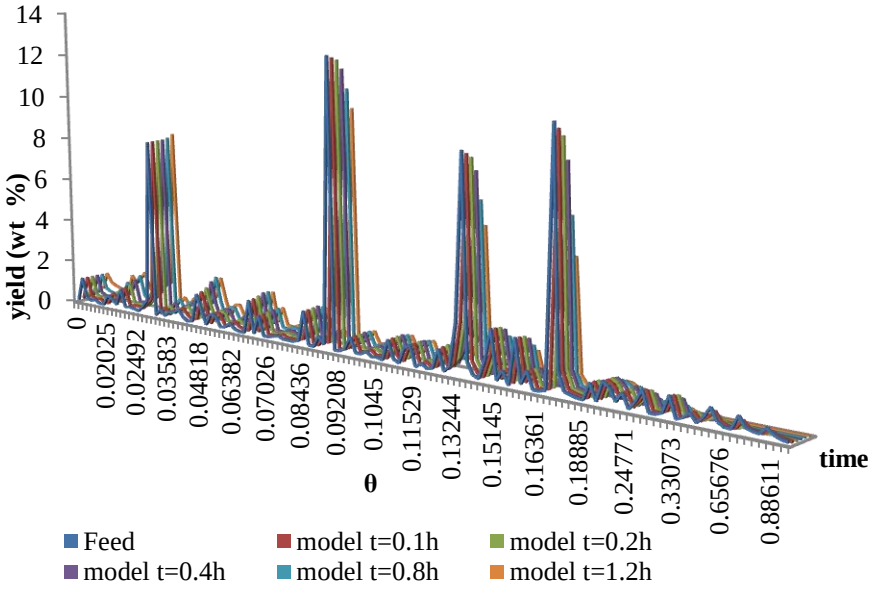

Figure 4.22. Feed and yield predicted from the model for different residence time.

Time (h)	a_0	a_1	k_{max}	α	δ
0.1	20.2	3.8	6.28	0.58	9.052e-07
0.2	32.2	3.8	9.48	0.54	9.052e-07
0.4	34.2	3.8	11.48	0.548	9.052e-07
0.8	5.2	3.8	13.28	0.488	9.052e-07
1.2	10.32	3.8	13.68	0.556	9.052e-07

Table 4.5. Model parameters.

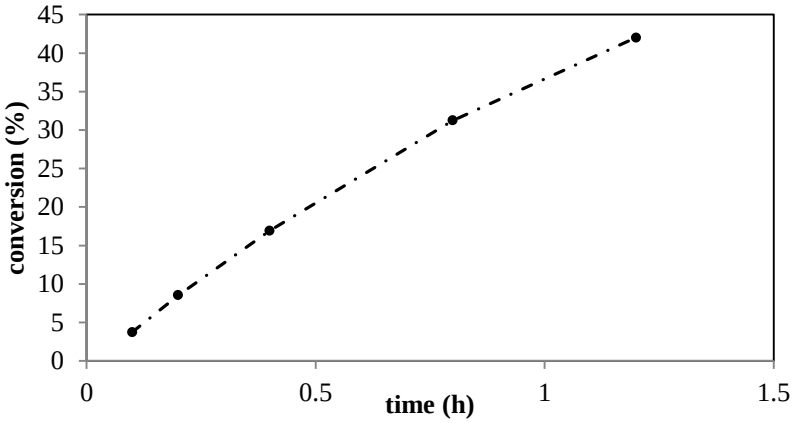

Figure 4.23. Predict degree of conversion for bio-oil (tar) that has a high molecular weight.

4.5 Conclusions

The experimental and the lumping model methodologies applied to the pyrolysis of lignin were studied in this chapter. The effect of the reactor temperature and mechanical mixing on the lignin decomposition during pyrolysis were investigated and how these parameters affected the models parameter was studied. The experimental yields were divided into three groups: liquid, gas and char. The yield of char decreased with temperature, whereas the yield of bio-oil was found to be maximised at 550 °C. It is observed that the tar production by using the mechanical mixing in a fluidised bed reactor is less than that produced from the fluidised bed reactor. This is a consequence of the fact that because of the residence time of the vapour in the FBM reactor is longer than in the FB reactor and consequently re-polymerisation might occur in the FBM reactor. It can be observed that secondary cracking takes place in the reactor in the gas phase at temperatures higher than 550 °C where the pyrolysis vapours undergo further degradation producing more compounds having a low molecular weight and gaseous species.

The discrete lumping model developed was implemented to predict the yield of Kraft lignin pyrolysis. The kinetic scheme involves three parallel reactions for primary reaction and an additional reaction for secondary reaction. Two different models for the kinetics are proposed: the “primary reaction kinetic” (PRK) model and “primary and secondary reaction kinetics” (PSRK) model. The PRK model is employed with the experimental data with mechanical mixing and the PSRK model applied to the

experimental data from the reactor without mechanical mixing. Computational results showed that the modelling simulation results are in good agreement with experimental data. The values of the kinetic parameters (activation energy, as well as the frequency factor) are calculated by using the Arrhenius plots for all kinetic rate constants.

The development of the PSRK model reflects the fact that, when the temperature increases, experimental data are indicative of a tendency towards the decomposition of the tar into gas. The data analysed and used in this study are such that a single model (PRK) would probably describe with a certain degree of approximation both reactors(with mixing and without mixing), the PSRK model is introduced as a general tool which would be more effective, and then recommended, if high temperature processes are considered.

The continuum kinetic lumping, with five adjustable parameters, was applied to the tar yield from the Kraft lignin pyrolysis. The model has been used to predict the cracking of the tar (bio-oil) with different retention time in a catalytic reactor; fractionation follows the primary pyrolysis of lignin in the fluidized bed reactor. The continuum kinetic lumping model is very effective in simulating the catalyst cracking reaction of tar and the product concentration profiles. The conversion of tar with increasing the retention time seems to be a linear conversion.

CHAPTER 5.

Case (III) – Continuum Lumping Modelling for Step-Growth Polymerisation Mechanism

The aim of the work reported in this chapter is twofold: to develop a continuum lumping model which could predict the molecular weight distribution of the polymer during polymerisation and to assess the suitability of the lumping methodology in describing the polymerisation process. Compared to the other studies presented in the previous chapters, the results obtained here are assessed only qualitatively; nevertheless, by analysing the weight distribution and the average of such distribution, conclusions can be obtained on the predictive capability of the lumping methodology. In this method a yield distribution function is used that was first introduced to describe the hydrocracking of oil cuts by Laxminarasimhan et al. (1996). Polymerisation follows a different mechanism compared to hydrocracking: the longest chain components are formed, whilst in hydrocracking they are broken. To the best of our knowledge, this is the first effort to use a yield distribution function to describe step growth polymerisation. The direct continuum lumping procedure requires a precise characterisation of the feed and this requirement is satisfied in polymerisation. The fact that the validity of the modelling procedure can be tested without any uncertainty related to the characterisation of the feed composition guarantees a more rigorous assessment of the predictive capabilities of the model.

5.1 Introduction

Polymers are usually characterised by a high molecular weight. These macromolecules are formed through polymerisation reactions starting from low molecular weight components called monomers. Because of their broad range of polymer properties, therefore they play an essential and ubiquitous role in everyday life. Polymers can be classified by different criteria such as chemical nature of the monomers, molecular structure of the polymers, polymer chain growth mechanism and

type of polymerisation process. Numerous papers in the open literature relate to polymerisation processes in general; however, only a small subset of these publications focuses on step growth polymerisation. The majority of the literature of polymerisation relates to chain growth polymerisation. This review attempts to give the general field of polymerisation as it relates to process modelling.

5.1.1 Type of polymerisation

Depending on the kinetic mechanism, polymerisation reactions can proceed by a step growth or chain growth process (Cowie and Arrighi, 2008). In chain growth polymerisation (also called addition polymerisation), growth centres in the reaction components are present and the monomers add to such centres until either all monomers are consumed or the active centre is rendered inactive by a termination reaction (e.g. when external agents are added to terminate the polymerisation reaction). Chain growth polymerisation can be further classified into free radical, anionic, cationic, and stereoregular polymerisation. Polymerisation of vinyl monomers such as ethane, propene, styrene and vinyl chloride is considered the most important group of chain growth polymerisation. In contrast, step growth polymerisation involves reactions between the functional groups (HO-, $HOOC^{-}$, etc.) of any molecule in the reaction mixture; consequently, by repeated reaction, long chains are gradually produced. In step growth polymerisation, the average molecular weight of the polymer increases with time and the life time of a growing polymer chain takes hours. In contrast, in chain growth polymerisation, the higher molecular weight components reach a maximum from the start, while the monomer quantity decreases slowly with time. Fig. 5.1 shows two types of polymerisation reaction examples: in the first reaction two different types of monomers react with each other as in the production of polyurethane; in the second reaction, one type of monomer reacts to produce an ester from hydroxyl-acid monomer.

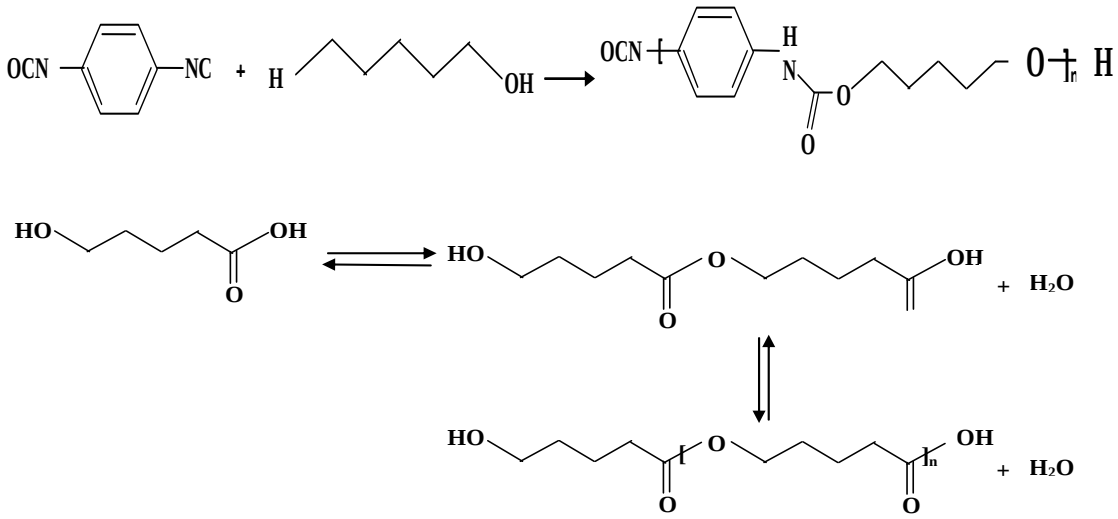

Figure 5.1. Polymerisation reaction.

5.1.2 Modelling

The polymer molecular properties (e.g. molecular weight distribution (MWD), the copolymer composition distribution (CCD), sequence length distribution (SLD), the long and short chain branching distribution (LCBD, SCBD)) as well as the morphological properties of the product (e.g., particle size distribution and bulk density) depend on the chemical nature of the monomer, polymerisation process, on the polymerisation mechanism, and on the reactor type (Kiparissides, 1996); modelling the problem in its entirety is a very difficult task. Consequently, the development of mathematical models for predicting the characteristics of the polymer produced is the key to improving the operation of the plant, to get sights into the process, and to increase the efficient production of high quality polymer. Therefore, the main objective of developing a polymerisation model is to understand how the physical transport phenomena, the kinetic mechanism, the reaction type and the operation conditions affect the polymer produced.

Various and extensive modelling efforts can be found in the literature and they have been devoted to modelling a number of aspects of polymerisation; the chemical kinetics, transport phenomena and the reactor dynamics are discussed by Ray (1991). One of the objectives of the mathematical modelling is the prediction of the MWD of the final product (polymer) and the MWD at different stages of the polymerisation

reaction. An early work by Floyd (1937) described the four main steps of the mechanism of free radical polymerisation (initiation, propagation, chain transfer and termination). The reaction system was represented by a very large set of nonlinear differential equations which describe concentration change with time of every component. Subsequently, a variety of modelling methods have been implemented to obtain information on the rate of polymerization and the resulting MWD (e.g., Ray, 1972).

The calculation of the molecular weight distribution, particle size distribution and chain-length distribution through mechanistic models is a hard task. Modelling polymerisation reactors implies the direct solution of the large system differential equations for each species present in the reactor. Consequently, efforts have been devoted to devise numerical techniques which can make the problem easier. The most common numerical methods, their advantages and disadvantages are discussed by Nele et al. (1999).

Skeirik and Grulke (1985) developed a technique where the dead and growing polymer chains were lumped together into equal size groups to reduce the calculation time. Chaimberg and Cohen (1990) developed a new computational model for free radical polymerisation reaction. The model is based on the use of a numerical technique to solve the differential equations for monomer and total growing polymer concentration. McCoy (1993) applied a moment model to describe the behaviour of chemical kinetics and equilibrium in reversible oligomerisation reactions. The model is based on distribution function of molecular weight and is modelled with fusion and fission rate expressions. Lumping methodology is used to reduce the continuous mixture mass balance equations. McCoy and Madras (2001) presented discrete and continuous models for polymerisation and depolymerisation by using a population balance equation for chain growth polymerisation. The models are dependent on the molecular weight distribution (MWD). In the continuous model the molecular weight distribution (MWD) is presented as a gamma distribution which gives a good comparison with exact polymerisation and depolymerisation MWD solutions of the discrete model. The theory of this model had been used by Smagala and McCoy (2006) to propose a model for branching kinetics during chain polymerisation based on

distribution kinetics as described by equations of population dynamics for flow reactors or batch reactors.

Since a polymer's end use properties are depended on its MWD, therefore controlling the polymer molecular weight distribution is very important in industrial polymerisation processes. Crowley and Choi (1997a) presented a method for calculating the weight chain length distribution in free radical polymerisation of vinyl monomers that is an extension of the method of molecular weight moments. The weight fraction of polymer is calculated in a specified range of molecular weight rather than at a single chain length in this method. And they named this proposed method the method of finite molecular weight moments. Crowley and Choi (1997b) proposed an approach for the control of weight chain length distribution of polymer instead of molecular weight averages in a batch free radical polymerisation reactor. The method is used in conjunction with the method of finite molecular weight moment to determine a sequence of reactor temperature set points which lead to the desired MWD. Pladis and Kiparissides (1998) developed a model to predict the joint molecular weight long chain branching distribution for branched polymers in free radical polymerisation. The technique is based on dividing the total polymer population into a number of classes with the same long chain branching. The overall MWD is calculated as a weighted sum of the individual molecular weight distributions. Developments on modelling and optimisation of polymerisation process are reviewed by Kiparissides (2006).

The process models that are found in the literature are usually a set of nonlinear coupled equations. And the kinetic parameters associated with these models are not well known and are difficult to estimate. The present work deals solely with the kinetics of polymerisation. Here, the model principles based on a continuum lumping approach that was developed in chapter three are used for step growth polymerisation to give a simple method for kinetic estimation and molecular weight distribution. The use of the continuum modelling in polymerisation is not new (e.g. McCoy and Madras, 2001; McCoy, 1993); however, the use of a yield distribution function, as present here, is novel.

5.2 Step growth polymerisation

In this study the step growth polymerisation was considered, where the macromolecules increase their molecular weight by reacting with monomers that are added to the polymer chain. The assumption in this study is that various monomers react creating larger chain polymers with no formation of smaller chain compounds; the polymer is indicated as $P(x)$, where x represents the molecular weight (MW)which is taken as a continuous variable. Two monomers or any other species in the reaction mixture can join by a step growth mechanism to form a new polymer whose mass equals the sum of two joining segments. The polymerisation reaction between a polymer and monomer is presented as (McCoy, 1993; McCoy and Madras, 2001):

$$P(x - x_s) + Q(x_s) \rightarrow P(x) \tag{5.1}$$

where Q is the monomer and P is the polymer. x_s represents the molecular weight of the monomer (equivalently, the degree of polymerisation). If, on the other hand, two polymers react to give a longer chain polymer, the polymerisation reaction is represented as:

$$P(x') + P(x - x') \rightarrow P(x) \tag{5.2}$$

The reaction mechanism for step growth polymerisation is shown in Fig. 5.2. All the monomers (M) are able to react and so larger and larger fragments are formed.

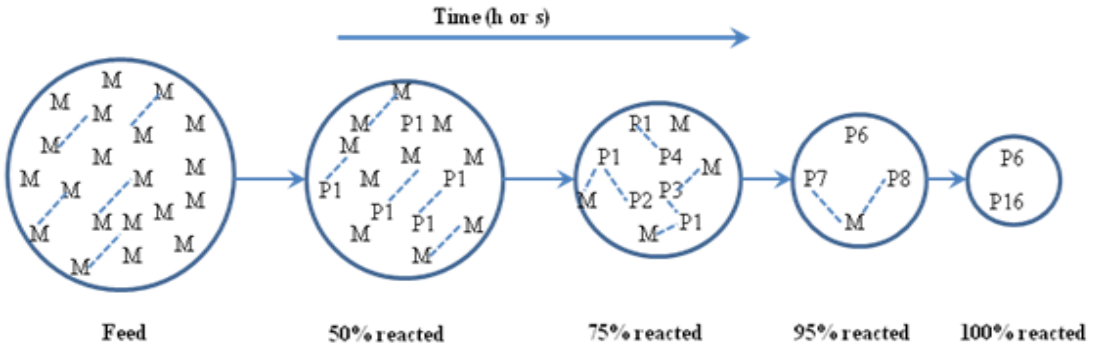

Figure 5.2. Schematics of the step growth polymerisation mechanism.

5.3 Mathematical model

Multi-component complex reactive systems are very common in industrial processes, such as hydrocracking, polymerisation, air pollution and pyrolysis. Those are systems where the individual components of the mixture are numerous and it is difficult to identify them in detail. The reduction of the dimensionality of the system having a large number of components furnishes systems constituted by a lower number of components. As an example, one could imagine substituting a subset of similar components, with a single component, or "lump" having the properties of the underling sub-mixture. In addition, when one is not interested in the fine-grained structure of the system, but only in some gross overall properties, (e.g. the total concentration of all species of a certain type) the "overall lumping approach" can be performed. It is important to note that the overall description can be attempted both in a discrete and continuous fashion; however, if the number of components is very large, it is more convenient to attempt a continuous description. More details about continuum lumping methodology were presented in the chapter two and three.

The continuum lumping approach is applied to the reactions (5.1 and 5.2), extending the procedure which has been applied previously to the hydrocracking of normal paraffins (waxes) in chapter three. In this case, the molecular weight (MW) of the polymer is used as the continuous variable and the index w is then introduced such that the "species" $P(w)dw$ represents the sub-mixture whose index (i. e. whose molecular weight) lies in the range $(w, w + dw)$. Here a yield distribution function, which was proposed by Laxminarasimhan and Verma (1996), has been introduced that determines the amount of formation of polymer that has a high molecular weight (W) from the reacting of monomer which has a low molecular weight (w).

5.3.1 Model formation

The model formulation involves the characterisation of the feed, of the reaction pathway and of the associated selectivity of the various polymerisation reactions. The distribution of MW characterises the composition of the reaction mixture at any time during polymerisation. As the residence time of the reacting mixture increases, the number of monomers and the concentration of lower molecular weight polymers

decrease, whilst the concentration of higher molecular weight polymers increases. Given the nature of the reaction, each monomer will exhibit the same rate constant when attaching to the polymer chain and consequently the rate of reaction is assumed to be the same for all reaction being a function of temperature alone. In addition, it is assumed that the "apparent" order of reaction is first order: this assumption is in line with an ample literature on continuum lumping. Indeed, the kinetics refers to lumped concentration and not to the real kinetics of a single reaction. Additionally, the study is interested to keep the number of adjustable parameters to a minimum, being the purpose of the study to investigate the feasibility of the continuum lumping approach to describe the polymerisation process. However, different orders of reaction can easily be considered in the model.

Having chosen the molecular weight, w, as the continuum index, the concentration of the generic component i, can be translated into the domain w, as follows:

$$c_i(t).di = D(w).c(w,t).dw \tag{5.3}$$

where $c_i(t)$ is the concentration of the component i in the discrete mixture and $c(w,t)dw$ is the concentration of the component with molecular weight lying in the range $(w, w+dw)$. The function $D(w)$, called the distribution-type function, was introduced by Chou and Ho (1988), and can be considered as a Jacobian of the transformation in Eq. 5.3. Discussion on the role of $D(w)$ can be found elsewhere (e.g., Adam et al., 2012; Laxminarasimhan et al., 1996); the assumption in this study, without loss of generality, is that $D(w) = 1$. This is a good approximation especially considering that the reactions are assumed to be linear and first order (Adam and Ocone, 2010). Also, the same reactivity for each component is assumed, contrary to what happens in cracking processes where heavier components may crack faster.

The mass balance equation for the component with molecular weight w, at a given t, in a plug flow reactor (or, equivalently in batch reactor) can be written as:

$$\frac{dc(w,t)}{dt} = -k.c(w,t) + k.\int_0^W P(W,w).c(w,t).dw \quad (5.4)$$

where k is a reaction kinetic rate constant and $c(w,t)$ is the concentration of reactant with molecular weight w at the time considered and W the highest fixed molecular weight produced in the mixture.

The term on the left-hand side of Eq. 5.4 represents the time variation of the concentration of the generic component of molecular weight w, whilst the first term on the right hand side represents the disappearance (death) of the same component due to reaction and the second term represents the formation (live) of the component due to the reaction. The term $P(W,w)$ in the integral part represents the yield distribution function and determines the amount of formation of the species with molecular weight w from the species with molecular smaller than w which reacts to form a component with higher molecular weight. The yield distribution function was first introduced by Laxminarasimhan et al. (1996) to describe the formation of shorter chain components after the longer chain ones undergo cracking. To adapt the procedure of Laxminarasimhan et al. (1996) to polymerisation processes, the yield distribution function P(W,w), expressing the formation of polymer of various molecular weights, is introduced. The yield function is defined through its properties in accordance with the physics of polymerisation; the properties of the yield function are defined in the following.

A skewed Gaussian type distribution function can be chosen as the yield distribution. The yield distribution function will be described as follows:

$$P(W,w) = \frac{1}{S_0.\sqrt{2\pi}}.\{\exp(-(\frac{\left(\frac{w}{W}\right)^{a_0}-0.5}{a_1})^2) - A\} \quad (5.5)$$

where:

$$A = \exp(-(\frac{0.5}{a_1})^2) \quad (5.6)$$

$$S = \int_0^W \left(\frac{1}{S_0.\sqrt{2\pi}} . \{\exp(-(\frac{\left(\frac{w}{W}\right)^{a_0} - 0.5}{a_1})^2) - A\} \right) . dw \quad (5.7)$$

5.3.2 Solution methodology

In the present treatment all polymers with the same molecular weight are assumed to belong to the same lump, namely they are characterised by the same label, w. The balance equation, for each spices, in a plug flow reactor (equivalently in a batch reactor), is then expressed by an integro-differential equation (Eq. 5.4), which is solved numerically. Considering the totality of species, a system of integro-differential equations must be solved at each time. The solution is attempted by solving the integral first and then evaluating $c(w,t)$ by foreword time. The integration is particularly demanding since the integral in Eq. 5.4 must be solved "forwards". Consider, as an example, the generic component i (of molecular weight w_i): at a given time t, the integral appearing in Eq. 5.4 must be solved by taking into account all components with a molecular weight lower than i, namely it must be solved by the interval $[c_1, c_i]$. The integration can then proceed forwards to $c_{(i+1)}$ and so forth till the concentration of the generic component n is calculated. A Matlap program was used to solve Eq. 5.4 where the trapezoidal rule was used to evaluate the integral and the differential equation was solved by using the Runge-Kutta method. At $t = t_0 = 0$ the component distribution corresponds to the feed distribution and, by using it as the input, the component concentration at $t = t_1$ is obtained. At $t = t_2$ the output is obtained by using the result at t_1 as the new "feed". The procedure is continued until the numerical time corresponds to the real time that the mixture spend in the reactor. A Matlab code that was used to solve the model equations is presented in appendix (4).

5.4 Results and discussion

The model for step-growth polymerisation reaction, represented in the previous section, has been solved for two test cases. The first case starts from a feed which consists of monomers and a pre-polymer having molecular weight distribution as shown in Fig. 5.3. The feed was chosen to analyse the model's behaviour and predictability for polymerisation processes which proceed via a pre-polymer synthetic route such as polyurethane synthesis. An equation ($w_x = x.(1-P)^2.P^{x-1}$), which was published by

Cowie and Arrighi (2008), has been used to give the weight fraction distribution for the feed in case one. Where, w is a mass fraction of polymer, P is the extent of reaction and equals 0.96 and x is a molecular weight. The second case considers the situation where the initial feed is formed by a single type of monomer with an assigned molecular weight equal to 5 kg/kmol.

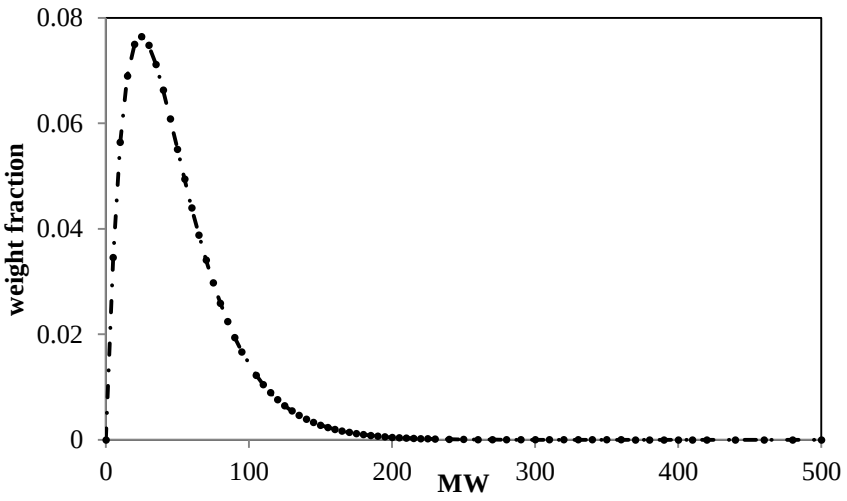

Figure 5.3. Feed data for first case study.

Fig. 5.4 summarises the calculations carried out starting from the feed distribution reported in Fig. 5.3 to explore the effect of the reaction times on the evolution of the molecular weight distribution of the monomer feed and the polymer produced; a constant rate of reaction, k, equals to 0.1 h^{-1} is assumed in all calculations. The model parameters a_0 and a_1, which are related to skewed Gaussian-type distribution function p(W,w), are assumed to be 2.67 and 28.86, respectively. These parameters were selected only for calculation reasons, to give a good performance of the yield distribution function $P(W,w)$, based on the model assumption as discussed early in the modelling section, and, at present, must not be related to any specific feature of the system. If the model is applied to a real process, then the values of the parameters would need to be validated against experimental data. However, since the purpose of this work is to test the model qualitatively, no further investigation of the parameters values was done.

Fig. 5.4 shows the decreasing concentration of monomers when they react to produce a polymer; the concentration of the polymer increases, as expected. An increase in the reaction time results in an increase of the amount of higher molecular weight polymers as compared to the amount of the lower molecular weight polymers: more monomers are consumed to produce a polymer with higher molecular weight. The polymer distribution at various residence times are reported; it can be noted that, as the time increases, the first peak, corresponding to the feed, becomes smaller, whilst the second peak, corresponding to the production of polymers with high molecular weight, becomes higher. The area under each curve is proportional to the total mass of initial monomers and it is conserved at each time.

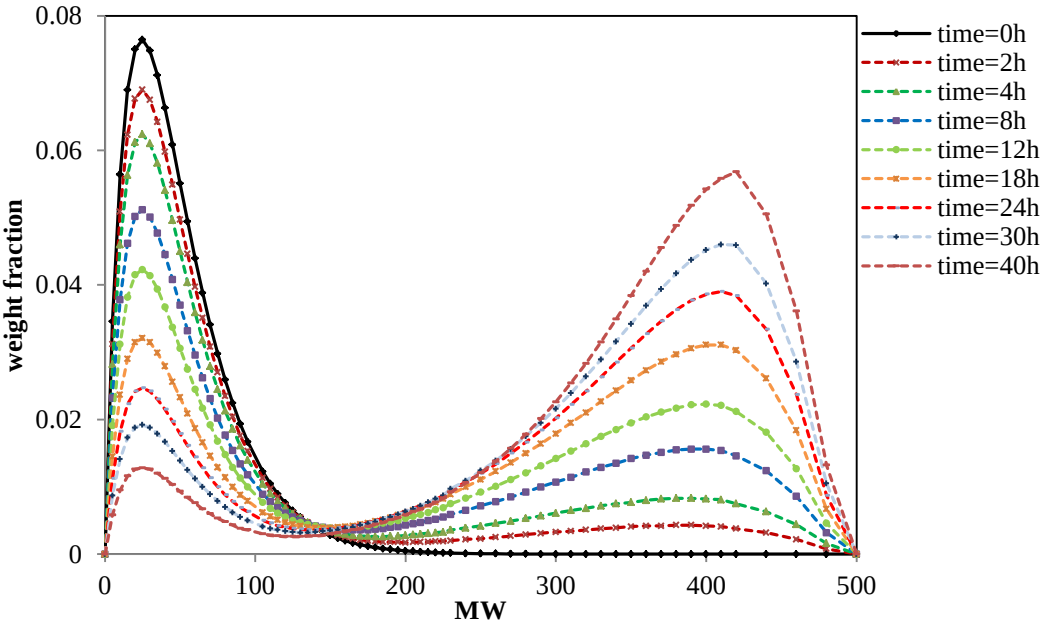

Figure 5.4. Feed and product distributions from the model for different reaction times ($\boldsymbol{t}$) and constant rate of reaction ($\boldsymbol{k}$) equals to 0.1 h^{-1}.

The influence of the rate reaction (k) on the polymer formation is also investigated. The assumption is made that, within each model run, all monomers in a selected feed have the same rate of reaction. An increase of rate of reaction for the monomer results in an increase in the rate of the formation of higher molecular weight product. Consequently, monomers with low rate of reaction need a longer time to produce a polymer with a higher molecular weight. Fig. 5.5 illustrates the effect of the reaction rate on the products at a fixed reaction time equals to two hours. The model parameters are kept the same for all calculation ($a_0 = 2.67$ and $a_1 = 28.86$), so that

variability does not affect the results. The results show that long reaction time and high conversion are necessary for the production of a polymer with large molecular weight.

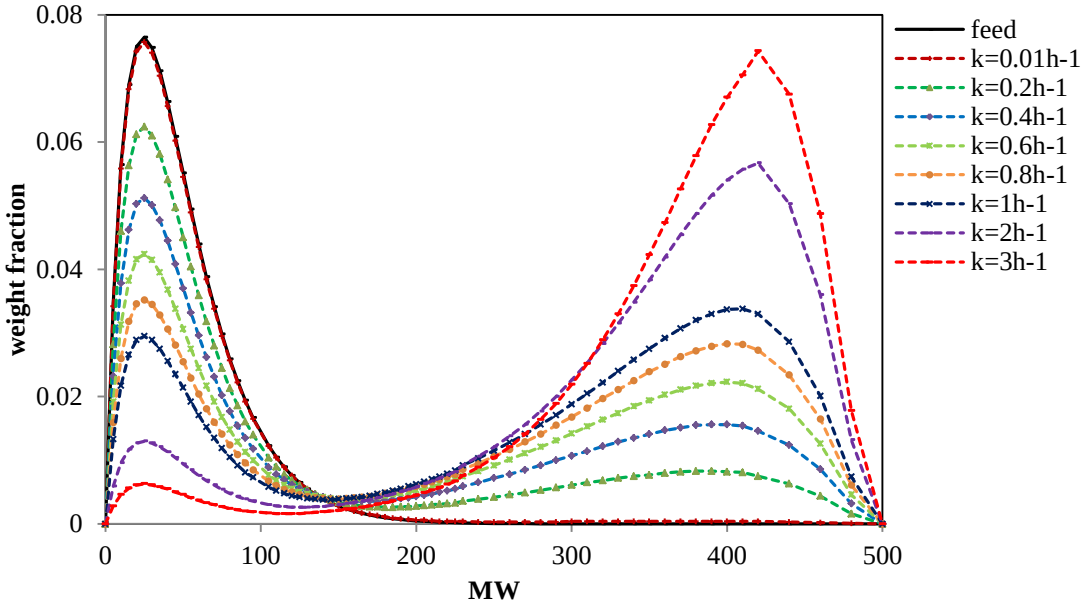

Figure 5.5. Feed and product distribution from the model calculations for different rate of reaction constant ($\boldsymbol{k}$) and reaction resistance time ($\boldsymbol{t}$) equals to two hours.

The second case study considers a feed of only one monomer, which has a molecular weight equal to 5 kg/kmol, reacting with each other to produce a polymer with high molecular weight. Fig. 5.6 reports the product distributions at various times. Starting from a reference 1 for the weight fraction of the feed monomer (left y-axis), for higher residence times, higher molecular weight polymer is produced (right y-axis). Notice the shift towards higher molecular weight polymers as the time increases; all calculations are performed keeping the model parameters constant and with a constant rate of reaction ($k = 0.1\ h^{-1}$). The same qualitative behaviour is observed if the value of rate constant is changed.

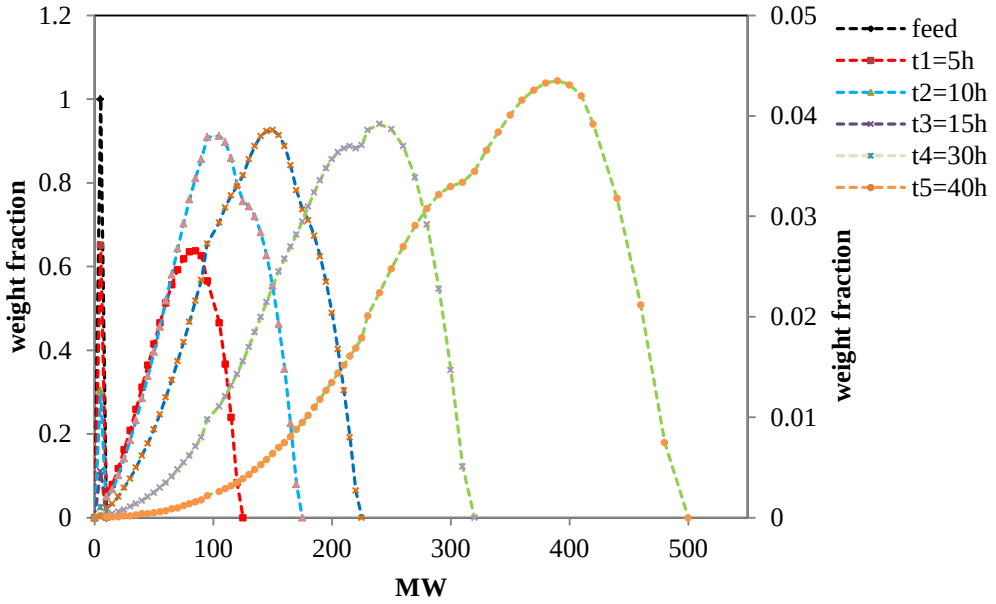

Figure 5.6. Product distribution at different times for the second case study where the feed is a monomer of molecular weight equal to 5 kg/kmol and $\boldsymbol{k = 0.1\ h^{-1}}$.

Fig. 5.7 reports the same calculation of Fig. 5.6, with a higher rate of reaction ($k = 0.2\ h^{-1}$). It can be noted that the production of higher molecular weight polymers increases, as expected.

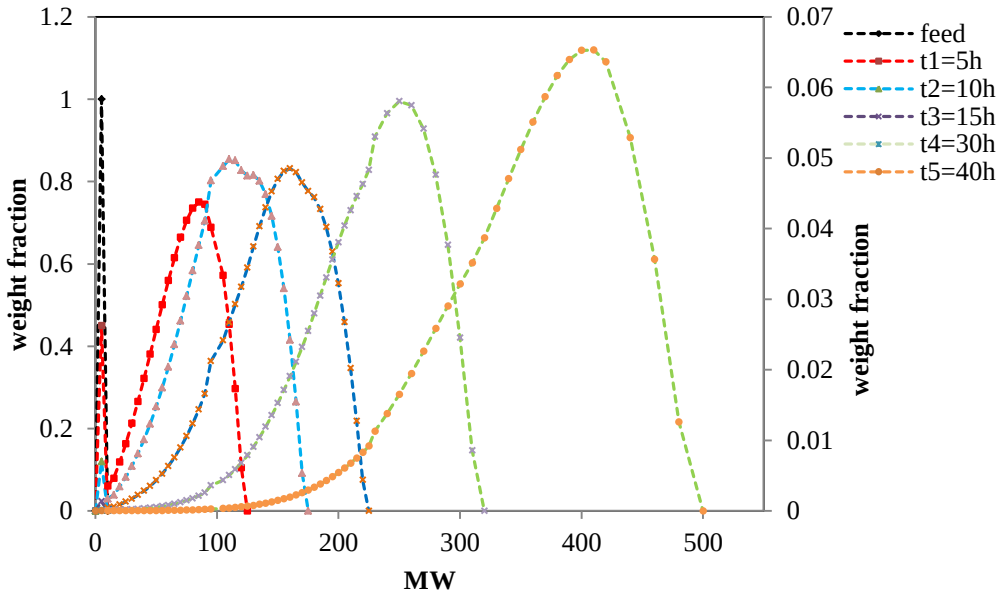

Figure 5.7. Product distribution at different times for second case study where the feed is a monomer of molecular weight equal to 5 kg/kmol and $\boldsymbol{k = 0.2\ h^{-1}}$.

Additional calculations were performed for the second case study, considering time steps to analyse how the polymerisation progresses with time. Starting from the feed of monomer of molecular weight equal to 5 kg/kmol, calculation are carried out using the product from the previous run as the feed: the product from the first run is used as the feed for the second step; the product from second step is used as the feed for the third step and so on. Fig. 5.8 reports the calculations corresponding to total of five steps. As the time increases, the concentration of the monomer decreases and the area under the curve increases, as more polymer is produced. A shift towards higher molecular weight polymers is observed, which, again, confirms the production of polymers with larger molecular weight. The reaction time is changed at each step. In the first step, the model is run until polymers with molecular weight less than 125 kg/kmol are produced; the corresponding reaction time is 5 hours. The product from this step is then used as the feed for the second step to produce polymers with molecular weight less than 175 kg/kmol; the corresponding reaction time is 10 hours. The times for the steps 3 to 5 are taken as 15, 30 and 40 hours, respectively and the corresponding polymers produced have molecular weight of these than 220, 320 and 500 kg/kmol, respectively.

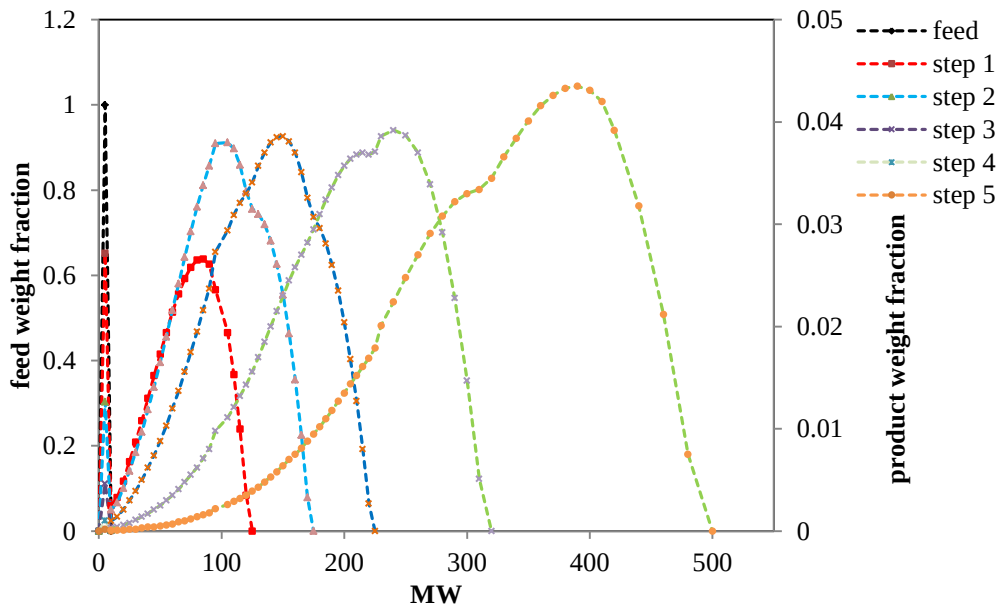

Figure 5.8. Effect of feed concentration on the MWD when used different steps.

The degree of conversion of the monomer to polymer is defined as: $conversion = \frac{(Monomer)_{in} - (monomer)_{out}}{(monomer)_{in}}$, and the variation of the conversion of the monomer with time is illustrated in Fig. 5.9 for the first case. It can be seen that the conversion of the monomer increases with increasing the resistance time of reaction but the increasing is not linear. The cumulative molecular weight distributions for the feed ($t = 0$) and for the polymerisation process at high conversion time ($40\ h$) are shown in Fig. 5.10 for the first case. The consumption of monomer and pre-polymers increases with the reaction time to produce polymers with a higher molecular weight. For example, the mixture contains about 30% of the components with a molecular weight less than 300 kg/kmol when the time of reaction reaches 40 hours. This implies that the monomers have to spend more than 40 hours in the reactor to be completely consumed.

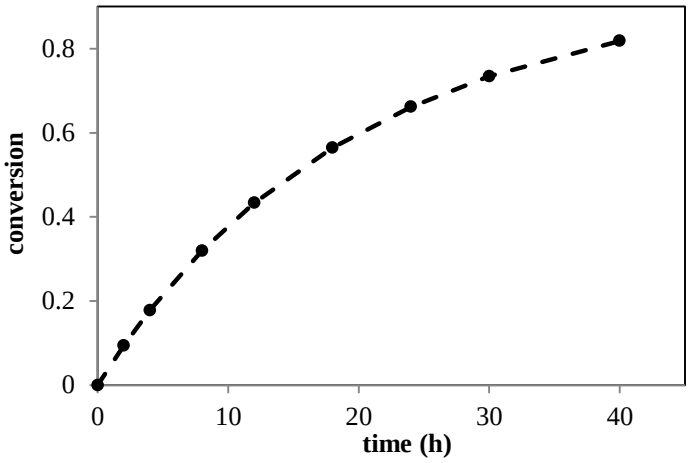

Figure 5.9. The degree of conversion of the monomer to polymer, for the first case.

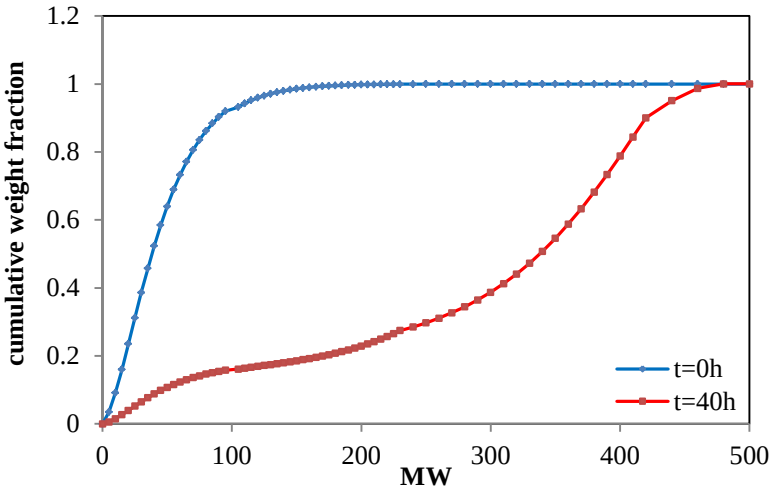

Figure 5.10. Predicted cumulative molecular weight distribution for first case.

The molecular weight distribution (MWD) is a continuous function in our model; therefore, the number and weight average molecular weights of the polymer for the first case study can be calculated by using the following equations:

$$\overline{M_N} = \frac{1}{\sum_{i=1}^{\infty} \frac{w_i}{M_i}} \tag{5.8}$$

$$\overline{M_w} = \sum_{i=1}^{\infty} w_i . M_i \tag{5.9}$$

where w_i is the weight fraction of polymer i. The time dependence of the number and weight average molecular weight M_N and M_w is shown in Fig. 5.11. As expected the value of M_N and M_w increase with increasing the conversion time.

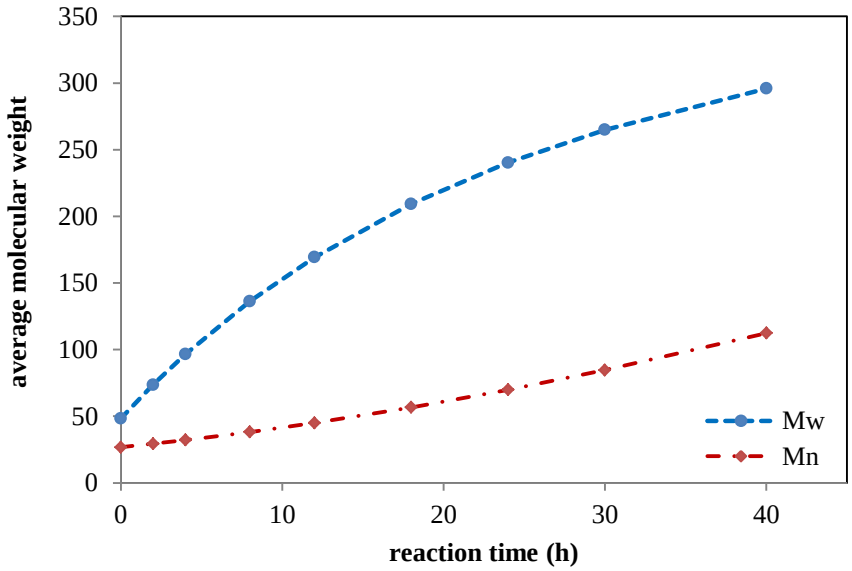

Figure 5.11. Predicted average molecular weight vs. time for $\boldsymbol{M_N}$ and $\boldsymbol{M_w}$.

5.5 Conclusions

There are many previous modelling works in the area of step growth polymerisation in the literature. However, most of these models were developed for a specific polymer system. In this study, a generalised modelling approach for step growth polymerisation systems has been developed. The developed model was based on the reduction methodology to avoid the complexity of polymerisation reactions. Therefore, a kinetic model has been developed to describe the polymerisation yield distribution based on the continuum lumping methodology. The model is based on the assumption that the molecular weight distribution evolves in time and it is described by an intgro-differential equation. The model has used a skewed Gaussian distribution function to determine the product yield distribution of the polymerisation reaction. As the time increases, the weight fraction of the monomer and oligomers decrease while the concentration of the polymers with higher molecular weight increases. The model captures successfully the effect of the reaction time and rate constant on the molecular weight distribution (MWD). A number and weight average molecular weights can be calculated from the predicted yield distribution; those are important and could be employed in determining the physical properties of the polymers.

CHAPTER 6.

Conclusions and Scope of the Future Work

6.1 Conclusions

The work undertaken in this thesis is focused on the development of lumping kinetic models for complex feedstocks. Three separate models are developed and applied to different practical problems encountered in industry. The problems selected are: hydrocracking of n-paraffins (Fischer-Tropsch waxes) in a catalytic reactor (Chapter Three); the pyrolysis of Kraft lignin in fluidised bed reactors (Chapter Four); and the step growth polymerisation (Chapter Five). Because of the complex structure of the molecules and large reaction network in the three case studies, some simplifying assumptions are made in the models. The model, which was developed for hydrocracking of n-paraffins in chapter three, has been modified to be applied for predicting catalytic hydrocracking of tar produced from lignin pyrolysis and extended to model step-growth polymerisation for deep understanding in detail; that is allowed to investigate kinetics of reactions on the yield distribution of the complex feedstocks. Of course the methodology cannot give all the information that one might want; but it can give the information that one needs in practical circumstances.

In the hydrocracking model of n-paraffin feed; the modelling approach used a continuous lumping methodology which allowed investigation of the effect of the operating conditions such as temperature, pressure, etc. on the model parameters. The molecular weight of the mixture has been used as the characterisation parameter and the rate constant of the hydrocracking has been assumed to be a monotonic function of the molecular weight in this model. Two functions of reactant-type distribution (the power law relation and the gamma function) are used in this model to investigate how this function affects the model predictions. Although, the gamma function gives less error than the power low relation, the power law relation has fewer parameters and needs less time to solve the model. The assumption in this model was dependent on first order of

reaction and the cracking has happened in the components which have high molecular weight first for producing components with low molecular weight. The proposed model has been validated against the experimental data and the yield of the different components can be predicted. The kinetics and product distribution parameters for both types of reaction type distribution have been fine-tuned by using the experimental data.

A number of simulations have been performed in this work using the estimated parameters to study the effect of the operating conditions on the product distribution. For the range of temperature, pressure and hydrogen feed ratio considered, the dependence on the temperature is much more marked than that on pressure and H_2/feed ratio, while the weight hour space velocity (WHSV) has been linked to the numerical time in the programme. As the residence time increases, the model predictions are less accurate. It is envisaged that for long residence time, other side reactions can take place and these are not included in the model at the present time. Another reason may be that the model uses the assumption that all the components in the feedstock will crack to produce components with low molecular weight, but in fact it may be that cracking occurs only on the components that have a molecular weight higher than 212 kg/kmol (C_{15} H_{32}). The reactivity (rate constant) of the components increases with increases in the temperature of reaction and decreases with increased pressure and WHSV.

The isomerisation between n-paraffins and iso-paraffins is not included in the model. The main equation in the model is an integrodifferential equation which can be solved numerically to find the product distribution in the reactor as a function of residence time and different conditions. The optimal set of model parameters were obtained by using the *MATLAB* regression function "*lsqcurvefit"* (Levenberg-Marquardt algorithm) to minimize the error between the experimental and calculated values of $c(k,t)$ by searching for the best values of the model parameters.

The second contribution in this research adds insight into the field of lignin pyrolysis kinetics and gives a catalytic kinetic model for bio-oil which is produced from lignin pyrolysis to improve the hydrocarbon fuel. The pyrolysis kinetics model developed was applied on two types of experiments of lignin pyrolysis. The first type was a fluidized bed reactor without mechanical mixing and the vapour residence time in

the reactor was 1.4 seconds while the second type was a fluidised bed reactor with mechanical mixing and 0.4 second for the vapour residence time in the reactor. Because Kraft lignin pyrolysis involves numerous extremely complex reactions and end products, devising an exact reaction mechanism and kinetic model for lignin pyrolysis is very difficult, therefore the developed pyrolysis models are modelled on the basis of lumping methodology to remove this difficulty. With applying the lumping technique on lignin pyrolysis, large sets of variables can be reduced. The mechanism models were based on a discrete lumping methodology with the different products split into three product groups: gas, tar and char. Thus, the lignin decomposition was described by three parallel reactions, called the primary reaction, whereas the tar decomposed according to one parallel reaction, referred to as a secondary reaction. In the first model the chemical processes of lignin pyrolysis were described through the primary reaction only while in the second model the processes were described through the primary and the secondary reaction. Assuming that all primary and secondary reactions were first order reaction in both models. The continuum kinetic model, which was developed from case one, was used on bio-oil product from lignin pyrolysis to increase the quality of lignin pyrolysis oil (tar). In short, this case study aimed at helping understanding of the pyrolysis process a whole. The kinetic description for primary and secondary reactions was connected to evaluation pathways of characteristics volatile products.

Finally, a new and simple kinetic model to describe the polymerisation yield distribution using continuum lumping methodology for the step-growth (or polycondensation) polymerisation has been proposed. This model is based on the molecular weight distribution (MWD) which is treated as a continuous variable. The time evolution of MWDs for monomers, copolymers, and polymers is governed by integro-differential equations. This model takes into account the constant rate of reaction between the functional groups of any molecule in the reaction mixture. The integro-differential equation is solved numerically to determine the $c(w,t)$. The model can predict MWD and can capture the effect of monomer feed concentration and residence time on the MWD. It is shown that, increasing the reaction time also increases the conversion of monomer that led to increases in both M_N and M_W. The results obtained are assessed only qualitatively; nevertheless, this study opens the door for many potential studies on polymerisation by using the continuum lumping approach.

The three case studies form a comprehensive project on understanding the methodology of lumping that can be applied in various complex reaction systems. This methodology gives good agreement with experimental data for Case one and two but Case three is not tested yet. Models are used to calculate the reactivity of the components and to predict the yield distribution from the reactor, while experimental data is used to improve the model parameters.

6.2 Recommendation for the future work

Several assumption and considerations in this study still require attention to encourage future research. The selections of experimental conditions applied in this study were dictated by available experimental data, as well as time limitations. The following recommendations are proposed for the future work:

1- Run experiments with different feed compositions and different kinds of catalyst to create a new type of yield distribution function ($P(k, K)$) to describe the hydrocracking phenomenon that can give more information on the mechanism of a process.

2- The exact nature of model parameters of the continuous kinetic approach depends on the activity and the formation of a catalyst. Therefore, correlating model parameters against operating variables such as pressure and hydrogen feed ratio need more investigation.

3- Although first order hydrocracking reactions, which were used in formulating the model, gives a very good result for the problems considered in this study, a more complicated kinetics can be inserted into the model for other problems. For example, if one considers the classical case of a Langmuir isotherm dominated kinetics (the kinetic equation for each reactant takes the form: $-dc/dt = kc/(1 + Kc)$) or if a n^{th} order hydrocracking reactions is considered, the main equation (Eq. 3.7) becomes:

$$\frac{dc(k,T)}{dt} = -k.c^n(k,t) + \int_k^{k_{max}} p(k,K).K.c^n(K,t).D(K).dK$$

4- The current continuum hydrocracking kinetic model does not account for isomerisation between n-paraffin and iso-paraffin due to the short age of experimental data available. The isomerisation could easily be inserted in the model, if data which can distinguish between two (or more) isomers were given. For example, if Fig 1.1 is considered, the model could be applied by steps. The model could be applied to the isomerisation step first obtaining two distributions, one for the n-paraffins and one for the iso-paraffins. By applying the model to those two feed distributions, the final cracking product can be evaluated, separating the two isomers. Two types of parameters are given by this procedure; one for isomerisation reaction and the other for cracking reaction. Therefore, the model parameters of isomerisation reactions help to select the type of catalyst that increases the isomer components in the catalytic reactor.

5- WHSV has been linked to the numerical time in the program. With increasing the time in the continuum kinetics model, the model predictions are less accurate. It is envisaged that for long residence time, other side reactions can take place and those are not included in the model at the present time.

6- Besides with the continuum lumping investigations, the discrete model was applied for estimating activation energy E and the frequency factor k_0 for pyrolysis of Kraft lignin, where parallel first-order reactions occur. Applying different order reactions for estimating the kinetic parameters and predicting pyrolysis yields would be useful.

7- Validating the polymerisation model with experimental data and modifying the yield distribution function to get a good prediction of the molecular weight distribution should be pursued.

8- After studying the continuum lumping approach and applying it to polymerisation we are confident that the methodology can be extended to other cases; and it is a very powerful technique. As an example it can applied to

crystallisation which is similar to polymerisation. This model could be used to predict the crystal size distribution during crystallisation at various times.

REFERENCES

Acrivos, A., Amundson, N.R. (1955). On the Steady State Fractionation of Multicomponent and Complex Mixtures in an Ideal Cascade: Part 1—Analytic Solution of the Equations for General Mixtures. *Chem. Eng. Sci., 4*(1), 29-38.

Adam, M., Ocone, R. (2010). *Application of the Lumping Kinetics Methodology*: EUROKIN Report.

Adam, M., Calemma, V., Galimberti, F., Gambaro,C., Heiszwolf, J., Ocone, R. (2012). Continuum Lumping Kinetics of Complex Reactive Systems. *Chem. Eng. Sci., 76*(9), 154-164.

Ancheyta, J., Sotelo, R. (2002). Kinetic Modeling of Vacuum Gas Oil Catalytic Cracking. *J. of the Mexican Chem. Society,, 46*(1), 38-42.

Ancheyta, J., Sanchez, S., Rodriguez, M.A. (2005). Kinetic Modeling of Hydrocracking of Heavy Oil Fractions: A Review. *Catal. Today, 109*(1-4), 76-92.

Ancheyta-Juarez, J., Lopeza-Isunza, F., Aguilar-Rodriguez, E., Moreno-Mayorga, J.C. (1997). A Strategy for Kinetic Parameter Estimation in the Fluid Catalytic Cracking Process. *Ind. Eng. Che. Res., 36*(12), 5170-5174.

Aris, R., Gavalas, G.R. (1966). On the Theory of Reactions in Continuous Mixtures. *Philos. Trans. R. Soc., 260*(1112), 351-393.

Aris, R. (1968). Prolegomena to the Rational Analysis of Systems of Chemical Reactions II. Some Addenda. *Arch. Ratl. Mach. Anal., 27*(5), 356-364.

Aris, R., Astarita, G. (1989). Continuous Lumping of Nonlinear Chemical Kinetics. *Chem. Eng. Proc., 26*(1), 63-69.

Aris, R. (1989). Reactions in Continuous Mixtures. *AIChE J., 35*(4), 359-548.

Astarita, G. (1985). *Scale Up: Overview, Closing Remarks and Cautions. Scale Up of Chemical Processes*. New York: A.L. Bisio, R.L. Kabel eds., Wiley.

Astarita, G., Ocone, R. (1988). Lumping Nonlinear Kinetics. *AIChE J. , 34*(8), 1299-1309.

Astarita, G., Ocone, R. (1989). Heterogeneous Chemical Equilibria in Multicomponent Mixtures. *Chem. Eng. Sci., 44*(10), 2323-1331.

Astarita, G., Nigam, A. (1989). Lumping Nonlinear Kinetics in a CSTR. *AIChE J., 35*(12), 1927-1932.

Astarita, G. (1989). Lumping Nonlinear Kinetics: Apparent Overall Order of Reaction. *AIChE J., 35*(4), 529-532.

Astarita, G., Ocone, R. (1992). Chemical Reaction Engineering of Complex Mixtures. *Chem. Eng. Sci., 47*(9-11), 2135-2147.

Avni, E., Coughlin, R.W., Solomon, P.R., King, H.H. (1985). Mathematical Modelling of Lignin Pyrolysis *Fuel, 64*(11), 1495-1501.

Balasubramanian, P., Pushpavanam, S. (2008). Model Discrimination in Hydrocracking of Vacuum Gas Oil Using Discrete Lumped Kinetics. *Fuel 87*(8-9), 1660-1672.

Baltanas, M. A., Vansina, H., Froment, G.F. (1983). Hydroisomerization and Hydrocracking. 5. Kinetic Analysis of Rate Data for n-Octane. *Ind. Eng. Chem. Prod. RD., 22*(4), 531-539.

Baltanas, M. A., Van Raemdonck, K. K., Froment, G.F., Mohedas, S.R. (1989). Fundamental Kinetic Modeling of Hydroisomerization and Hydrocracking on Noble-Metal-Loaded Faujasites. 1. Rate Parameters for Hydroisomerization. *Ind. Eng. Chem. Res., 28*(7), 899-910.

Basak, K., Sau,M., Manna, U., Verma, R.P. (2004). Industrial Hydrocracker Model Based on Novel Continuum Lumping Approach for Optimization in Petroleum Refinery. *Catal. Today., 98*(1-2), 253-264.

Blanding, F. H. (1953). Reaction Rates in Catalytic Cracking of Petroleum. *Ind. Eng. Chem., 45*(6), 1186-1197.

Boerjan, W., Ralph, J., Baucher, M. (2003). Lignin Biosynthesis. *Annu. Rev. Plant Biol., 54*, 519-546.

Bollas, G. M., Lappas, A.A., Iatridis, D.K., Vasalos, I.A. (2007). Five-Lump Kinetic Model with Selective Catalyst Deactivation for the Prediction of the Product Selectivity in the Fluid Catalytic Cracking Process. *Catal. Today., 127*(1-4), 31-43.

Bridgwater, A. V. (1994). Catalysis in Thermal Biomass Conversion. *Appl. Catal. A: General., 116*(1-2), 5-47.

Caballero, J. A., Font, R., Marcilla, A., Conesa, J.A. (1995). New Kinetic Model for Thermal Decomposition of Heterogeneous Materials. *Ind. Eng. Chem. Res., 34*(3), 806-812.

Caballero, J. A., Font, R., Marcilla, A. (1996). Study of the Primary Pyrolysis of Kraft Lignin at High Heating Rates: Yields and Kinetics. *J. Anal. Appl. Pyrolysis., 36*(2), 159-178.

Caballero, J. A., Font, R., Marcilla, A. (1997). Pyrolysis of Kraft Lignin: Yields and Correlations. *J. Anal. Appl. Pyrolysis., 39*(23), 161-183.

Calemma, V., Peratello, S., Perego, C. (2000). Hydroisomerization and Hydrocracking of Long Chain n-Alkanes on Pt/amorphous SiO_2–Al_2O_3 Catalyst. *Appl. Catal. A-Gen., 190*(1-2), 207-218.

Calemma, V., Correra, S., Perego, C., Pollesel, P., Pellegrini, L. (2005). Hydroconversion of Fischer–Tropsch Waxes: Assessment of the Operating Conditions Effect by Factorial Design Experiments. *Catal. Today., 106*(1-4), 282-287.

Chaimberg, M., Cohen, Y. (1990). Kinetic Modeling of Free-Radical Polymerization: a Conservational Polymerization and Molecular Weight Distribution Model. *Ind. Eng. Chem. Res., 29*(7), 1152-1160.

Chou, M. Y., Ho, T.C. (1988). Continuum Theory for Lumping Nonlinear Reactions. *AIChE J. , 34*(9), 1519-1527.

Chou, M. Y., Ho, T.C. (1989). Lumping Coupled Nonlinear Reactions in Continuous Mixtures. *AIChE J. , 35*(4), 533-538.

Clymans, P. J., Froment, G. F. (1984). Computer-Generation of Reaction Paths and Rate Equations in the Thermal Cracking of Normal and Branched Paraffins. *Comput. Chem. Eng., 8*(2), 137-142.

Collins, J. P., Font Freide, J.J.H.M., Nay, B. (2006). A History of Fischer-Tropsch Wax Upgrading at BP—from Catalyst Screening Studies to Full Scale Demonstration in Alaska. *J. Nat. Gas Chem., 15*(1), 1-10.

Cowie, J. M., Arrighi, V. (2008). *Polymers: Chemistry and Physics of Modern Materials* (3th edition ed.).

Crowley, T. J., Choi, K.Y. (1997a). Calculation of Molecular Weight Distribution from Molecular Weight Moments in Free Radical Polymerization. *Ind. Eng. Chem. Res. , 36*(5), 1419-1423.

Crowley, T. J., Choi, K.Y. (1997b). Discrete Optimal Control of Molecular Weight Distribution in a Batch Free Radical Polymerization Process. *Ind. Eng. Chem. Res., 36*(9), 3676-3684.

de Almeida, R. M., Guirardello, R. (2005). Hydroconversion Kinetics of Marlim Vacuum Residue. *Catal.Today. , 109*(1-4), 104-111.

de Donder, T. (1931). *L'Affinite*. 2nd part, Gautier Villars, Paris.

de Klerk, A. (2007). Thermal Cracking of Fischer−Tropsch Waxes. *Ind. Eng. Res., 46*(17), 5516-5521.

Di Blasi, C. (1996). Influences of Model Assumptions on the Predictions of Cellulose Pyrolysis in the Heat Transfer Controlled Regime. *Fuel, 75*(1), 58-66.

Dry, M. E. (2002). The Fischer–Tropsch Process: 1950–2000. *Catal. Today., 71*(3-4), 227-241.

Elizalde, I., Rodriguez, M.A., Ancheyta, J. (2009). Application of Continuous Kinetic Lumping Modeling to Moderate Hydrocracking of Heavy Oil. *Appl. Catal. A-Gen., 365*(2), 237-242.

Elizalde, I., Rodriguez, M.A., Ancheyta, J. (2010). Modeling the Effect of Pressure and Temperature on the Hydrocracking of Heavy Crude Oil by the Continuous Kinetic Lumping Approach. *Appl. Catal. A- Gen., 382*(2), 205-212.

Faravelli, T., Frassoldati, A., Migliavacca, G., Ranzi, E. (2010). Detailed Kinetic Modeling of the Thermal Degradation of Lignins. *Biomass Bioenerg., 34*(3), 290-301.

Feng, W., Vynckier, E., Froment, G. F. (1993). Single Event Kinetics of Catalytic Cracking. *Ind. Eng. Chem. Res. , 32*(12), 2997-3005.

Ferdous, D., Dalai, A.K., Bej, S.K., Thring, R.W. (2002). Pyrolysis of Lignins: Experimental and Kinetics Studies. *Energ. Fuel., 16*(6), 1405-1412.

Flory, P. J. (1937). The Mechanism of Vinyl Polymerizations. *J. Am. Chem. Soc. , 59*(2), 241-253.

Froment, G. F. (1987). Kinetics of the Hydroisomerization and Hydrocracking of Paraffins on a Platinum Containing Bifunctional Y-Zeolite. *Catal. Today., 1*(4), 455-473.

Froment, G. F. (2005). Single Event Kinetic Modeling of Complex Catalytic Processes. *Catal. Rev., 47*(1), 83-124.

Fushimi, C., Araki, K., Yamaguchi, Y., Tsutsumi, A. (2003). Effect of Heating Rate on Steam Gasification of Biomass. 1. Reactivity of Char. *Ind. Eng. Chem. Res., 42*(17), 3922-3928.

Fushimi, C., Araki, K., Yamaguchi, Y., Tsutsumi, A. (2003). Effect of Heating Rate on Steam Gasification of Biomass. 2. Thermogravimetric-Mass Spectrometric (TG-MS) Analysis of Gas Evolution. *Ind. & Eng. Chem. Res., 42*(17), 3929-3936.

Gamba, S., Pellegrini, L.A., Calemma, V., Cambaro, C. (2009). Introduction of a Breakage Probability Function in the Hydrocracking Reactor Model. *Ind. Eng. Chem. Res.*, *48*(12), 5656-5665.

Gamba, S., Pellegrini, L. A., Calemma, V., Gambaro, C. (2010). Liquid Fuels from Fischer–Tropsch Wax Hydrocracking: Isomer Distribution. *Catal. Today.*, *156*(1-2), 58-64.

Gambaro, C., Calemma, V., Molinari, D., Denayer, J. (2011). Hydrocracking of Fischer-Tropsch Waxes: Kinetic Modeling via LHHW Approach. *AIChE J.* , *57*(3), 711-723.

Gary, J. H., Handwerk, G.E. (1994). *Petroleum Refining: Technology and Economics*: 3rd Edition, Marcel Dekker, Inc.

Ghetti, P., Ricca, L., Angelini, L. (1996). Thermal Analysis of Biomass and Corresponding Pyrolysis Products. *Fuel.*, *75*(5), 565-573.

Guerra, A., Filpponen, I., Lucia, L.A., Argyropoulos, D.S. (2006). Comparative Evaluation of Three Lignin Isolation Protocols for Various Wood Species. *J. Agr. Food Chem., 54*(26), 9696-9705.

Haseli, Y., van Oijen, J.A., de Goey, L.P.H. (2011). Modeling Biomass Particle Pyrolysis with Temperature-Dependent Heat of Reactions. *J. Anal. Appl. Pyrol., 90*(2), 140-154.

Hillewaert, L. P., Dierickx, J. L., Froment, G. F. (1988). Computer Generation of Reaction Schemes and Rate Equations for Thermal Cracking. *AIChE J.*, *34*(1), 17-24.

Ho, T. C., Aris, R. (1987). On Apparent Second-Order Kinetics. *AIChE J.* , *33*(6), 1050-1051.

Ho, T. C., White, B.S. (1995). Experimental and Theoretical Investigation of the Validity of Asymptotic Lumped Kinetics. *AIChE J., 41*(6), 1513-1520.

Ho, T. C. (2008). Hydroprocessing Catalysis on Metal Sulfides Prepared from Molecular Complexes. *Catal. Today., 130*(1), 206-220.

Ho, T. C. (2008). Kinetic Modeling of Large-Scale Reaction Systems. *Catal. Rev., 50*(3), 287-378.

Huber, G. W., Iborra, S., Corma, A. (2006). Synthesis of Transportation Fuels from Biomass: Chemistry, Catalysts, and Engineering. *Chem. Rev., 106*(9), 4044-4098.

Iatridis, B., Gavalas, R. . (1979). Pyrolysis of a Precipitated Kraft Lignin. *Ind. Eng. Chem. Res. Dev., 18*(2), 127-130.

Ikeda, T., Holtman, K., Kadla, J., Chang, H., Jameel, H. (2002). Studies on the Effect of Ball Milling on Lignin Structure using a Modified DFRC Method. *J. Agr. Food Chem., 50*(1), 129-135.

Jacob, S. M., Gross, B., Voltz, S.E., Weekman, V.W. (1976). A Lumping and Reaction Scheme for Catalytic Cracking. *AIChE J., 22*(4), 701-713.

Jegers, H., Klein, M.T. (1985). Primary and Secondary Lignin Pyrolysis Reaction Pathways. *Ind. Eng. Chem. Process Des. Dev., 24*(1), 173-183.

Khorasheh, F., Chan, E.C., Gray, M.R. (2005). Development of a Continuous Kinetic Model for Catalytic Hydrodesulfurization of Bitumen. *Petroleum & Coal, 47*(1), 40-48.

Kiparissides, C. (1996). Polymerization Reactor Modeling: a Review of Recent Developments and Future Directions. *Chem. Eng. Sci., 51*(10), 1637-1659.

Kiparissides, C. (2006). Challenges in Particulate Polymerization Reactor Modeling and Optimization: a Population Balance Perspective. *J. Process Contr.l, 16*(3), 205-224.

Koufopanos, C. A., Papayannakos, N.,Maschio, G., Lucchesi, A. (1991). Modelling of the Pyrolysis of Biomass Particles. Studies on Kinetics, Thermal and Heat Transfer Effects. *Can. J. Chem. Eng., 69*(4), 907-915.

Krishan, P. C., Balasubramanian, P. (2009). Analytical Solution for Discrete Lumped Kinetic Equations in Hydrocracking of Heavier Petroleum Fractions. *Ind. Eng. Chem. Res., 48*(14), 6608-6617.

Krishna, R., Saxena, A. K. (1989). Use of an Axial-Dispersion Model for Kinetic Description of Hydrocracking. *Chem. Eng. Sci., 44*(3), 703-712.

Kumar, H. (2006). *Mechanistic Kinetic Modelling of the Hydrocracking of Complex Feedstocks.* Texas A&M University, Texas.

Kumar, H., Froment, G. F. (2007). A Generalized Mechanistic Kinetic Model for the Hydroisomerization and Hydrocracking of Long-Chain Paraffins. *Ind. Eng Chem. Res., 46*(12), 4075-4090.

Kumar, V. (2009). *Pyrolysis and Gasification of Lignin and Effect of Alkali Addition.* Goeorgia Institute of Technology, Georgia.

Lababidi, H. M. S., Al Humaidan, F.S. (2011). Modeling the Hydrocracking Kinetics of Atmospheric Residue in Hydrotreating Processes by the Continuous Lumping Approach. *Energ. Fuel., 25*(5), 1939-1949.

Laxminarasimhan, C. S., Verma, R.P., Ramachandran, P.A. (1996). Continuous Lumping Model for Simulation of Hydrocracking. *AIChE J., 92*(9), 2645-2653.

Leckel, D., Liwanga-Ehumbu, M. (2006). Diesel-Selective Hydrocracking of an Iron-Based Fischer−Tropsch Wax Fraction (C_{15}−C_{45}) Using a MoO_3-Modified Noble Metal Catalyst. *Energ. Fuel. , 20*(6), 2330-2336.

Lee, L. S., Chen, Y.W., Huang, T.N., Pan, W.Y. (1989). Four-Lump Kinetic Model for Fluid Catalytic Cracking Process. *Can. J. Chem. Eng., 67*(4), 615-619.

Li, B. Z., Ho, T.C. (1991). Lumping Weakly Nonuniform Bimolecular Reactions. *Chem. Eng. Sci., 46*(1), 273-280.

Li, G. (1984). A Lumping Analysis in Mono- or/and Bimolecular Reaction Systems. *Chem. Eng. Sci. , 39*(7-8), 1261-1270.

Li, G., Rabitz, H. (1989). A General Analysis of Exact Lumping in Chemical Kinetics. *Chem. Eng. Sci., 44*(6), 1413-1430.

Li, G., Rabitz, H. . (1990). A General Analysis of Approximate Lumping in Chemical Kinetics. *Chem. Eng. Sci., 45*(4), 977-1002.

Li, G., Rabitz, H. (1991). *A General Analysis of Lumping in Chemical Kinetics*: Kinetic and Thermodynamic Lumping of Multicomponent Mixtures. Editted by Astarita, G, and Sandlers, S.I., Elsevier.

Li, G., Tomlin, A.S., Rabitz, H., Toth, J. (1993). Determination of Approximate Lumping Schemes by a Singular Perturbation Method *J. Chem. Phys., 99*(5), 3562-3574.

Li, G., Tomlin, A.S., Rabitz, H., Toth, J. (1994). A General Analysis of Approximate Nonlinear Lumping in Chemical Kinetics. I. Unconstrained Lumping. *J. Chem. Phsys., 101*(2), 1172-1187.

Liao, J. C., Lightfoot, E.N. (1988). Lumping Analysis of Biochemical Reaction Systems with Time Scale Separation. *Biotech. Bioeng., 31*(8), 869-879.

Liu, Q., Wang, S., Zheng, Y., Luo, Z., Cen, K. (2008). Mechanism Study of Wood Lignin Pyrolysis by Using TG–FTIR Analysis. *J. Anal. Appl. Pyrolysis, 82*(1), 170-177.

Lora, J. H., Glasser, W.G. (2002). Recent Industrial Applications of Lignin: A Sustainable Alternative to Nonrenewable Materials. *J. Polym. Environ., 10*(1-2), 39-48.

Luo, Z., Wang, S., Cen, K. (2005). A Model of Wood Flash Pyrolysis in Fluidized Bed Reactor. *Renew. Energ., 30*(3), 377-392.

Martens, G. G., Marin, G. B., Martens, J. A., Jacobs, P. A., Baron, G. V. (2000). A Fundamental Kinetic Model for Hydrocracking of C_8 to C_{12} Alkanes on Pt/US–Y Zeolites. *J. Catal., 195*(2), 253-267.

Martens, J. A., Jacobs, P.A., Weitkamp, J. . (1986). Attempts to Rationalize the Distribution of Hydrocracked Products. I Qualitative Description of the Primary Hydrocracking Modes of Long Chain Paraffins in Open Zeolites. *Appl. Catal. , 20*(1-2), 239-281.

Martens, J. A., Jacobs, P.A., Weitkamp, J. (1986). Attempts to Rationalize the Distribution of Hydrocracked Products. II. Relative Rates of Primary Hydrocracking Modes of Long Chain Paraffins in Open Zeolites. *Appl. Catal., 20*(1-2), 283-303.

Martinis, J. M., Froment, G. F. (2006). Alkylation on Solid Acids. Part 2. Single-Event Kinetic Modeling. *Ind. Eng. Chem. Res., 45*(3), 954-967.

Mazloom, G., Farhadi, F., Khorasheh, F. (2009). Kinetic Modeling of Pyrolysis of Scrap Tires. *J. Anal. Appl. Pyrolysis, 84*(2), 157-164.

McCoy, B. J. (1993). Continuous-Mixture Kinetics and Equilibrium for Reversible Oligomerization Reactions. *AIChE J., 39*(11), 1827-1833.

McCoy, B. J., Madras, G. (2001). Discrete and Continuous Models for Polymerization and Depolymerization. *Chem. Eng. Sci., 56*(8), 2831-2836.

Miura, K. (1995). A New and Simple Method to Estimate f(E) and k0(E) in the Distributed Activation Energy Model from Three Sets of Experimental Data. *Energ. Fuel., 9*(2), 302-307.

Mohanty, S., Saraf, D.N., Kunzru, D. (1991). Modeling of a Hydrocracking Reactor. *Fuel Process Technol., 29*(1-2), 1-17.

Moller, K., Le Grange, P., Accolla, C. (2009). A Two-Phase Reactor Model for the Hydrocracking of Fischer−Tropsch-Derived Wax. *Ind. Eng. Chem. Res. , 48*(8), 3791-3801.

Montane, D., Torne-Fernandez, V., Fierro, V. (2005). Activated Carbons from Lignin: Kinetic Modeling of the Pyrolysis of Kraft Lignin Activated with Phosphoric Acid. *Chem. Eng. J., 106*(1), 1-12.

Morf, P., Hasler, P., Nussbaumer, T. (2002). Mechanisms and Kinetics of Homogeneous Secondary Reactions of Tar from Continuous Pyrolysis of Wood Chips *Fuel., 81*(7), 843-853.

Murugan, P., Mahinpey, N., Johnson, K.E., Wilson, M. (2008). Kinetics of the Pyrolysis of Lignin Using Thermogravimetric and Differential Scanning Calorimetry Methods. *Energ. Fuel., 22*(4), 2720-2724.

Nele, M., Sayer, C., Pinto, J.C. (1999). Computation of Molecular Weight Distributions by Polynomial Approximation with Complete Adaptation Procedures. *Macromol. Theory Simul., 8*(3), 199-213.

Nunn, T. R., Howard, J.B., Longwell, J.P., Peters, W.A. (1985). Product Compositions and Kinetics in the Rapid Pyrolysis of Milled Wood Lignin. *Ind. Eng. Chem. Process Des. Dev., 24*(3), 844-852.

Ocane, R. (2009). *Lumping Kinetics of Multi-Component Reactive mixture:* EUROKIN Report.

Okino, M. S., Mavrovouniotis, M.L. (1998). Simplification of Mathematical Models of Chemical Reaction Systems. *Chem. Rev., 98*(2), 391-408.

Pandey, M. P., Kim, C.S. (2011). Lignin Depolymerization and Conversion: A Review of Thermochemical Methods. *Chem. Eng. Technol., 34*(1), 29-41.

Patwardhan, P. R. (2010). *Understanding the Product Distribution from Biomass Fast Pyrolysis.* Iowa State University, Iowa.

Pellegrini, L., Locatelli, S., Rasella, S., Bonomi, S., Calemma, V. (2004). Modeling of Fischer–Tropsch Products Hydrocracking. *Chem. Eng. Sci., 59*(22-23), 4781-4787.

Pellegrini, L., Bonomi, S., Gamba, S., Calemma, V., Molinari, D. . (2007). The "All Components Hydrocracking Model". *Chem. Eng. Sci., 62*(18-20), 5013-5020.

Pellegrini, L., Gamba, S., Calemma, V., Bonomi, S. (2008). Modelling of Hydrocracking with Vapour–Liquid Equilibrium. *Chem. Eng. Sci., 63*(17), 4285-4291.

Pladis, P., Kiparissides, C. (1998). A Comprehensive Model for the Calculation of Molecular Weight–Long-Chain Branching Distribution in Free-Radical Polymerizations. *Chem. Eng. Sci., 53*(18), 3315-3333.

Pyle, D. L., Zaror, C.A. (1984). Heat Transfer and Kinetics in the Low Temperature Pyrolysis of Solids. *Chem. Eng. Sci., 39*(1), 147-158.

Ray, W. H. (1972). On the Mathematical Modeling of Polymerization Reactors. *J. Macromol. Sci.: Pol. Rev., 8*(1), 1-56.

Ray, W. H. (1991). Modelling of Addition Polymerization Processes — Free Radical, Ionic, Group Transfer, and Ziegler–natta Kinetics. *Can. J. Che. Eng., 69*(3), 626-629.

Sada, E., Kumazawa, H., Kudsy, M. (1992). Pyrolysis of Lignins in Molten Salt Media. *Ind. Eng. Chem. Res., 31*(2), 612-616.

Sadhukhan, A. K., Gupta, P., Saha, R.K. (2008). Modelling and Experimental Studies on Pyrolysis of Biomass Particles. *J. Anal. Appl. Pyrol., 81*(2), 183-192.

Sadighi, S., Ahmad, A., Rashidzadeh, M. (2010). 4-Lump Kinetic Model for Vacuum Gas Oil Hydrocracker Involving Hydrogen Consumption. *Korean J. Chem. Eng., 27*(4), 1099-1108.

Saiz-Jimenez, C., de Leeuw, J. W. (1986). Lignin Pyrolysis Products: Their Structures and Their Significance as Biomarkers. *Org. Geochem., 10*(4-6), 869-876.

Sanchez, S., Ancheyta, J. (2007). Effect of Pressure on the Kinetics of Moderate Hydrocracking of Maya Crude Oil. *Energ. Fuel., 21*(2), 653-661.

Schulz, H. F., Weitkamp J.H. (1972). Zeolite Catalysts. Hydrocracking and Hydroisomerization of n-Dodecane. *Ind. Eng. Chem. Process Des. Dev., 11*(1), 46-53.

Schweitzer, J. M., Galtier, P., Schweich, D. (1999). A Single Events Kinetic Model for the Hydrocracking of Paraffins in a Three-Phase Reactor. *Chem. Eng. Sci., 54*(13-14), 2441-2452.

Scott, D. S., Majerski, P., Piskorz, J., Radlein, D.J. (1999). A Second Look at Fast Pyrolysis of Biomass—the RTI Process. *J. Anal. Appl. Pyrol., 51*(1-2), 23-37.

Shafizadeh, F., Chin, P.S. (1977). Thermal Deterioration of Wood. In A. C. Society (Ed.), *Wood Technology: Chemical Aspects* (Vol. 43, pp. 57-81). Washington D.C.

Shahrouzi, J. R., Guillaume, D., Rouchon, P., da Costa, P. (2008). Stochastic Simulation and Single Events Kinetic Modeling: Application to Olefin Oligomerization. *Ind. Eng. Chem. Res., 47*(13), 4308-4316.

Skeirik, R. D., Grulke, E.A. (1985). A Calculation Scheme for Rigorous Treatment of Free Radical Polymerization. *Chem. Eng. Sci., 40*(3), 535-538.

Smagala, T. G., McCoy, B.J. (2006). Population Balance Modeling of Polymer Branching and Hyperbranching. *Chem. Eng. Sci., 61*(1), 3-17.

Stangeland, B. E. (1974). A Kinetic Model for the Prediction of Hydrocracker Yields. *Ind. Eng. Chem., Process Des. Dev., 13*(1), 71-76.

Surla, K., Guillaume, D., Verstraete, J. J., Galtier P. (2011). Kinetic Modeling using the Single-Event Methodology: Application to the Isomerization of Light Paraffins. *Oil Gas Sci. Technol., 66*(3), 343-365.

Svoboda, G. D., Vynckier, E., Debrabandere, B., Froment, G.F. (1995). Single-Event Rate Parameters for Paraffin Hydrocracking Oil a Pt/Us-Y Zeolite. *Ind. Eng. Chem. Res., 34*(11), 3793-3800.

Thurner, F., Mann, U. (1981). Kinetic Investigation of Wood Pyrolysis. *Ind. Eng. Chem. Process Des. Dev., 20*(3), 482-488.

Varhegyi, G., Antal, M. J., Jakab, E., Szabo, P. (1997). Kinetic Modeling of Biomass Pyrolysis *J. Anal. Appl. Pyrolysis, 42*(1), 73-87.

Varhegyi, G., Bobaly, B., Jakab, E., Chen, H. (2011). Thermogravimetric Study of Biomass Pyrolysis Kinetics. A Distributed Activation Energy Model with Prediction Tests. *Energ. Fuel., 25*(1), 24-32.

Vynckier, E., Froment, G.F. (1991). *Modeling of the Kinetics of Complex Processes based upon Elementary Steps*: Kinetic and Thermodynamic Lumping of Multicomponent Mixtures. ELSEVIER.

Weekman, V. W., Nace, D.M. (1970). Kinetics of Catalytic Cracking Selectivity in Fixed, Moving, and Fluid Bed Reactors. *AIChE J., 16*(3), 397-404.

Wei, J., Kuo, J.C.W. (1969). A Lumping Analysis in Monomolecular Reaction Systems. *Ind. Chem. Fundam., 8*(1), 114-123.

Wei, J. (1991). *Lumping Revisited: Global Environmental Changes*: Kinetic and Thermodynamic lumping of Multicomponent Mixture. G. Astarita and S.I. Sandler, Elsevier

Weismantel, G. E. (1992). *Petroleum Processing Handbook*. New York: Marcel Dekker.

Weitkamp, J. (1982). Isomerization of Long-Chain n-Alkanes on a Pt/CaY Zeolite Catalyst. *Ind. Eng. Chem. Prod. Res. Dev., 21*(4), 550-558.

Whetten, R., Sederoff, R. (1995). Lignin Biosynthesis. *The Plant Cell, 7*, 1001-1013.

Xu, R., Ferrante, L., Briens, C., Berruti, F. (2009). Flash Pyrolysis of Grape Residues into Biofuel in a Bubbling Fluid Bed. *J. Anal. Appl. Pyrolysis*, *86*(1), 58-65.

Xu, R., Ferrante, L., Briens, C., Berruti, F. (2011). Bio-Oil Production by Flash Pyrolysis of Sugarcane Residues and Post Treatments of the Aqueous Phase. *J. Anal. Appl. Pyrolysis*, *91*(1), 263-272.

Yen, L., Wrench, R., Ong, A. (1987). Reaction Kinetic Correlation for Predicting Coke Yield in Fluid Catalytic Cracking, *Presented at the katalistisks' 8th Annual fluid catalytic cracking symposium, Budapest, Hungary* (pp. 1-4).

Zeman, R. J., Amundson, N.R. (1965). Continuous Polymerization Models-Part I: Polymerization in Continuous Stirred Tank Reactors. *Chem. Eng. Sci., 20*(4), 331-361.

Zeman, R. J., Amundson, N.R. (1965). Continuous Polymerization Models—Part II: Batch Reactor Polymerization. *Chem. Eng. Sci., 20*(7), 637-664.

APPENDIX 1

In this appendix, it will provide a Matlab program codes that used for getting kinetic parameters.

- ***C.1 main Matlab program***

The following code belongs to the main structure of the Matlab program applied to get the local optimal model parameters.

```
%% MATLAB CODE FOR OPTIMISATION KINETIC MODEL PARAMETERS %%
clear all
close
clc
%$$$$$$$$$$$$$$$$$       INPUT DATA        $$$$$$$$$$$$$$$$
Conc=[0 0 0 0 0.038 0.095 0.696 1.353 2.156 2.885 3.374
3.715 3.906 3.984 4.016 3.968 3.906 3.904 3.747 3.624 3.501
3.408 3.347 3.329 3.268 3.137 2.215 2.656 2.372 2.092 1.865
1.67 1.52 1.415 1.434 1.336 1.246 1.172 1.09 1.114 0.954
0.97 0.933 0.879 0.717 0.739 0.594 0.522 0.478 0.431 0.389
0.36 0.315 0.295 0.272 0.252 0.235 0.222 0.213 0.204 0.195
0.187 0.176 0.162 0.249 0.195 0.109 0.086 0.056 0.057 ];
%
Exp=[0.046239 0.019042 0.12143 0.365646 0.385817 0.660189
0.943677  1.945919  2.871434  3.902147  4.734362  5.177179
5.339962  5.32404  5.225523  5.067716  4.966344  4.880419
4.584769  4.39694  4.096985  3.956406  3.776072  3.665358
3.385543  3.013365  2.630076  2.299849  1.920365  1.589686
1.353861  1.121074  0.978035  0.845882  0.718739  0.635399
0.551694  0.460902  0.401627  0.342205  0.300967  0.529537
0.165165 0.157165 0.145249 0 0 0 0 0 0 0 0 0 0 0 0 0 0 0 0
0 0 0 0 0 0 0 0 0];
%$$$$$$$$$$$$$$$$$$$$$$$$$$$$$$$$$$$$$$$$$$$$$$$$$$$$$$$$$$$
lb=[1,1,0.5,0.289,1.51e-9];   % LOWER VALUES FOR THE MODEL
                                PARAMETES
ub=[25,25,25,5,1.5e-3];       % HIGHER VALUES FOR THE MODEL
                                PARAMETERS
x0=[6.2,4.3,8.61,0.38,1.5e-8];% INITIAL VLUES FOR THE MODEL
                                PARAMETERS
%$$$$$$$$$$$$$$$$   MODEL OPTIMISATION      $$$$$$$$$$$$$$$
```

```
[x,resnorm,residual]=lsqcurvefit(@mymodelback,x0,Conc,Exp,l
b,ub)
%$$$$$$$$$$$$$$$$   THE OPTIMAL PARAMETERS   $$$$$$$$$$$$$$
a0 = x(1);
a1 = x(2);
kmax = x(3);
alpha = x(4);
delta = x(5);
%$$$$$$$$$$ USED THE OPTIMAL PARAMETERS IN THE MODEL $$$$$$
n=70; % NUMBER OF SPICES
AA=exp(-((0.5/a1)^2));
S0=1/(sqrt(2*pi));

for i=1 : n
    theta(i)=(i-1)./(n-1);
    k(i)=kmax*theta(i).^(1./alpha);
end
%$$$$$$$$$$$$$$$$$$$$$$$$$$$$$$$$$$$$$$$$$$$$$$$$$$$$$$$$$
Feed=Conc;
%$$$$$$$$$$$$$$$$$$$$$$$$$$$$$$$$$$$$$$$$$$$$$$$$$$$$$$$$$
SI=@(k)          ((S0)*(exp(-(((k./kmax).^a0-0.5)./a1).^2)-
AA+delta*(1-k./kmax)))*((n*alpha./kmax.^alpha)*k.^(alpha-
1));
SII=quadv(SI,0,kmax)

DI=@(k)(n*alpha./kmax.^alpha)*k.^(alpha-1);
DII=quadv(DI,0,kmax)

PI=@(k)((1./SII*S0)*(exp(-(((k./kmax).^a0-0.5)./a1).^2)-
AA+delta*(1-k./kmax)))*((n*alpha./kmax.^alpha)*k.^(alpha-
1));
PII=quadv(PI,0,kmax)
%$$$$$$$$$$$$$$$$$$$$$$$$$$$$$$$$$$$$$$$$$$$$$$$$$$$$$$$$$
h=0.01;        % TIME STEP
t=0:h:0.5;
ff=0;
for l=1:length(t)-1;
   ff=ff+h;
```

```
     time=t(l) ;
for i=n:-1:1
    ty=i;
    if i>=n

    Conc(n)=Conc(n)*(exp(-k(n)*h));

 else
    if k(i)==0
        m=k(i+1)-0.000000001;
    else
m=k(i);
    end
mm=k(i+1);

In=@(K)(((1./SII.*S0).*(exp(-(((m./K).^a0-0.5)./a1).^2)-
AA+delta.*(1-m./K))).*((n.*alpha./K.^alpha).*m.^(alpha-
1)).*(K-mm)./(m-mm));
I1=quadl(In,m,mm);
sum1=0;sum2=0;
for j=n-1:-1:i+1
    oo=j;
    xi=k(j);
    xx=k(j+1);
    zz=Conc(j);

 In2=@(K)(((1./SII.*S0).*(exp(-(((m./K).^a0-0.5)./a1).^2)-
AA+delta.*(1-m./K))).*((n.*alpha./K.^alpha).*m.^(alpha-
1)).*(K-xx)./(m-xx));
 I21=quadl(In2,xi,xx);

  sum1=sum1+I21*zz ;

 In22=@(K)(((1./SII.*S0).*(exp(-(((m./K).^a0-0.5)./a1).^2)-
AA+delta.*(1-m./K))).*((n.*alpha./K.^alpha).*m.^(alpha-
1)).*(K-x)./(xx-m));
  I22=quadl(In22,xi,xx);
```

```
  sum2=sum2+I22*zz;

end
  sum_int1=sum1;
  sum_int2=sum2;

k1=Conc(i)*(-m+I1)+sum_int1+sum_int2;
conc=Conc(i)+h*k1;
k2=conc*(-m+I1)+sum_int1+sum_int2;
Conc(i)=Conc(i)+h*(k1+k2)./2;

    end
end

C_Norm1=0;
for N_write1=1:n
    C_Norm1=C_Norm1+Conc(N_write1);
end

Total1=C_Norm1
subplot(2,2,1), plot(ff,Total1,'*')
grid on
xlabel('time(h)')
ylabel('total mass')
hold on

for N_cc=1:n
    Conc(N_cc)=(Conc(N_cc)./C_Norm1)*100;
end

end

C_Norm=0;
for N_write=1:n
    C_Norm=C_Norm+Conc(N_write);
    subplot(2,2,2),plot(N_write,C_Norm,'.');
```

```
    grid on
xlabel('carbon number')
ylabel('comulative wt %')
    hold on
    Total=C_Norm;

end

Total=C_Norm
for N_cc=1:n
    Conc(N_cc)=(Conc(N_cc)./C_Norm)*100;
end
Model1=Conc(:);
Feed1=Feed(:);
Exp1=Exp(:);
%$$$$$$$$$$$$$$$$$$   PLOT THE RESULT    $$$$$$$$$$$$$$$$$$
subplot(2,1,2), plot(k,Feed,k,Conc,'r+',k,Exp,'o');
grid on
xlabel('k')
ylabel('wt %')
hold off
```

➢ *C.2 main file of optimization*

```
function Conc = mymodelback(x,Conc)
a0=x(1);
a1=x(2);
kmax=x(3);
alpha=x(4);
delta=x(5);
n=70;
%%$$$$$$$$$$$$$$$$$$$$$$$$$$$$$$$$$$$$$$$$$$$$$$$$$$$$$$$$$$$$$$
AA=exp(-((0.5/a1)^2));
S0=1/(sqrt(2*pi));
for i=1 : n
    theta(i)=(i-1)./(n-1);
    k(i)=kmax*theta(i).^(1./alpha);
```

```
end
%%$$$$$$$$$$$$$$$$$$$$$$$$$$$$$$$$$$$$$$$$$$$$$$$$$$$$$$$$$$$$
SI=@(k)          ((S0).*(exp(-(((k./kmax).^a0-0.5)./a1).^2)-
AA+delta.*(1-
k./kmax))).*((n.*alpha./kmax.^alpha).*k.^(alpha-1));
SII=quadl(SI,0,kmax);
%$$$$$$$$$$$$$$$$$$$$$$$$$$$$$$$$$$$$$$$$$$$$$$$$$$$$$$$$$$$$$
h=0.01;                 % TIME STEP
t=0:h:0.5;
ff=0;

for l=1:length(t)-1;
   ff=ff+h;

     time=t(l)  ;
for i=n:-1:1
    ty=i;
    if i>=n

    Conc(n)=Conc(n)*(exp(-k(n)*h));

 else
    if k(i)==0
        m=k(i+1)-0.000000001;
    else
m=k(i);
    end
mm=k(i+1);

In=@(K)(((1./SII.*S0).*(exp(-(((m./K).^a0-0.5)./a1).^2)-
AA+delta.*(1-m./K))).*((n.*alpha./K.^alpha).*m.^(alpha-
1)).*(K-mm)./(m-mm));
I1=quadl(In,m,mm);

sum1=0;sum2=0;
for j=n-1:-1:i+1

    oo=j;
```

```
    x=k(j);
    xx=k(j+1);
    zz=Conc(j);

 In2=@(K)(((1./SII.*S0).*(exp(-(((m./K).^a0-0.5)./a1).^2)-
AA+delta.*(1-m./K))).*((n.*alpha./K.^alpha).*m.^(alpha-
1)).*(K-xx)./(m-xx));
 I21=quadl(In2,x,xx);

  sum1=sum1+I21*zz ;

 In22=@(K)(((1./SII.*S0).*(exp(-(((m./K).^a0-0.5)./a1).^2)-
AA+delta.*(1-m./K))).*((n.*alpha./K.^alpha).*m.^(alpha-
1)).*(K-x)./(xx-m));
  I22=quadl(In22,x,xx);

  sum2=sum2+I22*zz;

end
  sum_int1=sum1;
  sum_int2=sum2;

k1=Conc(i)*(-m+I1)+sum_int1+sum_int2;
conc=Conc(i)+h*k1;
k2=conc*(-m+I1)+sum_int1+sum_int2;
Conc(i)=Conc(i)+h*(k1+k2)./2;
    end
end

C_Norm=0;
for N_write=1:n
    C_Norm=C_Norm+Conc(N_write);
end

for N_cc=1:n
    Conc(N_cc)=(Conc(N_cc)./C_Norm)*100
end
end
```

APPENDIX 2

An effect of operating conditions such as temperature, pressure, WHSV, and H_2/feed ratio on experimental results:

1. **Temperature:**

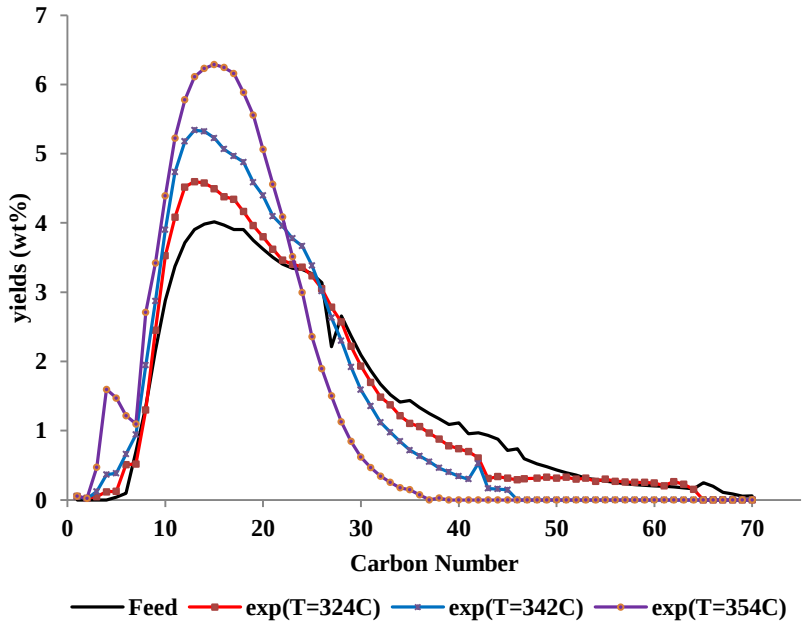

2. **Pressure:**

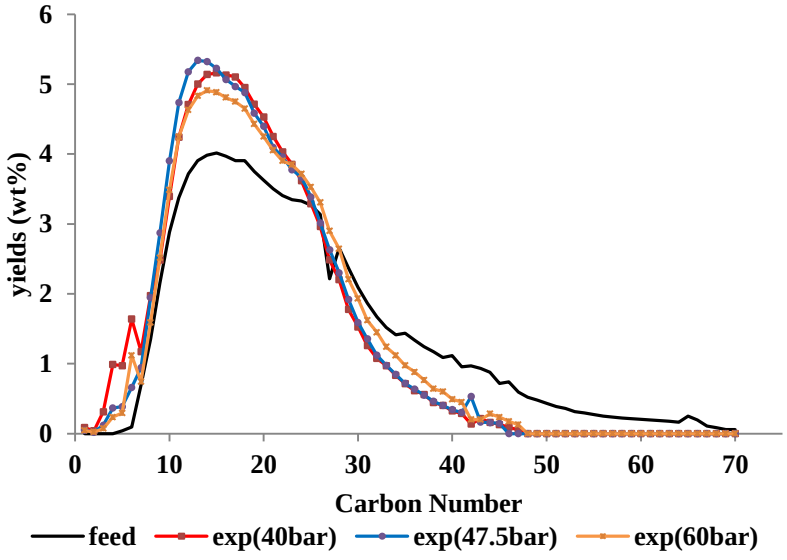

3. H_2/Feed ratio:

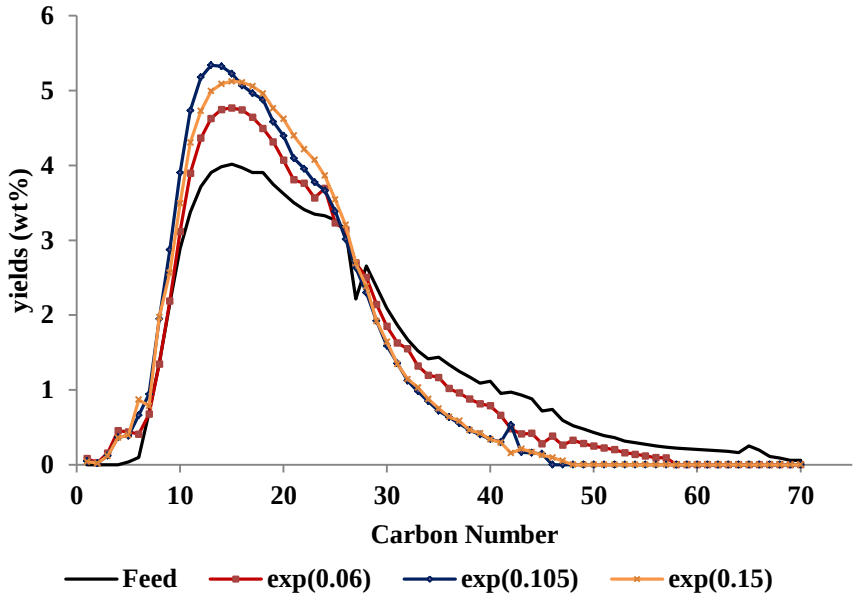

4. WHSV:

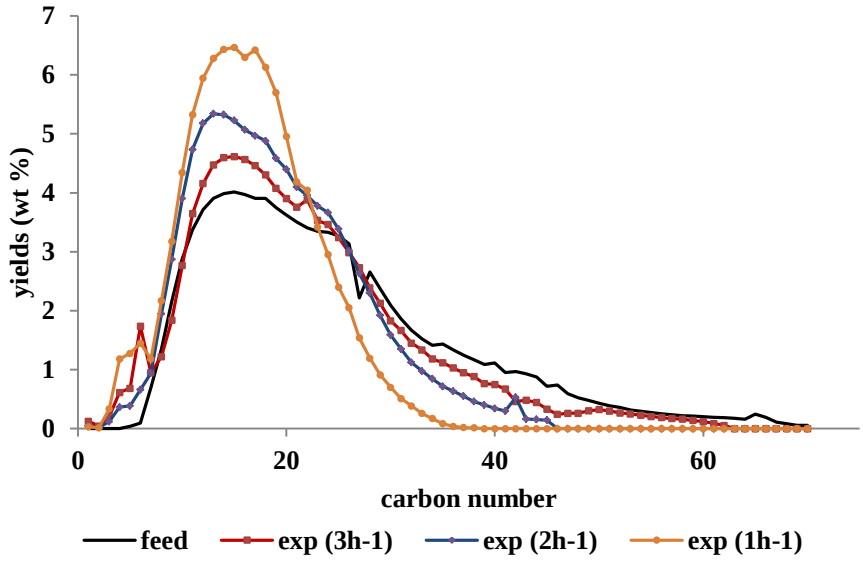

APPENDIX 3

This appendix includes the Matlab program code for Kraft lignin pyrolysis in a fluidized bed reactor as the following below (for the discrete lumping model):

- ***C.1 main program***

```
Clear
clc
close
%$$$$$$$$$$$$$$$$$$$$$$$$$$$$$$$$$$$$$$$$$$$$$$$$$$$$$$$$$$$$$$$$
exp=[ 0 5 25 70];                    % EXPERIMENTAL DATA
%$$$$$$$$$$$$$$$$$$$$$$$$$$$$$$$$$$$$$$$$$$$$$$$$$$$$$$$$$$$$$$$$
w0=[100 0 0 0 ];                     % FEED
%$$$$$$$$$$$$$$$$$$$$$$$$$$$$$$$$$$$$$$$$$$$$$$$$$$$$$$$$$$$$$$$$
lb=[0.0003 0.0003 0.0003 0.0003];  % LOWER VLAUES
ub=[400 400 400 400];                % HIGHER VALUES
%$$$$$$$$$$$$$$$$$$$$$$$$$$$$$$$$$$$$$$$$$$$$$$$$$$$$$$$$$$$$$$$$
x01=0.006;
Output=[];
for J=-9:1:9 % CALCULATE THE INTIAL VALUES FOR THE REACTION
               RATE CONSTANT
k0=[x01*(10+J)/10        x01*(20+J)/20        x01*(30+J)/30
x01*(40+J)/40];
[k,resnorm,residual]=lsqcurvefit(@reaction145b22,k0,w0,exp,
lb,ub)       % OPTIMISATION
kG_end=k(1);
kT_end=k(2);
kC_end=k(3);
kGT_end=k(4);
resnorm
output=[kG_end kT_end kC_end kGT_end resnorm];

Output=[Output; output]
```

```
end
[b,c]=size(Output);
%$$$$$$$$$$$$$$$$$$$$$$$$$$$$$$$$$$$$$$$$$$$$$$$$$$$$$$$$$$$$$$$$
z=1;
for jj=1:1:b;
    if (Output(jj,4)<0);
    else
        Output_new(z,:)=Output(jj,:);
        z=z+1;
    end
end
%%$$$$$ SEARCHIN THE OPTIMAL VALUES FOR THE KINETIC RATE
         CONSTANT
[b1,c1]=size(Output_new);
minimum=min(Output_new(:,5));
for p=1:1:b1;
    if (Output_new(p,5)==minimum);
        values(1,:)=Output_new(p,:);
    end
end
kG_end=values(1,1)
kT_end=values(1,2)
kC_end=values(1,3)
kGT_end=values(1,4)
%$$$$$$$$$$$$$$$$$$$$$$$$$$$$$$$$$$$$$$$$$$$$$$$$$$$$$$$$$$$$$$$$$
t=[0 20];
kk=[kG_end kT_end kC_end kGT_end];
wa=w0;
[t,wa]=ode45('reacts45b22',t,wa,[],kk);
subplot(2,1,1),plot(t,wa,'-');
grid on
xlabel('time (minute)')
ylabel('wt %')
hold on
%$$$$$$$$$$$$$$$$$$$$$$$$$$$$$$$$$$$$$$$$$$$$$$$$$$$$$$$$$$$$$$$$$
Lig=wa(end,1)
        t1=[0 0.4/60];
```

```
cc=wa(end,3);

f= @(t,c) -kGT_end.*cc;
[t1,cc]=ode45(f,t1,cc);
MM1=wa(end,3)-cc;
gas=wa(end,2)+MM1;
Gasend=gas(end)

tar=cc;
Tarend=tar(end)
Char=wa(end,4)
composation =[Lig Gasend Tarend Char];
subplot(2,1,2),plot(t1,cc,'-.',t1,gas,'--');
grid on
xlabel('time (second)')
ylabel('wt %')
hold off
```

➢ *C.2 main file of optimization*

```
function wt=reaction145b22(k,w)
t=[0 20];
[t,w]=ode45('reacts45b22',t,w,[],k);
k1=k(1);
k2=k(2);
k3=k(3);
k4=k(4);
%$$$$$$$$$$$$$$$$$$$$$$$$$$$$$$$$
wt(1)=w(end,1);

t1=[0 0.4/60];
c=w(end,3);
%kk=k(4);
f= @(t,c) -k(4).*c;
[t1,c]=ode45(f,t1,c);
MM=w(end,3)-c(end);
wt(2)=w(end,2)+MM;
```

```
        wt(3)=w(end,3)-MM;
        wt(4)=w(end,4);
```

➢ *C.3 kinetics model of the reaction*

```
function dwdt=reacts45a2(t,w,flag,k)
dwdt=zeros(size(w));
A=w(1);
B=w(2);
C=w(3);
D=w(4);
dwdt(1)=-(k(1)+k(2)+k(3)).*A;
dwdt(2)=k(1).*A+k(4).*C;
dwdt(3)=k(2).*A-k(4).*C;
dwdt(4)=k(3).*A;
```

APPENDIX 4

This appendix is introduced a Matlab code that explens how to solve model of polymerisation.

```
clear
close
clc
% ******************************************************
a0=2.67;a1=28.86;n=69;Pi=3.1415926536;;ka=1.5;Wn=500;
%******************************************************
PP=@(w)     ((1/SS0)*ss*(exp(-((((w./Wn).^a0)-0.5)./a1).^2)-
EE));
Pk=quad(PP',0,Wn);
%******************   INPUT DATA   *********************
w=[0 5 10 15 20 25 30 35 40 45 50 55 60 65 70 75 80 85 90
95 105 110 115 120 125 130 135 140 145 150 155 160 165 170
175 180 185 190 195 200 205 210 215 220 225 230 240 250 260
270 280 290 300 310 320 330 340 350 360 370 380 390 400 410
420 440 460 480 500];


Conc=[0  0.034590155  0.056407736  0.068989992  0.075003408
0.076444664  0.07479707  0.071152207  0.066303378  0.06081971
0.055100812  0.049420467  0.043959382  0.038830219  0.03409657
0.029787228  0.025906872  0.02244399  0.0193767  0.016676968
0.012254486 0.010467782 0.008923105 0.007591989 0.006448229
0.005468019 0.004629953 0.003914957 0.003306154 0.002788705
0.002349628 0.001977623 0.001662891 0.001396963 0.001172547
0.000983379 0.000824093 0.000690103 0.000577499 0.000482951
0.00040363 0.000337136 0.000281436 0.000234812 0.000195811
0.000163207 0.000113223 7.84106e-05 5.42151e-05 3.74303e-05
2.58065e-05 1.77698e-05 1.22213e-05 8.39596e-06 5.76197e-06
3.9504e-06 2.70598e-06 1.85194e-06 1.26641e-06 8.65335e-07
5.9085e-07 4.03155e-07 2.74903e-07 1.87334e-07 1.27583e-07
5.90774e-08 2.72993e-08 1.2591e-08 5.79713e-09];
%******************************************************
C=Conc;
%************************* PLOT THE FEED *************
plot(w,C)
```

```
% ******************************************************
AA=exp(-((0.5/a1)^2));
S0=1/(sqrt(2*Pi));
%************ CALCULATE S0 IN THE P(k,K) TERM **********
sum=0;
for jj=1:n-1;
    M(jj)=w(jj+1)-w(jj);
   t(jj)=exp(-(((w(jj)./Wn).^a0-0.5)./a1).^2);t(jj+1)=exp(-
(((w(jj+1)./Wn).^a0-0.5)./a1).^2);
    P(jj)=S0*(t(jj)-AA);P(jj+1)=S0*(t(jj+1)-AA);
        H(jj)=P(jj)+P(jj+1);
    sum=sum+M(jj)*H(jj)./2;
end
S=sum;
%******************************************************
h=0.01;                         % h IS THE TIME STEP.
t=0:h:2;                        % INITIALIZE TIME VARIABLE
for i=1:length(t)-1,
% **CALCULATE THE INTEGRAL PARTE IN THE MAIN EQUATION *
for j=2:n-1
    m=j;
    Sum_int=0;
for i=1:m
Delta(i)=w(i+1)-w(i);

temp(i)=exp(-(((w(i)./Wn).^a0-0.5)./a1).^2);temp(i+1)=exp(-
(((w(j+1)./Wn).^a0-0.5)./a1).^2);
Pee(i)=(1./S*S0)*(temp(i)-
AA);Pee(i+1)=(1./S*S0)*(temp(i+1)-AA);
H_trapez(i)= Pee(j)*ka*Conc(i)+Pee(i+1)*ka*Conc(i+1);
Sum_int=Sum_int+Delta(i)*H_trapez(i)./2;
end
integrals(j)=Sum_int;

k1=-ka*Conc(j)+integrals(j);
conc=Conc(j)+h*k1;
k2=-ka*conc+integrals(j);
```

```
Conc(j)=Conc(j)+h*(k1+k2)/2;

end
% ***********RENORMALISE THE CONCENTRATION *************
C_Norm=0;
for N_write=1:n
  C_Norm=C_Norm+Conc(N_write)
end
for N_cc=1:n
  Conc(N_cc)=(Conc(N_cc)./C_Norm);
end

end
% ***************** PLOT THE RESULTS ******************
hold on
plot(w,Conc,'r+');    % PLOT THE MODEL CALCULATION VS. w
hold off
```